Titre: Title:	Drinking water treatment of sources containing cyanobacterial blooms with Vacuum UV (VUV)
Auteur: Author:	Flavia Visentin
Date:	2020
Type:	Mémoire ou thèse / Dissertation or Thesis
Référence: Citation:	Visentin, F. (2020). Drinking water treatment of sources containing cyanobacterial blooms with Vacuum UV (VUV) [Thèse de doctorat, Polytechnique Montréal]. PolyPublie. https://publications.polymtl.ca/4228/

URL de PolyPublie: PolyPublie URL:	https://publications.polymtl.ca/4228/
Directeurs de recherche: Advisors:	Benoit Barbeau, & Sarah Dorner
Programme: Program:	Génies civil, géologique et des mines

POLYTECHNIQUE MONTRÉAL
affiliée à l'Université de Montréal

Drinking water treatment of sources containing cyanobacterial blooms with Vacuum UV (VUV)

FLAVIA VISENTIN
Département de génies civil, géologique et des mines (CGM)

Thèse présentée en vue de l'obtention du diplôme de *Philosophiæ Doctor*
Génie civil

Février 2020

POLYTECHNIQUE MONTRÉAL
affiliée à l'Université de Montréal

Cette thèse intitulée :

Drinking water treatment of sources containing cyanobacterial blooms with Vacuum UV (VUV)

présentée par **Flavia VISENTIN**
en vue de l'obtention du diplôme de *Philosophiæ Doctor*
a été dûment acceptée par le jury d'examen constitué de :

Yves COMEAU, président
Benoit BARBEAU, membre et directeur de recherche
Sarah DORNER, membre et codirectrice de recherche
Clara SANTATO, membre
Ronald HOFMANN, membre externe

DEDICATION

To Leandro, for his unconditional support.

To Bruno and Tiziano, for their smiles that charged me.

To my father for teaching me that the sky is the limit.

To my mother for transmitting the strength that only a woman is able to transfer.

ACKNOWLEDGEMENTS

To my supervisor, Prof. Benoit BARBEAU, for allowing me to enter the world of drinking water treatment, when I had no great knowledge in the subject, and teaching me everything he knows about this subject.

To my co-supervisor, Prof. Sarah DORNER, for her technical guidance, but above all her emotional support was key in the course of this stage.

To Prof. Clara SANTATO for accepting to be part of the jury during the thesis defense and allowing me to perfectly close a cycle since she was the one who strongly suggested me to go back to School.

To Prof. Madjid MOHSENI and his group, specially Siddharth Bhartia.

To Prof. Sigrid PELDSZUZ and her group, specially Lin Shen

To Prof. Sébastien SAUVÉ and his group, specially Dana SIMON, Sung Do GUY and Quoctuc DINH.

The whole team of Drinking Water Chair at Polytechnique.

To Arlene Van Leeuwen and Laura Dauphin for your great help in linguistic correction.

All my colleagues and friends that during these four years I have collected in and out of Poly.

A special thanks to my very first friend at Poly, Celso, who left us suddenly and surprisingly.

To Leandro, much more than my husband and father of my children, my life partner, my friend, my number one critic, my unconditional support. None of this would have been possible without you by my side.

To my children, Bruno and Tiziano, because they were the engine that forced me to move forward many times.

RÉSUMÉ

Assurer l'accès à l'eau potable peut être difficile pour les services d'approvisionnement en eau lorsque leur source d'eau est périodiquement affectée par les proliférations d'algues. Une solution potentielle à court terme ou temporaire est de changer la source d'eau à une autre source exempte d'algues. Cependant, cette solution est souvent impossible en raison des investissements requis pour modifier les infrastructures hydrauliques existantes ainsi que par manque de ressources financières.

La prolifération saisonnière des algues se produit généralement en été et au début de l'automne. Lors d'un événement de prolifération d'algues, la production de composés responsables aux goûts et odeurs tels que le 2-méthylisoborneol (MIB) et la géosmine (GSM), ainsi que la production potentielle de toxines doivent être surveillées et contrôlées.

Plusieurs technologies sont disponibles pour le traitement des eaux en présence de cyanobactéries. Parmi eux, la filtration sur charbon actif en poudre et granulaire, l'ozonation, et les membranes haute pression (nanofiltration et osmose inverse) se sont avérées efficaces pour adresser la problématique des toxines. Cependant, toutes ces solutions impliquent soit une technologie complexe et / ou des coûts d'investissement et d'exploitation importants. Compte tenu de la présence saisonnière des fleurs d'eau de cyanobactéries, les technologies à forte intensité de capital (par exemple l'ozonation ou les membranes) sont particulièrement difficiles à mettre en œuvre s'il n'y a pas d'autre objectif de traitement de l'eau pouvant justifier leur application.

En raison de ces problèmes, l'objectif principal de ce projet était d'évaluer une technologie simple, abordable et écoresponsable qui pourrait être utilisée par des systèmes d'approvisionnement en eau petits et éloignés. L'utilisation du rayonnement ultraviolet (UV) à 254 nm dans la désinfection de l'eau est appliquée depuis plusieurs décennies dans l'industrie de l'eau potable. La désinfection est atteinte lorsque les rayons UV à 254 nm attaquent l'ADN cellulaire rendant la reproduction des cellules impossible. La plage de photons avec des longueurs d'onde comprises entre 10 nm et 200 nm dans la région UV du spectre électromagnétique est communément appelée UV sous vide (VUV par son acronyme en anglais). Les photons VUV sont assez énergiques pour réaliser la photolyse des molécules d'eau, générant un fort et non sélectif radical hydroxyle ($^{\bullet}$OH). Contrairement à d'autres processus d'oxydation avancée, aucun produit chimique n'est injecté pour la formation de $^{\bullet}$OH, ce qui représente un avantage évident pour les petits systèmes en permettant l'oxydation simultanée de traces de contaminants organiques et la désinfection.

La viabilité du processus VUV doit être évaluée en termes de performances ainsi que de son impact sur la qualité de l'eau de source (matière organique naturelle, matière organiques algues et solutés inorganiques) en particulier pour les eaux de source affectées par les fleurs d'eau de cyanobactéries. Ce projet inclut pour la première fois l'application de VUV pour l'inactivation des cyanobactéries et cyanotoxines ainsi que la dégradation des gouts et odeurs dans les sources d'eau naturelles contaminées par une prolifération d'algues. L'influence de matière organique naturelle et algues et des solutés inorganiques naturellement présents dans les sources d'eau sur la performance de VUV a été évaluée tout au long du projet. Sur cette base, les objectifs suivants ont été fixés:

i. Évaluer la dégradation des cyanotoxines et des gouts et odeur par les VUV dans les eaux naturelles (Article 1)

ii. Comprendre le rôle de la matière organique naturelle et de la matière organiques des algues sur les performances et la formation de sous-produits de désinfection des VUV (Article 2)

iii. Confirmer la possibilité de désinfecter et de dégrader simultanément les traces de contaminants organiques avec les VUV après la chloration (Article 3)

L'originalité de ce projet provient de l'étude d'une technologie en développement, sans produits chimiques et avec l'utilisation de matrices d'eau chargées d'algues naturelles de trois lacs de la province du Québec au Canada. Les lacs sélectionnés pour ces travaux ont des qualités et des caractéristiques d'eau différentes. Bien que les trois soient régulièrement touchés par les cyanobactéries, des échantillons ont été prélevés en absences de proliférations, en présence modérée de cellules et en présence importante de cyanobactéries. De plus, un lac reconnu pour sa forte concentration de chlorures et d'alcalinité a été sélectionné pour évaluer l'influence de ces ions sur le traitement des VUV.

Les résultats obtenus tout au long de ce travail montrent:

i. 40% et 60% de dégradation des cyanotoxines et des gouts et odeurs dans les conditions de prolifération ont été atteints respectivement. Bien qu'il s'agisse d'une dégradation considérable, elle peut ne pas être suffisante pour éliminer la toxicité et les gouts et odeurs à la fluence appliquée (Article 1)

ii. l'application de VUV a entraîné une augmentation faible (<10%) ou modérée (jusqu'à 20%) de la formation de trihalométhanes et d'acide haloacétique (Article 2)

iii. Par rapport à l'inactivation des cyanobactéries, 5 log et 4 log ont été obtenus avec des eaux ultrapures et des eaux de surface respectivement (Article 3)

En conclusion, cette étude a démontré que les VUV est une option de traitement potentielle pour atteindre une photolyse directe sans produits chimiques ainsi qu'une oxydation avancée de l'une des toxines de cyanobactéries les plus communes et toxique (microcystin-LR) et des molécules de gouts et odeurs métabolites dérivés des algues (MIB et GSM). L'influence de la de la matière organique naturelle et algues sur les performances de VUV a été évaluée. Il a été constaté que la substance humique, une fraction de la matière organique naturelle, a la plus grande influence sur la formation de sous-produits de désinfection. Dans la dernière partie des travaux, l'influence des VUV sur l'intégrité cellulaire de deux celulles de cyanobactéries cultivées (*Microcystis aeruginsoa* et *Anabaena Sp.*) a été étudiée ainsi que la dégradation de leurs cyanotoxines. La désinfection et la dégradation des contaminants ont été obtenues simultanément. Un traceur, la carbamazépine (CBZ), a été utilisée pour mieux distinguer le rôle des radicaux $^{\bullet}$OH. La dégradation de CBZ obtenue par VUV a dépassé 99%.

Dans le cadre des futurs travaux dans ce domaine, la conception d'un réacteur à grande échelle qui permet l'utilisation d'ondes $UV_{185\,nm}$ dans une couche mince de quelques millimètres sera un grand défi. Une conception hydrodynamique améliorée est nécessaire pour atteindre des performances d'oxydation élevées en utilisant le $UV_{185\,nm}$.

Sans doute, un point à analyser avant d'appliquer un procédé d'oxydation de contaminants dans l'eau potable à l'échelle réelle est la formation de nouveaux produits / contaminants. Les futures études devront aborder la question, car les nouveaux produits / contaminants formés pourront possiblement être encore plus toxiques que les originaux.

ABSTRACT

Ensuring access to safe drinking water can be challenging for water utilities when their source water is periodically impacted by algae blooms. A potential short-term solution is to change the water supply to another source free of algae. However, this is most often impossible due to the investments required to modify the existing water infrastructures and the lack of financial resources.

Seasonal algal bloom usually occurs in summer and early autumn. During a bloom event, the production of compounds responsible for taste and odor (T&O), such as 2-Methylisoborneol (MIB) and geosmin (GSM), and the potential production of toxins must be monitored and controlled.

When the predominant species within a bloom is cyanobacteria, a so-called cyanobacterial bloom arises and cyanobacteria is responsible for the production of cyanotoxins.

Several technologies have been successfully applied to the treatment of water impacted by cyanobacteria,among them, powdered and granular activated carbon filtration, ozonation, and high-pressure membranes (nanofiltration and reverse osmosis). However, all these alternatives involve either a complex technology and/or significant capital and operational costs. Given the seasonal nature of cyanobacterial blooms, capital-intensive technologies (e.g. ozonation or membrane) are especially challenging to implement if there is not another water treatment objective justifying their application.

In view of these problems, the main objective of this project was to test an emerging simple, affordable and eco-friendly technology that could potentially be used by small and remote water supply systems.

The use of ultraviolet (UV) radiation at 254 nm in water disinfection has been applied for several decades in the drinking water industry. The disinfection is achieved when $UV_{254\,nm}$ attacks the cellular DNA making the cells reproduction not possible.

The range of photons with wavelengths between 10 nm to 200 nm in the UV region of the electromagnetic spectrum is commonly referred to as vacuum UV (VUV). VUV photons are energetic enough to photolyze the molecules of water, generating strongly and non-selective hydroxyl radicals ($^{\bullet}OH$). As opposed to other common advanced oxidation process (AOP), no chemicals are injected for the formation of $^{\bullet}OH$, a clear advantage of this treatment technique for small water systems which allows simultaneous oxidation of trace organic contaminants and disinfection.

The viability of the VUV process needs to be assessed in terms of its performance as well as its impact on source water quality (background natural organic matter (NOM), algal organic matter (AOM) and inorganic solutes) especially in the case of source waters impacted by cyanobacterial blooms. This project combines for the first time the application of VUV:

i. for cyanobacterial inactivation and

ii. cyanotoxins and T&O degradation in natural water sources contaminated by algal bloom

The influence on VUV perfromance of NOM, AOM and inorganic solutes, naturally present in the water sources,was evaluated throughout the project. On this basis, the following objectives have been set:

i. Assess cyanotoxins and T&O degradation by VUV in natural waters (Article 1)

ii. Understand the role of background NOM and AOM on VUV performance and disinfection by-products (DBP) formation after chlorination (Article 2)

iii. Confirm the possibility to simultaneously disinfecting and degrading organic trace contaminants with VUV (Article 3)

The originality of this project lies in the use of an incipient and chemical-free technology as applied to natural algae-laden waters matrix of three different lakes in the province of Quebec, Canada with correspondingly differing water qualities and characteristics. Although all three are regularly impacted by cyanobacteria, samples were collected in the absence of blooms, in the moderate presence of cells and in the presence of a significant cyanobacterial bloom. In addition, one lake, recognized for its high concentration of chlorides and alkalinity, was deliberately selected to assess the influence of these ions on VUV treatment.

The results obtained throughout this work show:

i. 40% and 60% degradation of cyanotoxin and T&O, respectively, were achieved under bloom conditions. While this represents a considerable degradation, it may not be sufficient to completely eliminate toxicity and T&O at the fluence applied (Article 1)

ii. the application of VUV led to, on average, a low ($< 10\%$) or moderate (up to 20%) increase in the formation of trihalomethanes (THM) and haloacetic acid (HAA) when chlorine was used as final disinfectant (Article 2)

iii. In terms of cyanobacterial inactivation, 5-log and 4-log were achieved in ultra-pure and surface water, respectively (Article 3)

In conclusion, this study demonstrated that VUV is a potential treatment option for achieving a chemical-free direct photolysis and advanced oxidation of one of the most common and toxic cyanobacterial toxins (microcystin-LR) and algae-derived T&O metabolites (MIB and GSM). The influence of NOM (background NOM and AOM) on VUV performance was evaluated. It was found that humic substance, a fraction of NOM, has the greatest influence on the formation of DBP.

In the last part of the research, the influence of VUV on the cellular integrity of two cultured cyanobacterial (*Microcystis Aeruginsoa* and *Anabaena Sp.*) was studied, as well as their cyanotoxin degradation. Disinfection and contaminants degradation was obtained simultaneously. A probe, carbamazepine (CBZ), was used to better discriminate the role of $^{\bullet}OH$ radicals. The degradation of CBZ obtained by VUV exceeded 99%.

Related to future work in this field, the design of a full-scale reactor allowing the use of $UV_{185\,nm}$ where $^{\bullet}OH$ radical are present in a thin layer measuring only a few millimeters will be a great challenge. Improved hydrodynamic design is needed to achieve high oxidation performance using $UV_{185\,nm}$.

Undoubtedly, another a point worth analyzing before applying any process of oxidation of contaminants in drinking water in real scale is the formation of new products or intermediates contaminants. Further studies should address the issue because formation of new products / contaminants that could be even more toxic than the original ones is a possibility.

VUV is a promising technology to be applied in the drinking water industry but there remain significant issues of concern such as the two aforementioned must be addressed before a real scale application.

TABLE OF CONTENTS

LIST OF TABLES

LIST OF FIGURES

LIST OF SYMBOLS AND ACRONYMS

$^{\bullet}$OH	Hydroxyl radical
Ana	*Anabaena Sp.*
ANA-a	*Anatoxin-a*
ANOVA	Analysis of variance
AOM	Algal organic matter
AOP	Advanced oxidation process
AP-A	*Anabaenopeptin-a*
APB	*Anabaenopeptin-b*
BB	Building blocks
BDOC	Biodegradable dissolved carbon
BP	Biopolymers
C	Contaminant concentration
C_0	Initial contaminant concentration
CBR	Collimated beam reactor
CBZ	Carbamazepine
c_{F}	Correction factor
C_{f}	Final concentration
C_{i}	Initial concentration
CYN	Cylindrospermopsin
DBP	Disinfection by-products
d_{F}	Divergence factor
dmMC-LR	[Asp3] Microcystin-LR
dmMC-RR	[Asp3] Microcystin-RR
DNA	Deoxyribonucleic acid
DOC	Dissolved organic carbon
DON	Dissolved organic nitrogen
DWTP	Drinking water treatment plant
E_0	Fluence rate NO EXISTE
EEO	Electrical energy per order
Ex:Em	Pair of excitation-emission wavelengths
FCM	Flow cytometry
FEEM	Fluorescence emission-excitation matrix
FTR	Flow-through reactor
FW	Filtered water

GSM	Geosmin
H	Fluence
H_0	Theoretical or uncorrected fluence
HAA	Haloacetic acid
HAA5	Group of five haloacetic acids
HAB	Harmful algal bloom
HANA-a	Homoanatoxin-a
HMW	High molecular weight
HPLC	High performance liquid chromatography
HPSEC	High performance size exclusion chromatography
HS	Humic substances
k', k''	Rate constants
LC-OCD-ONC	Liquid chromatography-organic carbon detector-organic nitrogen detector
LD_{50}	Lethal dose
LMWac	Low molecular weight organic acids
LMWne	Low molecular weight organic neutral
LOD	Limit of detection
LOQ	Limit of quantification
MA	*Microcystis aeruginosa*
MC-HilR	Microcystin-HilR
MC-HtyR	Microcystin-HtyR
MC-LA	Microcystin-LA
MC-LR	Microcystin-LR
MC-LW	Microcystin-LW
MC-LY	Microcystin-LY
MC-RR	Microcystin-RR
MCtot	Microcystin Total
MC-WR	Microcystin-WR
MC-YR	Microcystin-YR
MIB	2-methylisoborneol
MW	Molecular weight
NOM	Natural organic matter
PARAFAC	Parallel factor analysis
p_F	Petri factor
$R_{\bullet OH,UV}$	Hydroxyl radical exposure per ultraviolet fluence
r_F	Reflection factor

RFU	Relative fluorescence units
RNA	Ribonucleic acid
RW	Raw water
SEC	Size exclusion chromatography
SOM	Self-organizing maps
SUVA	Specific ultraviolet absorbance
SW	Surface water
t	Time
T&O	Taste and odor
THM	Trihalomethanes
TOC	Total organic carbon
TTHM	Total trihalomethanes
UFC	Uniform formation conditions
UFW	Untreated filtered water
UHPLC-MS/MS	Ultra-high performance liquid chromatography coupled to tandem mass spectrometry
UPW	Ultra-pure water
URI	Ultraviolet absorbance ratio index
URW	Untreated raw water
USEPA	United State Environmental Protection Agency
UV	Ultraviolet
$UV_{185\,nm}$	Ultraviolet at the wavelength of 185 nm
$UV_{254\,nm}$	Ultraviolet at the wavelength of 254 nm
UV-A	Ultraviolet light in the range of 314 nm to 400 nm
UVA_{254}	Ultraviolet absorbance at 254 nm
UV-B	Ultraviolet light in the range of 280 nm to 315 nm
UV-C	Vacuum ultraviolet light in the range of 200 nm to 280 nm
UV-LED	Ultraviolet by light emitting diode
V	Volume
VUV	Vacuum ultraviolet
VUVTFW	Vacuum ultraviolet treated filtered water
VUVTRW	Vacuum ultraviolet treated raw water
w_F	Water factor
WHO	World Health Organization
ε	Molar absorption coefficient
Φ	Quantum yield
λ	Wavelength

CHAPTER 1 INTRODUCTION

Access to quality drinking water should be guaranteed for every population, no matter its location. Unfortunately, many small communities experience significant challenges in providing safe drinking water. Insufficient resources and remote location are some of the common problems they face. Approximately 12% of the population of Canada is served by small drinking water systems or private water supplies (instead of large municipal treatment plants) [4]. While microbiological contamination is still the primary concern, disinfection by-products (DBP) formation, seasonal algal toxins and taste and odor (T&O) compounds pose significant risk to public health and represent major issues to be overcome [5].

Nowadays, lake eutrophication has become an important concern around the world [6]. The combination of several factors such as climate change, growth of the population and land use increase algal bloom occurrences. Seasonal algal blooms, usually occur during summer and have a direct impact on drinking water consumers because of the T&O compounds commonly generated during these events. Occasionally, summer recreational activities in a eutrophicated lake must be restricted because of the potential toxicity caused by these blooms [7]. The simple presence of a bloom does not imply toxicity, but it is an indication of possible toxin production.

When the predominant species within a bloom is cyanobacteria, the bloom, called a *cyanobacterial bloom*, can often lead to health concerns as a result of risks related to cyanotoxin production. Even once the bloom has disappeared, some toxins can remain in the water and in sediments [4]. Even though cyanotoxins can be considered as natural contaminants, the fact that the increased number of events is related to anthropic activities suggests that better management of land use at the watershed level would be the key to minimizing their occurrences. Meanwhile, treatment solutions are required to guarantee safe drinking water to the population being served.

Cyanotoxins can roughly be classified into three categories: i) hepatotoxins: microcystins, nodularis and cylindrospermopsins; ii) neurotoxins: anatoxin-a, anatoxina(s), and saxitoxins; and iii) dermatotoxins: lyngbyatoxin-a and aplysiatoxins [8]. Among the most common cyanotoxins found in natural water sources, microcystins are the most frequent. A survey of 227 New Zealand water bodies conducted between 2001 and 2004 revealed that microcystin is the most detected cyanotoxin in that country [9]. While more than 70 variants of microcystins were reported, microcystin-LR (MC-LR) is the most widespread species [8]. Its toxicity is estimated to be 50 µg MC-LR per kilogram bodyweight (lethal dose (LD_{50})). MC-LR is

released during cell death and lysis. Possible human health issues related to the development of this toxin are liver damage, increased risk of cancer and potential damage to the nervous system [10].

When talking about cyanotoxin removal in drinking water treatment, it should be considered that cyanotoxins can be either extracellular (released by the cells and already dissolved in water) or intracellular (within cells). While intracellular toxins can be removed by traditional treatment, removal efficacy is linked to the species of cyanobacteria present in the water. Samples from a full-scale drinking water treatment plant (DWTP) during a cyanobacterial bloom revealed that *Aphanizomenon* cells were poorly coagulated and thus were not retained by the filter. On the other hand, *Microcystis*, *Anabaena* and *Pseudanabaena* cells were removed by clarification and filtration processes [11]. Furthermore, the possibility of cell accumulation within the plant must be considered because a conventional coagulation / sedimentation / filtration treatment may not be efficient for all cells. Active cells could be retained within the plant and start producing toxins at any time [12].

The first treatment strategy in water sources contaminated with cyanobacteria involves the removal of the cells without producing lysis. In this way there is no release of intracellular toxins [13]. However, as mentioned above, cell removal efficiency is a function of the type of cells. Accumulation of improperly coagulated algae cells on the surface of settlers may also pose a risk, as discussed above. These constraints make the selection of an optimal water treatment strategy difficult to define. Westrick et al. (2010) suggest that additional treatment barriers must be implemented [13]. A multi-barrier strategy for intracellular and extracellular cyanotoxins is applied in many drinking water plants. This approach consists of choosing an appropriate intake location, physical treatment to remove cells by coagulation, flotation or settling and filtration, as well as additional treatments to degrade or adsorb extracellular toxins [13].

Among the additional treatments, powdered or granular activated carbon and/or O_3 are common treatment options. All of these add additional costs and complexity to water treatment, a difficult challenge for most small water systems. A simpler treatment option which does not require highly qualified operators for its operation is desirable for these small and remotely located communities. Throughout this project, UV radiation was used at a wavelength of $UV_{185\,nm}$ and $UV_{254\,nm}$ in natural water matrices, with and without cyanobacteria, to assess its efficiency and applicability as a simpler treatment option.

The region of the electromagnetic spectrum of light covered by photons with wavelengths between 10 nm to 200 nm in the UV region is called vacuum UV (VUV). VUV photons are energetic enough to photolyze water molecules, generating strongly and non-selective $^{\bullet}OH$.

By not requiring the addition of chemicals such as H_2O_2 for $^{\bullet}OH$ production, VUV technology is an easy and more environmentally-friendly solution for small and remote communities.

As it is producing $^{\bullet}OH$, it is considered an advanced oxidation process (AOP). An AOP relies on the availability of $^{\bullet}OH$, a highly reactive and non-selective oxidant. Nowadays, the most commonly available AOPs applied in drinking water treatment are [14]: $O_3 + H_2O_2$, UV light + O_3, UV light + H_2O_2, UV light + TiO_2, and different combinations of them.

However, given its non-selective oxidant characteristic, $^{\bullet}OH$ will react with other compounds present in water, such as natural organic matter (NOM), and VUV performance could be negatively affected. NOM is a complex mixture of organic substances in surface waters. Its presence adds color to water and may create aesthetic problems, such as T&O. The NOM fraction originating from algal growth is known as algal organic matter (AOM). The presence of cyanobacteria will increase this fraction. In addition, NOM acts as a reservoir of precursors for the production of disinfectant by-products (DBP) following its reaction with free chlorine.

The $UV_{254\,nm}$ lamps used in disinfection generate a minimum fraction of $UV_{185\,nm}$. When the material that surrounds the lamp (i.e., the sleeve) is made of ultra-pure quartz, the $UV_{185\,nm}$ fraction that reaches the water can be maximized. In this way, disinfection and degradation of contaminants can be targeted in parallel. Despite its interest, the use of VUV by the drinking water industry did not seem initially be practical due to the minimal $UV_{185\,nm}$ penetration length in water. About 90% of $UV_{185\,nm}$ photons are expected to be absorbed, but only in the 0.3 cm layer close to the lamp [15]. Nevertheless, ongoing research shows encouraging results, and VUV's application in small-scale water treatment plants appears promising [16, 17]. In line with this trend, this project tested VUV technology in natural water matrices regularly affected in differing degrees by cyanobacteria in order to assess its efficiency and applicability. To the best of our knowledge, there is no data published on this topic. As the problem of water sources impacted by cyanobacteria is increasing around the world, the need to find a simple and ecological treatment has become imperative. We hope the results of this research will contribute to assessing a possible solution.

We focused on the application of VUV with 185 nm energy and compared the performance of this technology and the characteristics of the treated water with that of 254 nm energy. This will provide key insights into this field, particularly as applied to natural waters, and strategies for the development of small and remote DWTP.

1.1 Objectives

The viability of the VUV process needs to be assessed in terms of its performance as well as its impact on water source quality (background natural organic matter (NOM), algal organic matter (AOM) and inorganic solutes), particulary in water sources affected by cyanobacterial blooms. This project encompasses for the first time the application of VUV for cyanobacterial inactivation and cyanotoxins and T&O degradation in natural water sources contaminated with algal blooms. We evaluate the influence of NOM, AOM and inorganic solutes naturally present in the water sources on VUV performance. On this basis, the following objectives are outlined:

i. Assess cyanotoxins and T&O degradation by VUV in natural waters (Article 1)

ii. Understand the role of background NOM and AOM on VUV performance and disinfection by-products (DBP) formation (Article 2)

iii. Confirm the possibility of simultaneously disinfecting and degrading organic trace contaminants with VUV (Article 3)

1.2 Hypothesis

Each objective has an associated hypothesis:

i. Cyanotoxin and T&O degradation from natural matrix water can be achieved by VUV (Article 1)

ii. AOM has a greater impact on VUV performance than NOM (Article 2)

iii. VUV can disinfect and degrade organic trace contaminants simultaneously (Article 3)

CHAPTER 2 LITERATURE REVIEW

2.1 Cyanobacterial blooms

Cyanobacteria, commonly known as "blue-green algae", are the Earth's oldest oxygenic photoautotrophs and have had major impacts on shaping its biosphere. They are photosynthetic prokaryotes with the ability to synthesize Chlorophyll-a. This chlorophyll production capacity gives them the popular name of "algae" when they actually are bacteria. Because of their long presence on Earth, they have a long evolutionary history that has enabled them to adapt several changes. Some of these include geochemical and climatic. Nowadays, anthropogenic modifications of aquatic environments, eutrophication, water diversions, withdrawals, and salinization are the most usual changes that this microorganism faces [18, 19].

During the Precambrian era, cyanobacteria's proliferation caused a significant modification to the biosphere. The evolution of terrestrial plant and animal life took place thanks to the fact that anoxic biosphere was modified by the concentration of O_2. Cyanobacteria played a key role at that time because it is presumed that they were responsible for this crucial development of life on Earth [19]. The reason why cyanobacteria population is a successful one is complex and it can be summarized in a short list. First, the optimum growing temperature, at least for many cyanobacteria, is higher than for most eukaryotic algae. This is the reason why they can survive warmer climates. Second, they can support water stress for a long period. Also, cyanobacteria are among the most successful organisms in highly saline environments (for example *Anabaena sp.* was found in the Baltic Sea [20]) [21]. Many genera have the ability to fix atmospheric nitrogen (N_2, an anaerobic process), while they can store phosphorus (P) and sequester iron (Fe) and a range of essential trace metals. These traits have enabled them to exploit both nutrient-scarce and nutrient-rich diverse terrestrial and aquatic environments worldwide [18].

At present, this ancestral microorganism has become a huge concern around the world since dense populations of freshwater cyanobacteria forming water blooms have increased. As this microorganism is able to produce a wide variety of toxins that cause animal poisonings and human health risks, their presence in water sources is a major problem. While some of the factors leading to the formation of such blooms are well understood, some others remain unknown. The toxicity of these blooms increases the awareness and concern of governmental agencies in charge of water management. Currently, the biggest challenge relates to the ability to predict the possible toxicity of a bloom [21]. How environmental factors impact cyanotoxin production is the subject of ongoing research, but nutrient (N, P and trace metals) supply

rates, light, temperature, oxidative stressors, interactions with other biota (bacteria, viruses and animal grazers), and most likely, the combined effects of these factors are involved [18].

Cyanotoxin becomes a health concern when a cyanobacteria bloom occurs in a water source. So, what is a bloom? There is not an exact definition for the term "bloom". Generally, a bloom refers to a phytoplankton biomass significantly higher than the water body average. Frequently, one or two species are dominant within a bloom, for instance, cyanobacterial bloom, diatom bloom [22]. A bloom usually takes place during the warm season, from early spring to late summer. As a consequence of a bloom, the water body's turbidity and color change [23].

Events named as red tides in the past are now grouped under the descriptor og harmful algal blooms (HABs) [24]. At this point, it is necessary to differentiate two types of HABs. One type of HABs includes toxins or harmful metabolites, such as toxins linked to wildlife death or human seafood poisonings. The other type of HABs that can be developed are nontoxic, but can still cause damage, even without being toxic. Sometimes, in the presence of small blooms a high algal toxin concentration is produced, while other times, nontoxic HAB causes highly invasive damage: an immense biomass developing, leading to foams or scums, the depletion of oxygen as blooms decay, or the destruction of habitat for fish or shellfish by shading of submerged vegetation [24].

In reference to cyanobacterial blooms, the concern is greater in the presence of a toxic bloom, especially if it occurs in a body of water that serves as a source of drinking water. The impossibility to predict the toxicity of a cyanobacterial HAB, is the focus of many investigations [25–27]. Cyanobacteria can bloom under low light availability by taking advantage of periods between episodic sediment loading events when the water clears, or by using mechanisms for buoyancy regulation to position themselves near the water surface [24]. Many cyanobacterial genera have optimal growth rates and bloom potentials at relatively high water temperatures; hence, global warming plays a key role in their expansion and persistence [19].

Regarding safe management of recreational water affected by cyanobacterial blooms the World Health Organization (WHO) proposed in 2003 the following guidelines based on the probability of adverse health effects [28]:

i. Low probability, when the concentration of cells is bellow 20,000 cells mL^{-1} or 10 µg Chlorophyll-a L^{-1}

ii. Moderate probability, when the concentration of cells is between 20,000 cells mL^{-1} to 100,000 cells mL^{-1} or between 10 µg to 50 µg Chlorophyll-a L^{-1}

iii. High probability, when cyanobacterial scum formation in areas where whole body contact and/or risk of ingestion/aspiration occur.

2.1.1 Cyanotoxins

Cyanobacteria are photosynthetic microorganisms found in diverse environments including oceans, freshwater, bare rock, and soil. They appear to be unable to colonize, invade, and grow in human or animal hosts to cause disease. In order to realize the photosynthesis, water serves as electron donor. Cyanobacteria can be found in water columns (planktonic), aggregated on the water surface (metaphytic), attached to other algae, cyanobacteria or macrophytes (epiphytic) and attached to substrates (benthic) [20]. Most of them produce the phycobilin pigment, phycocyanin, which gives the cells a bluish color when they are present in sufficiently high concentration, and is responsible for the popular "blue-green algae" name. In some cases the red accessory pigment, phycoerythrin, is formed as well [29].

This microorganism is able to produce a wide variety of toxins that cause animal poisonings and human health risk. They also produce a large number of bioactive compounds that have potential as drug leads and cell reagents [30]. Cyanotoxins can be classified as follow [8]:

i. Hepatotoxins: microcystins, nodularis, and cylindrospermopsins

ii. Neurotoxins: anatoxin-a, anatoxin-a(s), and saxitoxins

iii. Dermatotoxins: lyngbyatoxin-a and aplysiatoxins

The hepatotoxins are produced by various species (*Microcystis, Anabaena, Oscillatoria, Nodularia, Nostoc, Cylindrospermopsis*, and *Umezakia*) and most of them are microcystins [18]. More than 80 different structural variants of microcystins have been identified to date [31]. Among them, microcystin-LR (MC-LR) is the most widespread and one of the most toxic, with a lethal dose (LD_{50}) estimated to be 50 µg MC-LR per kilogram bodyweight. Table 2.1 shows a list with the main cyanotoxins. A survey conducted by Wood et al. in 227 different New Zealand water bodies between 2001 and 2004, verified that microcystin is the most detected cyanotoxin in that country [9]. Table 2.2 shows LD_{50}values for several cyanotoxin.

According to the WHO, there are insufficient data to derive a guideline value for cyanobacterial toxins other than MC-LR. The guideline value for total MC-LR (free plus cell-bound) is $1\,\mu g\,L^{-1}$ in drinking water. Due to the limited available database, this value is provisional [32]. In Canada, the maximum acceptable concentration (MCA) for the cyanobacterial toxin microcystin-LR in drinking water is $1.5\,\mu g\,L^{-1}$. Quebec has adopted this MCA from *Guidelines for Canadian Drinking Water Quality* produced by Heath Canada.

Potential risk for human exposure varies from short-term adverse health outcomes (skin irritations, gastrointestinal illness) to long-term illness with some cyanobacterial species [33]. This toxin is bioaccumulative and it has been found in different species used by human seafood consumption, such as mussels, crayfish, and fish. Therefore, it is important to monitor microcystin during and after the occurrence of cyanobacterial blooms [34].

2.1.2 Cyanobacteria within drinking water treatment plant

Extensive research has been performed on drinking water treatment plants (DWTP) fed by source contaminated with cyanobacterial blooms. Table 2.3 summarizes cyanobacterial species reported on DWTP from different studies.

In 2012, Zamyadi et al. analyzed bloom events during three consecutive years (2008, 2009, and 2010) breaking through a DWTP, located in the Missisquoi Bay on Lake Champlain (southern Quebec, Canada). This work was conducted based on two main objectives:

i. to estimate the breakthrough and accumulation of toxic cyanobacteria in water, scums and sludge inside a DWTP

ii. to determine whether chlorination can be an efficient barrier to the prevention of cyanotoxin breakthrough in drinking water

A high cyanobacterial cell numbers and total microcystins concentrations were measured at the clarifiers of the DWTP. Even for the chlorinated drinking water, microcystins was found in high concentration. Based on these results, authors suggested that natural bloom samples are more resistant than cultured cells [39].

Studying two different DWTP fed by the Richelieu River (southern Quebec, Canada) with low cyanobacterial occurrences, the same authors affirmed that pre-ozonation of raw water helped with the removal of cells in the clarification process. Samples from clarification and

Table 2.1: Cyanobacterial toxins (Adapted from [1])

Classification	Toxin	Toxigenic genera
Hepatotoxins	Microcystins	*Microcystis, Anabaena, Nostoc, Anabaenopsis, Planktothrix, Oscillatoria, Hapalosiphon*
	Nodularins	*Nodularia, Theonella* (spongecontaining cyanobacterial symbionts)
	Cylindrospermopsins	*Cylindrospermopsis, Aphanizomenon, Umezakia, Anabaena, Raphidiopsis*
Neurotoxins	Anatoxin-a (including homoanotoxin-a)	*Anabaena, Oscillatoria, Phormidium, Aphanizomenon, Rhaphidiopsis*
	Anatoxin-a(s)	*Anabaena*
	Saxitoxins	*Aphanizomenon, Anabaena, Lyngbya, Planktothrix Cylindrospermopsis*
Dermatotoxins and cytotoxins	Lyngbyatoxin-a	*Lyngbya, Schizothrix, Oscillatoria*
	Aplysiatoxins	*Lyngbya, Schizothrix, Oscillatoria*

filtration basin were analyzed in order to determine presence of cyanobacteria. *Microcystis* was the dominant specie in the clarification basin while *Gloetrichia* dominated the filtration basins. In this particular case, the low concentration and toxicity of the cells at the water intake studied, did not contribute significantly to the DBP production. Nevertheless, the potential DBP production has to be determined before the implementation of a pre-ozonation process [12].

The breakthrough of cyanobacteria in well water following bank filtration was evidenced and reported by Pazouki et al. (2016). The system under study comprises two artificial lakes located in Southern Quebec (Canada), near Lake of Two Mountains. The bank filtration system consists of wells that pump water through the bank from the lakes. The presence of cyanobacteria was monitored by using Phycocyanin. Causes of cyanobacteria passing through filters were associated to retention time. Lake travel times shorter than one week were found to facilitate the breakthrough. The authors emphasized on having an intensive monitoring system not only during bloom events, but throughout the year [40]. They based this recommendation on analyzing samples taken during winter season, where cyanobacteria accumulate within bank filters, considering the 1.7 RFU threshold recommended by Bartram et al. (1999) [41]. This limit corresponds to an Alert Level 1 associated to a total cyanobacterial biovolume of $0.2\,\mathrm{mm^3\,L^{-1}}$.

From August to November 2017 Almuhtaram et al 2018 sampled intakes of the four plants: Lake Erie, Lake Ontario, the Bay of Quinte in Lake Ontario, an inland reservoir. Authors reported cell accumulation and presence of cyanotoxins across the treatment trains of four plants. Even when low cell influx was measured (under $1000\,\mathrm{cells\,mL^{-1}}$) significant cell accumulations (over $1\times10^{-5}\,\mathrm{cells\,mL^{-1}}$) were observed in clarifier sludge and filter backwash samples. As a conclusion, they affirmed that DWTP receiving a low influx of cells can be at

Table 2.2: Cyanobacteria toxic LD_{50}(Adapted from [2, 3])

Classification	**Toxin**	**Toxigenic genera**	**LD_{50}**
Hepatotoxins	Microcystins	*Anabaena flos-aquae*	50
		Microcystis, Anabaena, Nostoc, Planktothrix, Anabaenopsis, Hapalosiphon	25-1000
		Oscillatoria agardhii var. isothrix	300-500
		Oscillatoria agardhii	500-1000
	Nodularins	*Nodularia spumigena*	30-50
	Cyanoginosins	*Microcystis aeruginosa*	50
Neurotoxins	Anatoxin-a	*Anabaena flos-aquae*	200-250
	Anatoxin-a(s)	*Anabaena flos-aquae*	20-40
	Aphantoxin	*Aphanizomenon flos-aquae*	10
	Saxitoxins	*Aphanizomenon, Planktothrix, Anabaena, Cylindrospermopsis and Lyngbya*	10-30

risk of toxic cyanobacterial accumulation. However, the absence of a bloom at the drinking water source does not imply absence of risk [42].

The above review provides an excellent source of information which demonstrates that cyanobacterial bloom persists within water treatment systems. As suggested by Bai et al. (2019), the key to cyanobacterial treatment is to achieve cell deactivation and cyanotoxin degradation without causing lysis [43]. In this way, the risk associated with the accumulation within the plant is minimized.

2.2 Natural organic matter

Natural organic matter (NOM) is a complex mix of organic substances present in fresh water, especially in surface water. The origin of NOM could be either autochthonous, within a water body, or allochthonous, generated from an external source and transported to the water body [44]. Its presence gives color to water inducing aesthetic problems, such as taste and odors. One of the main problems with NOM is the ability to produce disinfectant by-products (DBP) by reacting with oxidant and disinfectant agents. Moreover, it is considered a source of biofilm growth in distribution system, decreases the effectiveness of UV disinfection, increases the coagulant demand, induce fouling of GAC absorbers and membranes [44].

Related to water affinity, NOM is divided in two categories: hydrophobic and hydrophilic [40]. The hydrophobic fraction, so-called high molecular weight (HMW) represents the major fraction of NOM, with approximately 50% of the DOC. Hydrophobic fraction is described as humic substances and it is considered to be mainly responsible of DBP production [45, 46]. On the other hand, the hydrophilic fraction, referred as low molecular weight (LMW), Conventional water treatment seems to be less efficient in LMW removal than HML removal [46].

The concern about DBP has increased in the last decades due to their anticipated negative health effects. As the detection methods improve new components are discovered and smaller detection limits are reached [47]. In 1974, Rook reported the formation of trihalomethanes (THM) in water disinfection for the first time. THM form when chlorine or bromide reacts

Table 2.3: Cyanobacterial species found in DWTP

Species	Location within DWTP	Reference
Microcystis sp. and *Anabaena sp.*	Full scale sludge bed clarifier	[35, 36]
Aphanizomenon sp. and *Aphanothece sp.*	Scums over the clarifiers, dual sand-anthracite filter, and post chlorination	[35, 36]
Microcystis Gloetrichia	Clarification and filtration basins	[12]
Oscilatatoria sp., *Psedanabaena sp.* and *Lyngbya sp.*	Flocculation basin, surface of clarifiers, and surface of filters	[37]
Oscillatoria and *Phormidium*	Biofilm of the sedimentation basin walls	[38]
Lyngbya	Walls of overflow weirs and troughs of the sedimentation basin and sedimentation basin scum	[38]

with organic compounds in water. Here lies the importance of removing NOM previous to disinfection [48]. Two years later, a national survey conducted by the US Environmental Protection Agency (USEPA) showed ubiquitous presence of THMs and DBP in chlorinated drinking water [49]. Also in 1976, results published by the US National Cancer Institute proved the relationship between chloroform and cancer in laboratory animals. Consequently, major problems linked to public health entered the agenda [48–50].

The NOM fraction from algal growth is known as algal organic matter (AOM). AOM consists mainly of LMW components and it is composed of intracellular organic matter (IOM) and extracellular organic matter (EOM) [51]. EOM is the result of metabolic activity of cells during exponential and stationary growth phases, while IOM can be released in the aquatic environment following cell lysis. AOM could be produced by several processes [52]:

i. through extracellular release in response to low nutrient stress or other stressful conditions

ii. invasion by bacteria or virus

iii. through disruption and decay of algal cells

iv. release from algae species under normal conditions

AOM has a different character than allochtonous NOM [53]. In order to minimize DBP formation and avoid cyanotoxin breakthrough to finished drinking water, it is useful to distinguish AOM from other background NOM to establish an appropriate water treatment strategy. Thus, distinguishing AOM from the NOM background present in raw water could help to establish an appropriate water treatment strategy [53].

2.2.1 Algal organic matter from cyanobacteria

Henderson et al. (2008) characterized four algae species: *Chlorella vulgaris*, a green algae; *Microcystis aeruginosa*, a cyanobacteria and two diatoms *Asterionella formosa* and *Melosira sp.* by measuring DOC, specific UV absorbance (SUVA), zeta potential, charge density, hydrophobicity, protein and carbohydrate content, molecular weight and fluorescence. According with their results, all AOM was predominantly hydrophilic with low SUVA. *Microcystis aeruginosa* SUVA values range from $0.48\,\mathrm{L\,m^{-1}\,mg^{-1}}$ to $1.65\,\mathrm{L\,m^{-1}\,mg^{-1}}$ [53]. These results are consistent with Wang et al. (2009) who affirmed that hydrophobic materials with a HMW were mainly from allochthonous origin [54]. AOM was reported with negative zeta potential

values in the range pH 2–10, while lower charge density was related to higher hydrophobicity. The authors concluded that AOM characteristics differ from NOM [53].

Leloup et al. (2013) performed a characterization in two cyanobacteria: *Euglena gracilis* and *Microcystis aeruginosa*. The AOM characterization was carried out by DOC, XAD fractionation and SUVA analyses. Although AOM was found to be mainly hydrophilic, it became more hydrophobic over the time [55]. The periodical character of algal blooms may cause impacts on water sources because they have a significant contribution to organic matter. In fact, an increase of NOM hydrophilic content and a decrease of SUVA index were determined. The situation could be aggravated considering that organic matter accumulates.

The authors concluded that AOM characteristics showed a high dependency on growth phase and species. They also declare that the evolution of the organic matter produced by a phytoplankton bloom does not stop once the bloom has collapsed. In agreement with Henderson et al (2008), the authors affirmed that AOM properties are very different when compared to those of NOM [53, 55]. Villacorte et al. (2015) tested three algae (*Alexandrium tamarense*, a dinoglafellate; *Chaetoceros affinis*,a diatom and *Microcystis sp.* a cyanobacteria) to evaluate membrane fouling. The main conclusion of the work was that during algal blooms AOM composition; size distribution and physico-chemical characteristic (stickiness) may dictate severity of fouling in membrane [52]. However, there is no reported evidence of similar behaviour in a natural bloom.

Khan et al. (2019) applied fluorescence emission-excitation matrix (FEEM) and PARAllel FACtor analysis (PARAFAC) to investigate the possibility of using fluorescence to characterise the AOM released by cyanobacterial and algal species. they used (*Dolichospermum circinalis, Cylindrospermopsis raciborskii*, four strains of *Microcystis aeruginosa* and algal *Chlorella vulgaris*). They observed that certain wavelengths could help for AOM monitoring in conjunction with cell pigments. For example, the fluorescence of amino acid-like material at Ex:Em = 290:345 nm dominated in the AOM originating from *Chlorella vulgaris*, while that of *Microcystis aeruginosa* was dominated by fluorescence at Ex:Em = 355:475 nm (previously been associated only with terrestrially delivered substances). They proposed that fluorophores typically associated with "terrestrially-derived or humic-like" fluorescence (Ex:Em = 335:438; Ex:Em = 355:475 and Ex:Em = 300:390) can also be produced by microorganisms [56]. Henderson et al. (2008) reported similar tendency. They found that tryptophan-like rather than humic/fulvic acid-like fluorescence dominated. During the transition to the stationary phase they found that the excitation wavelengths related to tryptophan-like (protein-like) decreased. Assuming that the sample condition did not change (temperature and pH remain unchanged) they related that decrease to culture age. In relationship with

AOM fluorescence from *Microcystis aeruginosa*, they affirmed that it was similar to that obtained for cyanobacteria in previous studies. However, additional fluorescence was detected in locations attributable to humic/fulvic-like [57].

2.2.2 Natural organic matter characterization

The significant variety of compounds present in NOM makes impractical the determination of its exact composition. Therefore, there exists a wide range of techniques used to retrieve different parameters depending on their measurement complexity. There are denominated bulk parameters such as TOC, DOC, biodegradable dissolved organic carbon (BDOC), assimilable organic carbon (AOC), ultraviolet and visible UV-Vis absorption spectroscopy, UVA absorbance, and specific UV-absorbance (SUVA), are used to determine the amount of NOM within a sample [14]. These parameters are simple to measure and provide a general idea of what is present in the water. On the other hand, numerous methods are currently available for a more profound characterization, for example: resin adsorption, size exclusion chromatography (SEC), nuclear magnetic resonance (NMR) spectroscopy, and fluorescence spectroscopy. Methods such as pyrolysis gas chromatography-mass spectrometry (Py-GC–MS), multidimensional NMR techniques, and Fourier transform ion cyclotron resonance mass spectrometry (FTICR-MS) allow to determine the NOM structures more precisely [46].

Indubitably, the availability of techniques to measure NOM is numerous. The main question is to find a combination of these techniques that is accurate enough to aid the decision-makers during the treatment plant operation. Additionally, the chosen technique should not require considerable investments in equipment or highly trained personnel. For example, Her et al. (2008) used ultraviolet absorbance ratio index (URI = UVA_{210}/UVA_{254}) plus high performance size exclusion chromatography (HPSEC) to characterize NOM. Authors assert that the method is simple and can be easily applied to the characterization of bulk water samples. However, they also recognize that URI results obtained on their experiment contradict SUVA measurements [58]. Consequently, the verification of this contradiction is required in order to ensure an accurate NOM characterization. In contrast, Villacorte et al. (2015) have performed an excellent NOM characterization by using six different techniques. This characterization has an invaluable contribution in the academic field because it allows thoroughly understanding the NOM composition in the three studied species [52]. However, it is an impracticable combination to carry out in a water treatment plant, as it requires a variety of equipment as well as specialized technical support. Once more, an accessible characterization procedure should be found in order to help water treatment suppliers, especially

small community's suppliers.

2.3 Oxidation processes and cyanobacterial blooms

Since cyanobacterial blooms affect drinking water sources more frequently, the need to treat properly the affected water has become a challenge for many DWTPs. Conventional drinking water treatment (coagulation/settling/filtration), under appropriate coagulation conditions, can be effective for removing cells without provoking lysis but offers limited control of extracellular cyanotoxin and T&O [59, 60]. Cyanotoxins are formed within the cyanobacterial cells and typically remain as intracellular toxin. When the cell lysis occurs due to age or an external stress on the cells toxins are released (extracellular toxins). Ideally, an effective treatment against both intra and extracellular toxins should be applied [61].

In this way the need arises to apply technologies that are efficient in the removal of intracellular and extracellular cyanotoxins as well as T&O components. Lately, different technologies have been tested at various scales (laboratory and pilot and even some are already applied in DWTP) to solve this problem. Among the available technologies we can cite: photocatalysis, membrane technology, ozonolysis, chlorination. In the following section focus on oxidation processes will be discussed.

The main goal of oxidation is the reduction of harmless inorganic or organic species found in water. Ideally, oxidation should convert toxic compounds to carbon dioxide and mineral acids and reduce T&O compounds [14]. Other reason why oxidation is applied for disinfection. The presence of pathogens in drinking water is responsible for numerous diseases in consumers.

There are three types of oxidation processes: conventional oxidation processes, oxidation processes carried out at elevated temperatures and/or pressure, advanced oxidation processes (AOP). The most common conventional oxidation processes applied during drinking water treatment are: chlorine (Cl_2), chlorine dioxide (ClO_2), chloramine (NH_2Cl), and permanganate (MnO_4). These four oxidants will be developed in the next section.

When cyanotoxin are the target organic compound to oxidize the biggest drawback is that a single oxidant is not effective for all possible cyanotoxins that can be produced in a bloom. Rodriguez et al. (2007) affirm that O_3 can effectively oxidize microcystin-LR (MC-LR), cylindrospermopsin (CYN), and anatoxin-a (ANTX). However, special attention must be paid in relation to bromate DBP formation when O_3 is applied. MnO_4 is efficient for ANTZ and MC-LR degradation but not cylindrospermopsin or saxitoxin [62, 63]. Although Cl_2 is effective again CYN and MC-LR [62].

2.3.1 Chlorination and chloramination

Cl_2 is an excellent biocide because of the strong oxidizing characteristics of free chlorine. Free chlorine will destroy bacterial cell membranes and oxidizing enzymes and proteins. Free chlorine consists of molecular Cl_2, hypochlorous acid ($HOCl^-$), and hypochlorite ion (OCl^-). Besides being a very good disinfectant, chlorine is also a good oxidant [64]. The reduction half reaction for chlorine at 25 °C and its dissociation products $HOCl^-$ and OCl^- are given by the following reactions:

$$Cl_2(aq) + 2\,e^- \rightleftarrows 2\,Cl^-\,, \quad E^0_{aq} = 1.396V \tag{2.1a}$$

$$2HOCl + 2\,H^+ + 2\,e^- \rightleftarrows Cl_2(aq) + 2\,H_2O\,, \quad E^0_{aq} = 1.61V \tag{2.1b}$$

$$2HOCl + H^+ + 2\,e^- \rightleftarrows Cl^- + H_2O\,, \quad E^0_{aq} = 1.50V \tag{2.1c}$$

$$OCl^- + H_2O + 2\,e^- \rightleftarrows Cl^- + 2\,OH^-\,, \quad E^0_{aq} = 0.90V\,. \tag{2.1d}$$

Zamyadi et al. (2013) evaluated toxin release and oxidation from of *Microcystis aeruginosa* by Cl_2, along with DBP formation. Dose applied range from $2\,mg\,L^{-1}$ to $10\,mg\,L^{-1}$ caused lysis and oxidation of toxins produces by *Microcystis aeruginosa*. They observed 76% reduction of cells [65]. These results are very important because *Microcystis aeruginosa* is responsible of microcystin, the most common cyanotoxin found in fresh water [9] and upon which most of the regulations are based.

Chloramines are formed when ammonia is added to water in presence of Cl_2. The most common form of chloramines is monochloramine. In lower concentration, dichloramine, trichloramine, and organic chloramines are also produced. Monochloramine has been used as a drinking water disinfectant for more than 90 years because it has been shown to be an effective disinfectant. It is applied in addition to chlorination and it helps to maintain water quality in the pipes and help to minimize DBP formation [66]. Formation of the three chloramine species can be described by the following reactions:

$$HOCl + NH_3 \rightleftarrows NH_2Cl(\text{monochloramine}) + H_2O, \tag{2.2a}$$

$$HOCl + NH_2Cl \rightleftarrows NHCl_2(\text{dichloramine}) + H_2O, \tag{2.2b}$$

$$HOCl + NHCl_2 \rightleftarrows NCl_3(\text{trichloramine}) + H_2O\,. \tag{2.2c}$$

Chloramines are frequently used to provide residual disinfectant because they are poor oxi-

dants. Its application is usually recommended when it is necessary to minimize DBP. However, chloroamine and chlorine dioxide are not effective treatment barriers for microcystin, CYN, ANTX, and saxitoxins. If a DWTP is using chlorine dioxide or chloramines as disinfectant in order to reduce DBP formation then it is possible that cyanotoxin inactivation is not complete [13].

2.3.2 Chlorine Dioxide

The main advantage of oxidation by ClO_2 is that does not produce THM or HAA associates with free chlorine [14]. The reduction half reaction for chlorine dioxide at 25 °C is given by the reaction [14]:

$$ClO_2(g) + 2\,H_2O + 5\,e^- \longrightarrow Cl^- + 4\,OH^-\,, \quad E^0_{red} = 0.799\,V\,. \tag{2.3}$$

However, ClO_2 produce chlorite ($ClO_2{}^-$) and chlorate ($ClO_3{}^-$) ions as by-products. Regulation related to those ions limited ClO_2 doses. The formation of ($ClO_2{}^-$) and ($ClO_3{}^-$) is given by the reaction [14]:

$$2\,ClO_2 + 2\,OH^- \longrightarrow ClO_2{}^- + ClO_3{}^- + H_2O\,. \tag{2.4}$$

2.3.3 Permanganate

Permanganate (MnO_4) is used for T&O control since 1960s. It is a very versatile oxidant that was well accepted on DWTP since that date. Under acidic conditions the principal reduction half reactions are [14]:

$$MnO_4{}^- + 4\,H^+ + 3\,e^- \rightleftarrows MnO_2(s) + 2\,H_2O\,, \quad E^0_{red} = 1.680\,V\,, \tag{2.5a}$$
$$MnO_4{}^- + 8\,H^+ + 5\,e^- \rightleftarrows Mn^{2+} + 4\,H_2O\,, \quad E^0_{red} = 1.510\,V\,. \tag{2.5b}$$
$$\tag{2.5c}$$

Under alkaline conditions the corresponding reduction half reaction is:

$$MnO_4{}^- + 2\,H_2O + 3\,e^- \rightleftarrows MnO_2(s) + 4\,OH^-\,, \quad E^0_{red} = 0.590\,V\,. \tag{2.6}$$

Rodriguez et al (2007) applied MnO_4 to oxidize microcystins below regulated limit ($1\,\mu g\,L^{-1}$)

with MnO_4 dose ranging from $1.00\,mg\,L^{-1}$ to $1.25\,mg\,L^{-1}$ [67].

2.4 Advanced oxidation process and cyanotoxins

Processes where the concentration of hydroxyl radical ($^{\bullet}OH$) is enough to modify the quality of water are considered advanced oxidation process (AOP) [80]. AOP consist on a complex chain-reaction mechanism that involve intermediate radical species [81]. The "$^{\bullet}$" presiding OH symbolize that the outer electron orbital has an unpaired electron. $^{\bullet}OH$ is a highly reactive and non-selective oxidant. The nonselective reactivity characteristic of $^{\bullet}OH$ is based on the broad range of values that the rate constant (from $107\,M^{-1}\,s^{-1}$ to $1010\,M^{-1}\,s^{-1}$). While several components, such as atrazine, benzene, geosmin, trichloroethene and tetrachloroethene do not react in presence on O_3 they are oxidized by $^{\bullet}OH$ [81]. Nowadays, the available AOP applied to drinking water treatment are [14]: O_3 + H_2O_2, UV light and O_3, UV light and H_2O_2, UV light and TiO_2 and combinations of the previous technologies listed.

The main reason why AOP are practicable in DWTP stems from the possibility to generate $^{\bullet}OH$ at ambient conditions of temperature and pressure, unlike other oxidation processes also producing $^{\bullet}OH$ [80]. Park et al. (2018) analized the effectiveness of several AOP in MC-LR removal. They applied photo-Fenton-like process (UV-C/FeIII/H_2O_2) and achived 80% of MC-LR removal after 15 min [68]. Bai et al. (2019) applied plasma reactor to produce $^{\bullet}OH$ among other radicals (H_2O_2, $HO_2{}^-$, $O_2{}^-$, $O_3{}^-$, HO_3) that they call total reactive oxidants in a DWTP. They compared $^{\bullet}OH$ and NaClO performance form cyanobacterial inactivation as well cyanotoxins degradation. DBP formation was also analyzed. Regarding DBP, authors affirm that both oxidants produce DBP under regulated limits. In relation to cell inactivation and degradation of MC-LR, $^{\bullet}OH$ proved to be much more effective than NaClO [43].

Kumar et al. (2018) suggest that efficient cyanotoxin removal with reduced toxicity level could be achieved with a hybrid technique such as photocatalytic, ozonation and chlorination assisted by UV and/or peroxides [61].

2.4.1 Ozone

Ozonolysis has two mechanisms of oxidation, O_3 and $^{\bullet}OH$. O_3 reacts with alkene groups, activated aromatic and neutral amine functional groups. On the other hand, $^{\bullet}OH$ based in its non-selective oxidation characteristic attacks carbon-hydrogen bonds in organic molecules [69]. MC-LR, CYN and ANTX have second order rate constants (k_{O_3}) at pH 8 ($4.15\times10^5 \pm 0.1\times10^5$ $M^{-1}\,s^{-1}$, 3.4×10^5 $M^{-1}\,s^{-1}$, 6.4×10^4 $M^{-1}\,s^{-1}$ respectively) [70]. Coral et al. (2013) preoxydaized *Microcystis aeruginosa* and *Anabaena flos-aquae* with O_3 and analyzed cell

integrity as well DBP formation. An immediately cell membrane damage and not significant cell lysis were observed at the conditions tested. However, DBP increase considerably [7]. Nonetheless O_3 is not effective for saxitoxin degradation [71].

2.4.2 UV, UV+H_2O_2, UV+O_3 and UV+Cl_2

The UV region of the spectrum can be decomposed into four different zones (Figure 2.1): UV-A (314 nm to 400 nm), UV-B (280 nm to 315 nm), UV-C (200 nm to 280 nm) and vacuum UV (VUV, 100 nm to 200 nm). The UV light from regions UV-B and UV-C has a germicidial effect when acting on microorganisms, and its combination with other disinfection techniques offer more advantages for water treatment. Although is feasible to use the UV-A range, it would require longer exposure times to reach significant disinfection efficiencies. The two main wavelengths used in UV disinfection lie in the VUV (185 nm) and UV-C (254 nm) regions.

While chemical disinfectants such as Cl_2 and O_3 produce inactivation of microorganisms through cellular damage, UV disinfects by oxidation mechanisms, causing damage directly to the DNA and RNA upon absorption of UV-C light. Thus, UV disinfection affects the cells turning their chances of reproduction null. The absorption of electromagnetic radiation also induces photochemical reactions to occur, among them photolysis. Molecules inside the water to treat can absorb light with discrete levels of energy (photons) and are responsible for the photochemical change [72].

The efficiency of photolysis for degraded contaminants is defined through two main quantities:

i. the molar absorption coefficient (ε [$M^{-1}\,cm^{-1}$]), which determines the strength of the absorption of each chemical species at a certain wavelength

ii. the quantum yield (Φ), which is the efficiency of the absorbed energy for causing a photochemical degradation reaction.

He et. al (2015) compared the degradation of common mycrocystins (MC-LR, MC-RR, MC-YR and MC-LA) using UV disinfection at 254 nm only, and the same UV combined with different oxidants separately (H_2O_2, ${S_2O_8}^{2-}$ and ${HSO_5}^{-}$). They observed an improvement in the degradation efficiency with the addition of oxidants [73].

MC-LR removal efficiencies of 94% in surface waters with UV-C/H_2O_2 were reported by He et al (2012). They showed that by using higher H_2O_2 concentrations, increases the removal efficiency of MC-LR but with significant $^{\bullet}OH$ scavenging by the H_2O_2 [74].

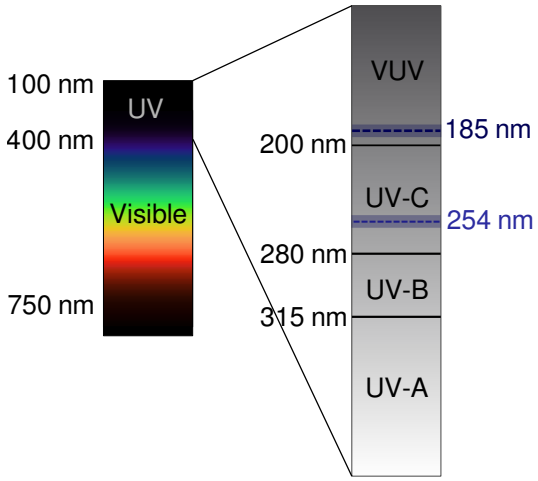

Figure 2.1: Ultraviolet-near infrared electromagnetic spectrum of light. The detail on the right shows the discrimination of the UV region into UV-A (314 nm to 400 nm), UV-B (280 nm to 315 nm), UV-C (200 nm to 280 nm) and vacuum UV (VUV, 100 nm to 200 nm). The two main wavelengths used in water treatment (185 nm and 254 nm) are depicted inside their corresponding regions.

Liu et al. (2010) used a two steps disinfection process (UV/O_3) where they applied first a UV process, with a consecutive ozonation. They compared this process with other three (O_3, UV, and $UV+O_3$) and found better performance for decreasing the concentration and toxicity of MC-LR. They also reported significant transformation of micropollutants and NOM into moieties unfavorable for O_3 decomposition, when using UV treatment [75].

Analysis on the performance of UV combined with Cl_2 showed efficiencies achieving a 92.5% reduction of MC-LR, and enhanced degradation and reduced toxicity compared to the UV only and the Cl_2 only treatments, due to the presence of $^{\bullet}OH$ and reactive Cl_2 species ($Cl_2^{\bullet -}$, $ClO^{\bullet}$). Increasing the chlorine concentration (lowering the pH) favored MC-LR removal [76].

UV/Cl_2 preoxydation process was demonstrated to be responsible for the inactivation of *Microcystis aeruginosa*. This effect is stronger for higher Cl_2 concentrations. The surface characteristics of *Microcystis aeruginosa* are changed to the UV/Cl_2 process, enhancing the coagulation efficiency favoring their removal [77].

2.5 Vacuum UV and drinking water treatment

UV light in the range from 100 nm to 200 nm is called vacuum UV (VUV). These UV light range is absorbed by almost all substances, including liquid water and oxygen in air. In

presence of air, O_3 will be produced from O_2 [72]. For this reason experiments with UV light below 200 nm were historically conducted under vacuum conditions. However, experiments may also be conducted purging the system with nitrogen.

Although VUV allows to achieve disinfection and degradation of contaminant at the same time, it is not applied on a large scale in DWTP due to the low penetration of photons of short wavelength. About 90% of 185 nm photons are expected to be absorbed in the 0.3 cm layer close to the lamp [15, 78]. The absorption coefficient at 185 nm of pure water is 0.79 $\pm$ 0.11 cm^{-1} at 3.6 °C and increases to 1.53 $\pm$ 0.09 cm^{-1} at 25 °C [79]. However, in recent years, promising advances in the application of technology have been achieved, especially on a small and medium scale [17, 80–88]. Bagheri and Mohseni (2015) afirm that introducing baffles into a VUV reactor significantly increase the degradation of target pollutants [84].

VUV has the advantage of photolyzing water to generate $^{\bullet}OH$ without any chemical addition required [89]. Consequently it is a chemical free AOP. Futhermore, several reactive species are produced: $HO_2^{\bullet}$, $O_2^{\bullet}$, $H^{\bullet}$ and e^-_{aq} (equiatons 2.7) [90, 91] . There are two primary reactions initiating a series of oxidation and reduction reactions: the homolysis (equation 2.7a) and ionization (equation 2.7a) of water [90].

$$H_2O \xrightarrow{h\nu_{185\ nm}} {}^{\bullet}OH + H^{\bullet}, \quad \Phi = 0.3 \tag{2.7a}$$

$$H_2O \xrightarrow{h\nu_{185\ nm}} {}^{\bullet}OH + H^{\bullet} + e^-, \quad \Phi = 0.045 \tag{2.7b}$$

$$H^{\bullet} + O_2 \longrightarrow HO_2^{\bullet}, \quad k = 2{\times}10^{10}\ M^{-1}\,s^{-1} \tag{2.7c}$$

$$HO_2^{\bullet} \rightleftarrows O_2^{\bullet -} + H^+ \quad pK_a = 4.8, \tag{2.7d}$$

$$O_2^{\bullet -} + {}^{\bullet}OH \longrightarrow O_2 + OH^-, \quad k = 7{\times}10^{9}\ M^{-1}\,s^{-1} \tag{2.7e}$$

$$HO_2^{\bullet} + {}^{\bullet}OH \longrightarrow H_2O + O_2, \quad k = 6{\times}10^{9}\ M^{-1}\,s^{-1}\,. \tag{2.7f}$$

A review in $UV_{185\,nm}$ in water treatment was published by Zoschke et al. (2014) [92]. They underline that the main advantage of $UV_{185\,nm}$ generated by a low-pressure mercury vapor lamp (that generated $UV_{254\,nm}$ + $UV_{185\,nm}$) is that the energy consumption is the same as for the emission of UV light at $UV_{254\,nm}$ exclusively. Then the disinfection can be achieved by $UV_{254\,nm}$ while the on-site generation of $^{\bullet}OH$ by $UV_{185\,nm}$ can degrade a wide range of contaminants. Once again, the biggest disadvantage lies in the poor penetration of $UV_{185\,nm}$ in the water matrix making the technique difficult to apply in large DWTP. However, the authors mention that $UV_{185\,nm}$ is a good option to prepare ultrapure water or as a main treatment process for decentralized systems.

2.5.1 Vacuum UV and cyanotoxins

VUV, as it was mentioned before, is the portion of the UV spectrum ranging from 100 nm to 200 nm. These high energy photons react with water molecules to produce $^{\bullet}OH$ from the water itself without the need to add other chemicals, such as H_2O_2 or O_3 [90]. VUV technology will be deeply discuss in the following section.

Liu et al. (2016) applied VUV to degradate MC-LR from a *Microcystis Aeruginosa* culture. They reported a positive impact on MC-LR removal under pH < 7 and aeration conditions, such that the maximal removal achieved was 44% after 20 min of exposure for a low initial MC-LR concentration ($C_0 = 1.24\,\mu g\,L^{-1}$). A lower removal was reported for a higher initial concentration ($C_0 = 18.8\,\mu g\,L^{-1}$). The final concentration was lower than that recommended by WHO ($1.00\,\mu g\,L^{-1}$) when $C_0 = 1.24\,\mu g\,L^{-1}$ [93].

Anatoxin-a was irradiated at 172 nm with a fluence of $200\,mJ\,cm^{-2}$ by Afzal et al. (2010). A second order rater between Anatoxin-a and $^{\bullet}OH$ of $5.2\times10^9 \pm 0.3\times10^9\ M^{-1}\,s^{-1}$ was found in their work. They reported that constant was independent of pH, temperature, and initial concentration of anatoxin-a. When $30\,mg\,L^{-1}$ of H_2O_2 was added more than 70% of toxin was degraded that the dose applied [94].

Chintalapati et Mohseni (2019) applied $UV_{254\,nm}$ and $UV_{185\,nm}$ to degrade MC-LR in synthetic and natural waters. 70% degradation was achieved by $UV_{254\,nm}$ (fluence applied = $200\,mJ\,cm^{-2}$). When $UV_{185\,nm}$ was added, removal increase up to 90% for the same fluence ($H = 200\,mJ\,cm^{-2}$).

2.5.2 Fluence applied in Vacuum UV: Actinometry

An actinometer is a chemical system that undergoes a light induced reaction at a certain wavelength, λ, with a quantum yield, Φ. By measuring the reaction rate of the actinometer the calculation of the absorbed photon flux is possible [95].

Actinometry at 185 nm with actinometers described in the literature required gas-tight assemblies and gas chromatography analysis [95]. In contrast, actinometry at 254 nm is a relatively simple to determinate by using Ki-KIO_3 actinometer [96–98].

The most accurate method to evaluate 185nm irradiation will be through a convenient actinometer for 185 nm, that is insensitive to 254 nm radiation. Meanwhile, Furatian (2017) proposes the use of Ki-KIO_3 on his works with VUV [99]. Its recommendation is based on the fact that the Ki-KIO_3 actinometer does not respond to the 185 nm radiation present. While this actinometer cannot be used to quantify 185 nm radiation in his experiments, neither does 185 nm interfere with 254 nm measurements. Standard Ki-KIO_3 actinometric is

widely applied in $UV_{254\,nm}$. Bolton and Linden (2003) proposed an standard method to measured fluence ($UV_{254\,nm}$ dose). This proposal includes several correction factors to be applied when an actinometry is realized [96]. Among them are:

i. Water factor: when the water absorb at the λ applied then decrease of irradiation must be estimated as:

$$w_F(UVA_{254}) = \frac{1 - 10^{-a\ell}}{a\ell \ln 10}, \tag{2.8}$$

where a is the decadic absorption coefficient cm^{-1} or absorbance for a 1 cm path length and ℓ is the vertical path length of the water in the Petri dish. Equation (2.8) is derived from Beer-Lambert Law and valid only in well mixed samples [100].

ii. Divergence factor: Accounts for the fraction of light that diverge because the light in not perfectly collimated.

$$d_F = \frac{L^2}{(L + \ell)}, \tag{2.9}$$

where L is the distance from the UV lamp to the surface of the cell suspension.

iii. Petri factor: is the ratio of the average of the incident irradiance over the area of the Petri dish to the irradiance at the center of the dish. It is applied to correct the irradiance reading at the center of the Petri dish.

iv. Reflection factor: Accounts for the fraction of light reflected in the interface air-water. For these two media $R = 0.025$.

$$r_F = 1 - R, \tag{2.10}$$

These four factors are those that have been taken into account throughout this work.

CHAPTER 3 GENERAL ORGANIZATION

This thesis consists of one published article, one submitted and a chapter that contains data to be published. The thesis is divided into 8 Chapters and 1 Appendices. The approach and main contributions of each chapter are described below.

Chapter 1 is the **Introduction**. It presents background information, explaining the global context of this thesis, as well the problem that has motivated the development of this research. In addition, the objectives and original scientific hypotheses are presented.

Chapter 2 presents a **Literature review** on cyanobacterial blooms, cyanotoxin, cyanobacteria within drinking water treatment plant, natural and algal organic matter and the main methods used to characterize the organic matter, oxidation processes and cyanobacterial blooms, advanced oxidation process and cyanotoxins, vacuum UV (VUV) and drinking water treatment, VUV and cyanotoxins, measurement of fluence applied in VUV by actinometry.

Chapter 3 presents the approach of research and the **General Organization** of the thesis.

Chapter 4 presents a scientific article published in the "Environmental Science Water Research & Technology" journal (accepted on September 6th 2019) titled: **Performance of Vacuum UV (VUV) for the degradation of MC-LR, geosmin, and MIB from cyanobacteria-impacted waters**. The article analyses VUV process performance using two cyanobacterial-laden Canadian source waters with different inorganic and natural organic matter contents. Degradation of MC-LR and two T&O components (MIB and GSM) were studied. It was observed that although MC-LR, GSM, and MIB were impacted by VUV treatment, the degradation achieved may not be sufficient to completely eliminate toxicity and T&O at the tested fluences (up to 400 $\mathrm{mJ\,cm^{-2}}$). In average 20% increase of DBP was observed in treated water by VUV when chlorination was applied.

Chapter 5 presents a scientific article published in the "Environmental Science Water Research & Technology" journal (accepted on January 20th 2020) titled: **Impact of vacuum UV on natural and algal organic matter from cyanobacterial impacted waters**. In this article, water samples from three Canadian lakes periodically affected by cyanobacteria were used to assess the impact of NOM and AOM on VUV treatment. NOM and AOM were characterized before and after VUV by SEC and FEEM. DBP formation after VUV treatment was analyzed and THM yield was calculated. THM yield increased between 15 and 20% after VUV treatment. Regarding DBP formation and NOM/AOM fractions from SEC, it was found that humic substances are the most important fraction causing the increase

in DBP formation with yield at least 3 times higher than the other fractions (biopolymers, building blocks, low weight molecular acids and neutrals)

Chapter 6 consists data to be published as an article titled **Impact of Vacuum UV on cyanobacteria cell integrity and cyanotoxin degradation**. Disinfection and cyanotoxin oxidation could be reached without provoking cell lysis by VUV. Additionally, dissolved toxins are oxidized as well given the non-selective oxidation characteristic of $^{\bullet}$OH produced by VUV. MilliQ and surface water were spiked with *Microcystis aeruginosa* and *Anabaena Sp.* (cell concentration = 10^6 cells mL^{-1}). Both cultured strains produce toxins. Carbamazepine was used as a probe component to track and asses the $^{\bullet}$OH radical formation. VUV was more performant than $\mathrm{UV}_{254\,\mathrm{nm}}$ in terms of cell inactivation determined by FCM.

Chapter 7 presents a **General Discussion** of the three articles constituting Chapters 4 to 6.

Chapter 8 contains the major **Conclusions** of this project and provides Recommendations for future research based on the findings of this study.

The Appendix A presents the supplementary information of Article 2.

CHAPTER 4 Article 1 - Performance of Vacuum UV (VUV) for the degradation of MC-LR, geosmin, and MIB from cyanobacteria-impacted waters

Article authors

Flavia Visentin, Siddharth Bhartia, Madjid Mohseni, Sarah Dorner and Benoit Barbeau

Journal and citation

Environmental Science: Water Research and Technology

F. Visentin, S. Bhartia, M. Mohseni, S. Dorner and B. Barbeau, Environ. Sci.: Water Res. Technol., 2019, DOI: 10.1039/C9EW00538B.

4.1 Abstract

The increasing frequency with which cyanobacterial blooms are affecting sources of drinking water is a growing concern worldwide. Such events are usually responsible for the presence of cyanotoxins as well as taste and odor (T&O) compounds. Vacuum UV (VUV) is a promising advanced oxidation process used to treat water impacted by cyanobacterial blooms, with potential applicability in small and remote communities because of its simplicity. Here, we present the performance of a VUV process, in both a collimated beam reactor (CBR) and a pilot scale flow-through reactor, using two cyanobacterial-laden Canadian source waters with different inorganic and natural organic matter contents. First, VUV performance was assessed by comparing the removal of microcystin-LR (MC-LR), 2-methylisoborneol (MIB), and geosmin (GSM). The average rate constants obtained in the CBR case were $2.9\times10^{-3}\,\mathrm{cm^2\,mJ^{-1}}$ for MIB and GSM and $6.6\times10^{-3}\,\mathrm{cm^2\,mJ^{-1}}$ for MC-LR. Under bloom conditions, removals of 40-60% for T&O compounds and MC-LR were achieved in the flow-through reactor. It was observed that although MC-LR, GSM, and MIB were impacted by VUV treatment, the removals achieved may not be sufficient to completely eliminate toxicity and T&O at the tested fluences (up to $400\,\mathrm{mJ\,cm^{-2}}$). In addition, we observed a 20% increase in disinfection by-products (DBPs), on an average. Hence, achieving high MC-LR, MIB, and GSM removals with VUV may cause the generation of more DBPs.

4.2 Introduction

Over recent decades, the occurrence of cyanobacterial blooms has increased worldwide due to climate change, legacy nutrient loads, water resource management strategies, population growth, and changes in land usage affecting the quality of drinking water sources [101]. Cyanobacterial blooms often lead to health concerns as a result of risks related to the presence of cyanotoxins. These cyanotoxins can roughly be classified as follows: i) hepatotoxins: microcystins, nodularis, and cylindrospermopsins; ii) neurotoxins: anatoxin-a, anatoxin-a(s), and saxitoxins; and iii) dermatotoxins: lyngbyatoxin-a and aplysiatoxins [8]. Codd et al. (2005) proposed two additional categories: cytotoxins (inhibitor of protein synthesis, genotoxic, and can cause chromosome loss and DNA strand breakage) and irritants and gastrointestinal toxins [102]. As reported by Kardinaal and Visser (2005), more than seventy different structural variants of microcystins have been identified to date [8]. Among them, microcystin-LR (MC-LR) is the most widespread and one of the most toxic, with a lethal dose (LD_{50}) estimated to be 50 µg MC-LR per kilogram of body weight. Between 2001 and 2004, a study conducted by Wood et al. in New Zealand verified that microcystin is the most frequently detected cyanotoxin in that country [9]. Possible human health issues linked to MC-LR include liver damage, increased risk of cancer, and potential damage to the nervous system [10]. According to the World Health Organization (WHO) there are insufficient data to derive a guideline value for cyanobacterial toxins other than MC-LR. For this reason, the WHO and several countries have established guidelines and standards for maximum MC-LR levels in drinking water, ranging from $1.0\,\mu g\,L^{-1}$ to $1.5\,\mu g\,L^{-1}$ depending on the jurisdiction [103–105]. In 2015, the U.S. Environmental Protection Agency health advisory recommend $0.3\,\mu g\,L^{-1}$ for bottle-fed infants and young children of preschool age and $1.6\,\mu g\,L^{-1}$ for school-age children through adults. The health advisory applies to total microcystins using microcystin-LR as a surrogate [106]. Because other microcystins could be also present in drinking water, a Canadian guideline for a maximum total microcystins level of $1.5\,\mu g\,L^{-1}$ has been proposed to protect human health [104].

Blooms events are also responsible for adverse taste and odor compounds (T&O), with the most common metabolites being 2-methylisoborneol (MIB) and geosmin (GSM). Although these compounds do not pose any risk to human health, their presence is noticeable by humans in very low concentrations ($5\,ng\,L^{-1}$ to $10\,ng\,L^{-1}$), and its removal implies challenges [107]. Consequently, effective water processes to reduce T&O along with cyanotoxins are also sought by water regulation institutions.

Under appropriate coagulation conditions, conventional water treatment (coagulation, settling, filtration) can be effective for removing cells without provoking lysis but offers limited

control of extracellular cyanotoxin and T&O [59, 60]. Pre-oxidation processes, using strong oxidants such as ozone (O_3) or permanganate (MnO_4^-), can effectively remove these contaminants [77, 108, 109]. Moreover, Zamyadi et al. suggested that pre-oxidation should be considered to minimize the accumulation of potentially toxic cyanobacteria within a drinking water treatment plant that uses raw water from a source predisposed to cyanobacterial blooms. These plants are vulnerable to the accumulation and breakthrough of cells and toxins. Thus, in these cases, early destruction of cells during treatment could be the best option. Nevertheless, the impact of pre-oxidation, such as DBP's formation, must be considered [12].

Alternative advanced oxidation processes (AOPs), such as (O_3) + hydrogen peroxide (H_2O_2), ultraviolet light (UV) + (O_3), UV + (H_2O_2), and UV + (TiO_2), have also been proposed to control T&O and cyanotoxins [110–112]. Pre-oxidation and AOP both add complexity to the treatment train. Oxidation-based processes are expected to lead to the release of intracellular cyanotoxins [113,114]. Thus, their proper control is of paramount importance to achieve the oxidation reaction, a challenging goal for small communities with limited technical resources. In view of this, robust oxidation technologies with minimal operational and chemical use requirements would be beneficial, especially for small water systems.

Recently, VUV has been suggested as a potentially simple AOP to control organic micropollutants in drinking water treatment [15, 16, 78, 92, 115]. VUV relies on the use of a standard UVC lamp with a high purity quartz envelope and sleeve that enables a portion of short wavelength (lower than 200 nm) photons to irradiate the water. These high energy photons react with water molecules to produce $^{\bullet}OH$ from the water itself without the need to add other chemicals, such as H_2O_2 or (O_3) [90]. This characteristic simplifies the operation of the system, and this process is deemed effective against pathogens (with UVC) [72] and micropollutants [16].

The ability of VUV to destroy MC-LR from an artificial *M. aeruginosa* bloom, under various water conditions, was tested by Liu et al. [93]. They reported a positive impact on MC-LR removal under pH < 7 and aeration conditions, such that the maximal removal achieved was 44% after 20 min of exposure for a low initial MC-LR concentration ($C_0 = 1.24\,\mu g\,L^{-1}$). A lower removal was reported for a higher initial concentration ($C_0 = 18.8\,\mu g\,L^{-1}$). The final concentration was lower than that recommended by WHO ($1.00\,\mu g\,L^{-1}$ of MC-LR) when $C_0 = 1.24\,\mu g\,L^{-1}$. Unfortunately, no information about the fluence responsible for the degradation was reported.

Kutschera et al. [116]) studied MIB and GSM degradation under 254 nm and 185 nm radiation in ultrapure and natural waters. The authors confirmed that these two T&O compounds were not photolyzed at 254 nm, suggesting that the formation of $^{\bullet}OH$ radicals from

the 185 nm radiation was the main mechanism responsible for T&O degradation. The degradation followed pseudo first-order kinetics with rate constants of $1.2\times10^{-2}\,cm^2\,mJ^{-1}$ for both GSM and 2-MIB in ultrapure water. A fluence of $200\,mJ\,cm^{-2}$ induced 90% removal in ultrapure water, while complete degradation was achieved by a fluence of $400\,mJ\,cm^{-2}$. In natural water (DOC = $3.0 \pm 0.3\,mg\,L^{-1}$, $[HCO_3^-] = 0.3\,mmol\,L^{-1}$, specific UV absorbance at 254 nm = $2.3 \pm 0.2\,L\,mg^{-1}\,m^{-1}$), the authors reported a decrease in the rate constants, $2.7\times10^{-3}\,cm^2\,mJ^{-1}$ for GSM and $2.5\times10^{-3}\,cm^2\,mJ^{-1}$ for 2-MIB, attributed to the presence of scavenged natural organic matter [116].

Previous studies have all been conducted under controlled conditions, such as artificial *M. aeruginosa* blooms or in the absence of cyanobacterial cells. In addition, most of the previous studies used batch VUV set-ups that do not represent actual flow-through UV reactors, which are affected by hydrodynamics. In this study, we focused on testing the efficacy of VUV to remove MC-LR and T&O compounds using natural cyanobacterial blooms in a flow-through UV reactor. As the presence of minerals is expected to impact VUV reactions, water from two lakes with very different quality characteristics were selected. In parallel, the performances of the flow-through reactor were compared to a lab-scale collimated beam reactor for which the fluence was characterized by actinometry [117].

4.3 Materials and methods

4.3.1 Source water location

Source water samples from two Canadian cyanobacterial-impacted lakes, identified as Lakes A and B (Table 4.1) were collected to conduct this work. Lake A is located 40 km west of Montreal (Quebec, Canada) and constitutes a system of two lakes that supplies a bank filtration water system. Lake B, located 160 km east of Montreal (Quebec, Canada), is a recreational water body currently under consideration to become a source of drinking water for the area. Samples were collected from Lake A and Lake B on August 25, 2017 and September 7, 2017, respectively.

4.3.2 Source water characterization

Source waters were analyzed for total organic carbon (TOC), dissolved organic carbon (DOC), and biodegradable dissolved carbon (BDOC) concentrations using a TOC analyzer (5310C Sievers Instruments Inc., USA). BDOC analysis was performed using the 30-d incubation batch method of Servais et al. [118]. The pH was measured using a Fisher Scientific pH-meter (Accumet, Fisher Scientific Instruments, USA), pre-calibrated with pH 4, 7, and 10 standard

buffers (BDH VWR Analytical). Turbidity measurements (Hach 2100N turbidimeter) were assessed following Standard Methods #2130B [119]. Ions were measured by ionic chromatography ICS 5000 AS-DP DIONEX (Thermo Scientific) with an As18-4µm column. Alkalinity was measured by titration according to Standard Methods #2320 [119]. A YSI 6600 V2-4 water-quality multi-probe (YSI, Yellow Springs, Ohio, USA) equipped with a self-cleaning wiper was used to determine the presence of cyanobacteria (i.e., the phycocyanin measured was higher than 2.4 relative fluorescence units (RFU)) [120]. Lugol's iodine preserved the water samples for further taxonomic identification and cell counting.

4.3.3 Targeted cyanobacterial metabolites detection

The initial intent was to collect waters during bloom events with the hope that cyanobacterial metabolites (GSM, MIB, and cyanotoxin) would be simultaneously present in sufficiently high concentrations to avoid spiking. However, due to their low abundance, we had to resort to spiking the three target compounds in the waters collected from both lakes. The source waters were always spiked with $100\,\mathrm{ng\,L^{-1}}$ of MIB and GSM and $10\,\mathrm{\mu g\,L^{-1}}$ of MC-LR.

Because microcystin is the most common cyanotoxin and MC-LR the most frequent and one of the most toxic [8,9], we decided to spike our samples with MC-LR ($C_0 = 10\,\mathrm{\mu g\,L^{-1}}$). Most studies of cyanotoxin oxidation by AOP are performed using MC-LR [73,111,121]. For this purpose, dry MC-LR was purchased from Alexis Chemical (Cedarlane, Canada). MC-LR was measured by an on-line solid phase extraction coupled with ultra-high performance liquid chromatography, heated electrospray ionization, and high-resolution mass spectrometry detection, Q-Exactive (Thermo Fisher Scientific, Waltham, MA) (UHPLC-HESI-HRMS), as described in Fayad et al. [122]. The limit of detection (LOD) of the method was $10\,\mathrm{ng\,L^{-1}}$, and the limit of quantification (LOQ) was $33\,\mathrm{ng\,L^{-1}}$.

GSM (purity $\geq 97\%$), MIB (purity $\geq 98\%$) and cis-decahydro-1-naphthol, used as an internal standard (IS, purity $\geq 99\%$), were purchased from Sigma-Aldrich (St. Louis, MO). Individual stock solutions were prepared daily in ultrapure water (Milli-QTM) at a concentration of $10\,\mathrm{mg\,L^{-1}}$ in HPLC grade methanol (MeOH) from Fisher Scientific (Whitby, ON, Canada). The contribution to carbon concentration in the water by MeOH was $4.2\times10^{-7}\,\mathrm{mg\,L^{-1}}$. This represented a negligible amount of carbon introduced to the samples (0.001%).

For the MIB and GSM analysis, a GC 3800 coupled to a MS 4000 from Varian (Palo Alto, CA) equipped with a PAL auto sampler (Zwingen, Switzerland) and a Gerstel Twister system (Baltimore, MD) was used. The LOD and LOQ for MIB and GSM were respectively determined as 8/27 $\mathrm{ng\,L^{-1}}$ and 8.5/29 $\mathrm{ng\,L^{-1}}$ ($100\,\mathrm{ng\,L^{-1}}$).

4.3.4 Disinfection by-products

Samples were chlorinated under uniform formation conditions (UFC) (1 ± 0.5 ppm Cl_2 at pH = 8.0 after 24 h incubation at 20 °C, and disinfection by-product formation was analyzed in terms of trihalomethanes (THMs) and haloacetic acids (HAAs). Four THMs (bromoform, chloroform, bromodichloromethane, and dibromochloromethane), total THM (TTHM) and six haloacetic acids (HAAs) (bromoacetic acid, bromochloroacetic acid, chloroacetic acid, dibromoacetic acid, dichloroacetic acid, and trichloroacetic acid) were measured. THMs were acquired according to USEPA Method 524-2 (purge and trap [Aquatek 100 - Stratum 9800 de Teledyne Tekmar] coupled with GC-MicroECD [7890B de Agilent]). HAA compounds were extracted by liquid/liquid extraction with methyl tertbutyl ether (MtBE) followed by derivatization with acidic methanol in accordance with USEPA Method 552.2 (GC-MicroECD [7890B de Agilent]).

4.3.5 Vacuum UV experiments

For each sampling campaign, experiments were first conducted in duplicate using a lab-scale collimated beam UV/VUV reactor (referred hereafter as CBR). In parallel, experiments were also conducted in duplicate on a flow-through UV/VUV reactor (referred hereafter as FTR).

The stirred CBR setup allows observation of the precise kinetics of VUV induced reactions. Pollutant concentrations and the local incident radiation are uniform inside the CBR, allowing proper interpretation of the kinetics of reactions [124]. The CBR is equipped with an ozone-generating amalgam Hg lamp (Light Sources GPHVA357T5VH/4W) placed in a T-shape polyvinyl chloride (PVC) enclosure that is continuously purged with nitrogen to remove oxygen present in air (Figure 4.1). To irradiate water samples, a special cylindrical reaction vessels made with regular quartz (except the bottom part made of Suprasil® quartz to allow 185 nm and 254 nm radiation to be transmitted) was used. The diameter and height are 4.8 cm (path length = 4.67 cm) and 1.5 cm, respectively.

The FTR experiments were conducted using a lab-scale annular photoreactor, 30 cm in length, in a configuration similar to what could be installed for application in a small water system (Figure 4.2). The FTR was equipped with an ozone generating low-pressure mercury lamp (Light Sources GPHVA357T5VH/4W) with a dome-ended high purity quartz sleeve housed in a cylindrical Plexiglass® chamber. The fluence inside the FTR was controlled by adjusting the inlet flow, which feeds a 5 mm thick water layer located between the inner core and the outer sleeve [125]. The flow was varied from 1.0 L min^{-1} to 5.3 L min^{-1}, providing a theoretical contact time of 9.4 s to 1.8 s, respectively. Under the tested conditions, laminar

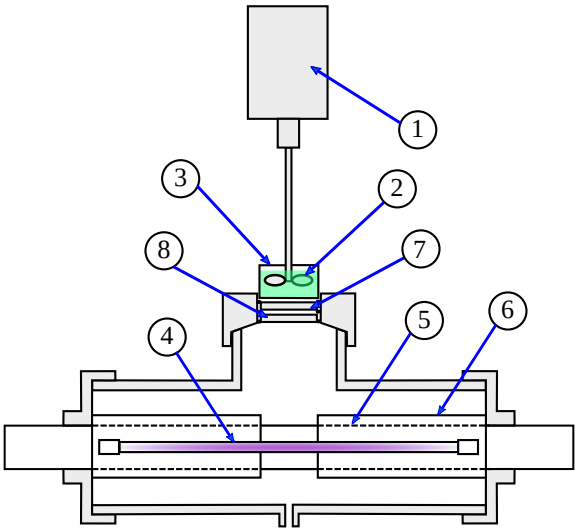

Figure 4.1: Scheme of the collimated beam reactor (CBR) used: (1) motor, (2) stirrer, (3) reaction vessel, (4) vacuum UV lamp, (5) quartz sleeve, (6) Teflon cylinder, (7) optical filter, (8) Suprasil® quartz. Adapted from reference [123].

flow was obtained where Reynolds numbers in the water layer ranging from 320 to 1700.

4.3.6 Kinetic analysis

VUV treatment involves a potential direct photolysis pathway (for MC-LR) and an indirect pathway (for MC-LR, GSM & MIB) due to the formation of free radicals according to equations (4.1),

$$\mathrm{H_2O} + h\nu_{185\ \mathrm{nm}} \longrightarrow {}^{\bullet}\mathrm{OH} + {}^{\bullet}\mathrm{H}, \quad \Phi = 0.3 \tag{4.1a}$$

$$\mathrm{H_2O} + h\nu_{185\ \mathrm{nm}} \longrightarrow {}^{\bullet}\mathrm{OH} + \mathrm{H^+} + \mathrm{e^-}\,, \tag{4.1b}$$

where ${}^{\bullet}$OH radicals are highly reactive and non-selective oxidants. Due to the high reactivity of ${}^{\bullet}$OH, the generation rate is equal to the consumption rate such that a steady state is reached in a short period of time in comparison with the exposure time [99]. It has been shown that the fluence at 185 nm is approximately equivalent to 5% to 16% of the fluence at 254 nm [99, 126]. Therefore, the fluence at 254 nm can be used as an indirect metric of the formation of ${}^{\bullet}$OH radicals [89]. Assuming that the degradation in the VUV system is solely the result of direct photolysis at 254 nm and indirect hydroxyl radical pathways originating

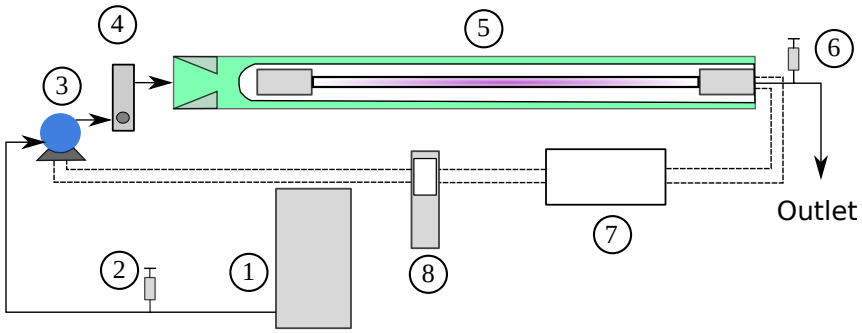

Figure 4.2: Scheme of the flow through reactor (FTR) used: (1) water reservoir, (2) inlet sampling point, (3) pump, (4) flow meter, (5) photoreactor, (6) outlet sampling point (the dashed lines represent the electric connections and the solid lines indicate the water connections), (7) ballast, (8) power meter. Adapted from reference [82].

from the fluence at 185 nm, the degradation kinetics can be described by equation (4.2) [116]:

$$-\frac{\mathrm{d}C}{\mathrm{d}H} = \left(k_{d,C} + k_{^{\bullet}\mathrm{OH},C}\,[^{\bullet}\mathrm{OH}]\right) C = \left(k_{d,C} + k'\right) C = k''\,C\,, \tag{4.2}$$

where C is the concentration of contaminant (MIB, GSM or MC-LR), H is the fluence at 254 mJ cm^{-2}, [$^{\bullet}$OH] is the hydroxyl radical concentration, $k_{d,C}$ is the first-order direct photolysis rate constant at 254 nm, and $k_{^{\bullet}\mathrm{OH},C}$ is the rate constant for an $^{\bullet}$OH based reaction.

Since MIB and GSM do not photolyze [116], $k_{d,C}$ can be neglected. Also, the $^{\bullet}$OH steady state is rapidly reached, so the [$^{\bullet}$OH] can be considered constant. The contaminant degradation can then be expressed as follows [116]:

$$-\frac{\mathrm{d}C}{\mathrm{d}H} = k'\,C\,, \tag{4.3}$$

where k' is the pseudo-first order rate constant, in units of cm^2 mJ^{-1}.

In contrast, MC-LR does photolyze, and thus, $k_{d,C} = 3.65{\times}10^{-3} \pm 0.21{\times}10^{-3}$ cm^2 mJ^{-1} [73] cannot be neglected [73, 88]. Therefore, equation (4.2) also describes the degradation of MC-LR, where a modified becomes the pseudo-first order rate constant in cm^2 mJ^{-1}.

CBR experimental data were fitted to equation (4.3) in order to determine a kinetic model for each contaminant. For the FTR, the fluence cannot be directly computed, hence, using an approach similar to biodosimetry [127–129], fluences were back-calculated using the kinetics derived in the CBR and the measured performances (C/C_0) in the FTR.

4.3.7 Fluence calculations

The fluence applied in the CBR is calculated based on equation (4.4):

$$H_0 = E\,t\,, \tag{4.4}$$

where H_0 is the theoretical fluence in units of $\mathrm{mJ\,cm^{-2}}$, E is the irradiance in units of $\mathrm{mW\,cm^{-2}}$, both at 254 nm, and t is exposure time in s. Irradiance at 254 nm was measured through potassium iodide-potassium iodate KI–KIO_3 actinometry [99, 117, 130]. To obtain the applied fluence in the reactor, the fluence in equation (4.4) was multiplied by the correction factor, c_F, as defined in [96, 124]:

$$H = H_0\,c_F = E\,t\,w_F(\mathrm{UVA_{254}})\,r_F\,p_F\,d_F \tag{4.5}$$

where $w_F(\mathrm{UVA_{254}})$ is the water factor which is a function of $\mathrm{UVA_{254}}$ and source-water specific, r_F is the reflection factor (which considers the light reflected at the air-water interface), p_F is the petri factor (accounting for non-uniformity of irradiance), and d_F is the divergence factor of the beam. The values adopted were: $r_F = 0.98$, $p_F = 0.95$ and $d_F = 0.73$ [124]. Knowing the irradiance and the correction factors, the time for each irradiation was adjusted to provide the targeted fluences, which ranged from $0\,\mathrm{mJ\,cm^{-2}}$ to $400\,\mathrm{mJ\,cm^{-2}}$ at 254 nm.

4.3.8 Statistical analysis

Kinetic constants were obtained by performing regression analysis, imposing to pass through $x = 0$ at $y = C_0$. Main Effects ANOVA was conducted to discriminate the roles of source water quality (Lake A vs Lake B), reactor type (FTR vs CBR), and contaminant type (MIB, GSM, or MC-LR) with respect to kinetic constants. Statistical analyses were realized using the Statistica 13 software (TIBCO, CA, USA), with the level of significance set at $\alpha = 0.05$. Outliers were removed from the dataset prior to the statistical analysis.

4.4 Results and discussion

4.4.1 Source water characteristics

Table 4.1 summarizes the water quality parameters measured during the sampling campaigns of Lakes A and B. Lake A source water had a high alkalinity and moderate DOC. Despite the absence of a cyanobacterial bloom at the time of sampling from Lake A, this source water was selected due to the high concentration of alkalinity (an $^{\bullet}OH$ scavenger) and chloride

(Cl^-) (a strong absorber of 185 nm photons). For example, when the Cl^- concentration is higher than 20 mg L^{-1}, it becomes the major absorber of 185 nm photons [130], resulting in the formation of chlorine radicals ($^{\bullet}Cl$). When this radical is present, both $^{\bullet}Cl$ and $^{\bullet}OH$ can degrade contaminants [130].

The source water from Lake B was sampled during an important cyanobacterial bloom, which is reflected by the high levels of DOC and the presence of particulate organic carbon from the 200,000 cells mL^{-1} (88% of cells were *Cyanophyceae* class and 83% of the cyanobacterial cells corresponded to *Planktothrix agardhii*). However, this source water exhibited low mineralization, with an alkalinity of 14 mg L^{-1} and a Cl^- concentration of 12 mg L^{-1}.

4.4.2 Measurements of irradiance and fluence correction factors

The irradiance value obtained for the collimated beam reactor by KI–KIO_3 actinometry was 1.24 ± 0.04 mW cm^{-2} at 254 nm. The UVA_{254} values for Lake A and B waters were 0.085 cm^{-1} and 0.296 cm^{-1}, respectively, which translate into water factors of $w_{F,A} = 0.65$ and $w_{F,B} = 0.30$, respectively. The overall fluence correction factor (including reflection, Petri, and divergence factors) results $c_{F,A} = 0.44$ and $c_{F,B} = 0.20$, for each lake. summarizes the uncorrected (H_0) and corrected (H) fluences tested in the CBR for both Lakes.

4.4.3 Reactions in the collimated beam reactor

Figures 4.3 and 4.4 show the degradation kinetics of MC-LR, MIB, and GSM in the CBR, for Lakes A and B, respectively. The removal of MC-LR was higher than the removal of MIB and GSM in both source waters as a result of direct photolysis. During these tests, the removals of T&O metabolites reached a maximum of 50%, while an MC-LR removal of almost 80% was observed at the highest fluence. Kutschera et al. [116] analyzed the effectiveness of 254 nm and 185 nm radiation on ultra-pure and natural water (DOC = 3.0 ± 0.3 mg L^{-1}) spiked with MIB and GSM (C_0 = 100 ng L^{-1}). They proved that 254 nm was ineffective for removing MIB and GSM. However, when the samples were irradiated with both 254 nm and 185 nm simultaneously, around 80% removal rates for MIB and GSM were observed at a

Table 4.1: Characteristics of the waters sampled from Lakes A and B

Lake	TOC mg C L^{-1}	DOC mg C L^{-1}	BDOC mg C L^{-1}	pH	Turbidity NTU	UVA_{254} cm^{-1}	Nitrate+Nitrite mg N L^{-1}	Sulfate mg SO_4^- L^{-1}	Alkalinity mg $CaCO_3$ L^{-1}	Chloride mg Cl^- L^{-1}
A	4.5	4.5	0.6	8.4	0.9	0.085	-	40	170	94
B	14.7	12.2	2.4	7.7	15.7	0.296	0.078	-	14	12

fluence of 200 mJ cm^{-2} [116]. In our experiments, 50% removal was obtained with a fluence of 160 mJ cm^{-2} for the Lake B.

The apparent rate constants k' and k'' for the waters of both lakes are summarized in Table 4.3 and compared to those reported by Kutschera et al. [116]. For Lake B, k' values for MIB and GSM were greater than those from Lake A (1.4 and 2.5 times greater, respectively), suggesting that higher degradation was achieved in Lake B, where the water had a bloom/high DOC/low mineral content. The presence of alkalinity and chloride in Lake A affect VUV performance, as reported by Furatian [130]. However, the k' values obtained in our experiments were similar to the k values reported by Kutschera et al. [116] (except for the k' for GSM in Lake A where our value is 1.7 times lower). According to an ANOVA test, the rate constants for T&O metabolites were marginally, yet statistically significantly, lower ($p = 0.057$) in Lake A (with high minerals) compared to those in Lake B (with high DOC). GSM rate constants were also lower than those of MIB in Lake A ($p < 0.05$).

Regarding MC-LR, kinetic values exhibited a similar trend to MIB and GSM, with higher kinetic in Lake B than Lake A. The k'' value from Lake B was three times higher than the k'' value from Lake A when photolysis was considered. This reinforce the idea that inorganic components interfere with VUV performance more than the cyanobacterial bloom (high organic carbon concentration).

The removal of MC-LR was more effective than that of MIB and GSM due to the added effect of direct photolysis. Approximately 80% MC-LR removal efficiencies were achieved for the highest tested fluences. The apparent rate constants were two times greater than those of the two T&O metabolites (Table 4.3) for Lake B. It was also observed that the apparent rate of MC-LR removal was higher in Lake B than in Lake A ($p < 0.01$), a similar conclusion to the source-water matrix effect observed for GSM and MIB. Assuming that the rate of MC-LR direct photolysis is 3.65×10^{-3} cm^2 mJ^{-1} [73], the rates provided by the action of free

Table 4.2: Uncorrected (H_0) and corrected (H) fluences for Lakes A and B using the CBR

Time, s	**Uncorrected fluence,** H_0, mJ cm^{-2}	**Corrected fluence,** H, mJ cm^{-2}	
		Lake A	Lake B
80	100	44	20
159	200	88	40
318	400	176	80
477	600	264	120
636	800	352	160

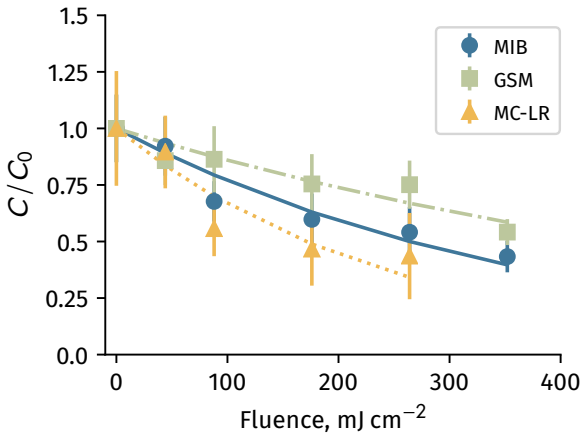

Figure 4.3: Degradation of micropollutants in the CBR for Lake A (Error bars denote standard deviation). Experiments conducted in duplicate using a lab-scale CBR UV/VUV reactor.

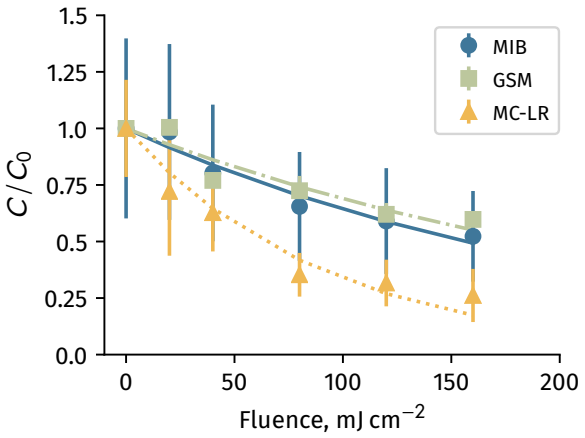

Figure 4.4: Degradation of micropollutants in the CBR for Lake B (Error bars denote standard deviation). Experiments conducted in duplicate using a lab-scale CBR UV/VUV reactor.

radicals represented 40% of the overall removal of MC-LR for Lake B. Consequently, it is important to account for the role of direct photolysis in the prediction of MC-LR removals.

The raw water from Lake B impacted by a natural cyanobacterial bloom with a cell concentration of 200,000 L^{-1} was spiked with MC-LR. After irradiation, a maximum 80% MC-LR removal was achieved (Figure 4.4), with an estimated k'' value of $9.2\times10^{-3} \pm 0.0$ $cm^2\,mJ^{-1}$ (Table 4.2). For Lake A, without cyanobacterial bloom and the same exposure time, 80% removal was also obtained with a k'' value of $3.9\times10^{-3} \pm 0.9\times10^{-3}$ $cm^2\,mJ^{-1}$. It should be noted that although the exposure times were the same, the applied fluences were different because they depended on the UVA_{254} values. The same removal (80%) was achieved for both water matrices but with different fluences: 264 mJ cm^{-2} and 160 mJ cm^{-2} for Lakes A and B, respectively. This also suggest that higher concentrations of major solutes, such as chloride and alkalinity, result in the need for higher fluences to obtain desirable MC-LR removal.

Liu et al. [93] studied the degradation of microcystins in natural waters using 185 nm UV irradiation on an artificial bloom of *M. aeruginosa* (cultured for 3 weeks with a cell concentration of 10^6 cells mL^{-1}. They observed a maximum removal of 44% ($C_0 = 1.24$ µg L^{-1}). At a higher initial concentration ($C_0 = 18.8$ µg L^{-1}), higher exposure times were required and lower removals were obtained, around 30%. From a graph presented in their article where the degradation of MC-LR for different pH values were plotted, it was possible to estimate the rate constants, ranging from 0.005 min^{-1} to 0.01 min^{-1} (for pH values from 12 to 7)

when $C_0 = 1.55\,\mu g\,L^{-1}$ [93]. However, there was no mention to whether the authors applied correction factors in their analysis.

The major solutes, Cl^- and $HCO_3{}^-$ and DOC, of a water matrix, are expected to interfere with contaminant removal. In particular, Cl^- plays a significant role, and its concentration is more important when using VUV technologies compared to other AOPs, such as UV-H_2O_2 and O_3-H_2O_2 [99,130], due to the strong absorption of Cl^- at 185 nm. Furatian et al. investigated the influence of Cl^- in VUV water treatment using carbamazepine as a probe and two sources of carbon (t-butanol, an effective $^\bullet$OH radical scavenger, and NOM) [99,130]. They found that the carbamazepine degradation rate increased with the addition of Cl^- in the presence of t-butanol to scavenge $^\bullet$OH radicals. However, the opposite trend was observed when t-butanol was replaced by NOM as a source of carbon. The authors concluded that Cl^- has a negative influence on contaminant removal rates. When the Cl^- concentration is higher than $20\,mg\,L^{-1}$, it becomes the major 185 nm absorber [130]. In our case, Lake A had Cl^- concentration of $94\,mg\,L^{-1}$ (Table 4.1), yielding a Cl^- absorbance at 185 nm of $9.37\,cm^{-1}$ (assuming a molar absorption coefficient $\varepsilon_{185\,nm} = 3540\,M^{-1}\,cm^{-1}$ [130], and $\varepsilon_{185\,nm} = 1.8\,cm^{-1}$ for pure water [131]. The fraction f_{Si} of absorbed photons for each absorbing solute is given by $f_{Si} = \alpha_{Si}/\alpha_{Total}$, where α_{Si} is the absorption coefficient for solute Si, and α_{Total} is the absorption coefficient for the overall solution. Considering only the main 185 nm absorbances (water, Cl^-, $HCO_3{}^-$ ($\varepsilon_{185\,nm} = 290\,M^{-1}\,cm^{-1}$) [99]) and NOM ($\varepsilon_{185\,nm}$, referred as Specific UV Absorbance), we calculated that Cl^- absorbs 75% of the 185 nm photons for Lake A, whereas H_2O absorbed 15%, and the remaining 10% is absorbed by $HCO_3{}^-$ and NOM. In contrast, for Lake B (where $[Cl^-] < 20\,mg\,L^{-1}$, water is the dominant 185 nm absorber, since 50% of the 185 nm photons are absorbed by water and 35% by Cl^-. Once more, $HCO_3{}^-$ and NOM absorption were lower than 10%.

The reduced performance in Lake A is related to the presence of a high Cl^- concentration. As shown by Furatian et al., the impact of Cl^- on the VUV efficiency is specific to each

Table 4.3: Rate constants (k' and k'') for MIB and GSM. In parenthesis, the R^2 of the fitting are reported

	k' or $k''[\times 10^{-3} cm^2\,mJ^{-1}]$		
	MIB	**GSM**	**MC-LR**
Lake A	2.5 ± 0.3 ($R^2 = 0.79$)	1.6 ± 0.0 ($R^2 = 0.56$)	3.9 ± 0.9 ($R^2 = 0.65$)
Lake B	3.4 ± 0.1 ($R^2 = 0.85$)	4.0 ± 0.0 ($R^2 = 0.85$)	9.2 ± 0.0 ($R^2 = 0.82$)
Kutschera et al. [116]	2.5	2.7	-

water source. With a high Cl^- concentration, the success of VUV treatment relies on Cl^- reactivity with NOM and target contaminants [99, 130]. Therefore, the negative impact of Cl^- on the removal efficiencies of MIB, GSM, and MC-LR observed here is consistent with the conclusions of Furatian et al. [99, 130]. When Cl^- absorbs photons at 185 nm, it will generate chlorine radicals ($^{\bullet}Cl$) equation (4.6). The $^{\bullet}Cl$ reacts with Cl^- (equation (4.6)) and dichlorine radical anion ($^{\bullet}Cl_2^-$) are generated [132]. $^{\bullet}Cl$ and $^{\bullet}Cl_2^-$ are expected to react with the background water matrix to produce $^{\bullet}OH$ (equation (4.6)) [91]. Details of these reactions between the radicals are discussed by Gonzalez et al (2004) [90].

$$Cl^- + h\nu_{185\ nm} \longrightarrow {}^{\bullet}Cl + e_{aq}{}^-, \quad \Phi = 0.4 \tag{4.6a}$$

$$^{\bullet}Cl + Cl^- \rightleftarrows {}^{\bullet}Cl_2^- \tag{4.6b}$$

$$^{\bullet}Cl/\ {}^{\bullet}Cl_2^- + H_2O \rightleftarrows H^+ + HOCl^{\bullet -} \tag{4.6c}$$

$$^{\bullet}Cl/\ {}^{\bullet}Cl_2^- + H_2O \rightleftarrows Cl^- + {}^{\bullet}OH + H^+ . \tag{4.6d}$$

An important difference between Lakes A and B can also be found in their respective alkalinities. Bicarbonate is responsible for radical scavenging as well as 185 nm photo-absorption [99]. Bicarbonates may react with $^{\bullet}OH$ according to:

$$^{\bullet}OH + HCO_3{}^- \longrightarrow CO_3{}^{\bullet -} + H_2O . \tag{4.7}$$

The kinetic constant rate of the reaction ranges from $8.5\times10^{-6}\,M^{-1}\,s^{-1}$ to $1.5\times10^{-7}\,M^{-1}\,s^{-1}$ [91,133]. Duca et al. reported that atrazine removal was reduced by ten times in the presence of $50\,mg\,L^{-1}$ as $CaCO_3$ of bicarbonate [134]. The high alkalinity of Lake A water source ($170\,mg\,L^{-1}$ as $CaCO_3$) compared to Lake B ($14\,mg\,L^{-1}$ as $CaCO_3$) is therefore suggested as the main reason for the lower VUV performance in Lake A. If the apparent rate constant k_{app} is calculated for each lake (as the product of k times the inorganic compounds concentration, in this case $HCO_3{}^-$) we obtained $k_{app} = 3.4\times10^4\,s^{-1}$ for Lake A, which is 12 times higher than that of Lake B, $k_{app} = 2.8\times10^3\,s^{-1}$). This suggest that the high bicarbonate concentration in Lake A may detriment the VUV performance.

DOC also acts as a radical scavenger and 185 nm photo-absorber [99, 135]. DOC in Lake B was almost three times higher than that in Lake A (Table 4.1). The kinetic constant of the reaction between NOM and $^{\bullet}OH$ (based on moles of organic carbon) is in the range of $1.6\times10^8\,M^{-1}\,s^{-1}$ to $1.0\times10^{10}\,M^{-1}\,s^{-1}$ [91, 133, 136]. This gives us a k_{app} of $3.75\times10^5\,s^{-1}$ and $1.2\times10^6\,s^{-1}$, for Lake A and B respectively, suggesting that DOC concentration in our study had less influence than inorganic components on the VUV performance. Nevertheless, rate

constants of contaminants tested during this work (MC-LR, MIB and GSM) were higher in Lake B, allowing to infer that the presence of major inorganic solutes is more important than DOC for explaining differences in performance.

In 2007, Rosenfeldt and Linden propose to analyze the parameter $R_{\bullet OH,UV}$ in order to experimentally determine the $^{\bullet}$OH radical exposure per UV fluence given a water matrix and initial H_2O_2 concentration. $R_{\bullet OH,UV}$ is defined as follow [137]:

$$R_{\bullet OH,UV} = \frac{1}{H} \int_0^t [^{\bullet}OH]\, dt\,, \tag{4.8}$$

where $R_{\bullet OH,UV}$ is in units of $M\,s\,cm^2\,mJ^{-1}$ and H is the corrected fluence defined in equation (4.5). Although the work mentioned above uses UV+H_2O_2 instead of VUV as is our case, we applied the concept of $R_{\bullet OH,UV}$ to estimate the concentration of $^{\bullet}$OH in Lake A and B. It was found that the $R_{\bullet OH,UV}$ was two times larger in Lake B than in Lake A (Table 4.4), mainly due to the lower $^{\bullet}$OH concentration in Lake A.

Assuming the same operation conditions of the reactor to treat water sources from Lakes A and B, the explanation why $R_{\bullet OH,UV}$ is lower in Lake A than Lake B is directly related to the water matrix.

4.4.4 Flow-through reactor

A bench scale FTR was used to study the degradation of MIB, GSM, and MC-LR. For the Lake A, 40% of MIB and 50% of GSM were removed with a residence time of 9.5 s, which gave a reduction equivalent dose of $360\,mJ\,cm^{-2}$ (Figure 4.5). The equivalent fluence for MIB and GSM in Lake B was $150\,mJ\,cm^{-2}$ and removal efficiencies achieved were 60% and 35%, respectively (Figure 4.6). An MC-LR removal efficiency of 50% was achieved in both Lakes A (Figure 4.5) and B (Figure 4.6), but the dose required for that removal in Lake A was two times larger than that in Lake B, $230\,mJ\,cm^{-2}$ and $100\,mJ\,cm^{-2}$, respectively. In

Table 4.4: $R_{\bullet OH,UV}$ for Lake A and Lake B

	$R_{\bullet OH,UV}[M\,s\,cm^2\,mJ^{-1}]$		
	MIB	**GSM**	**MC-LR**
Lake A	8.33×10^{-13}	1.95×10^{-13}	2.50×10^{-14}
Lake B	1.13×10^{-12}	4.88×10^{-13}	5.55×10^{-13}

order to achieve the same removal, a higher fluence was used to treat the water source of Lake A. The differences in removal efficiencies could be explained in one hand by the water matrix characteristics and its impact on the fluence received by the sample and the kinetics involved, and on the other hand by the hydrodynamics of the reactor.

According to Bagheri and Mohseni (2015) the hydrodynamics of the reactor is correlated with its performance [84]. About 90% of 185 nm photons are expected to be absorbed in the 0.3 cm layer close to the lamp [15] (details of the propagation of 254 nm and 185 nm photons are presented in reference [78]). In our study, the Reynolds number in the FTR varied from 320 to 1700, suggesting a laminar flow regime and thus a strong influence of hydrodynamics on reactor performance. The lack of turbulence along with poor distribution of VUV photons in the reactor may also explain why we observed a plateau of performance in the FTR at higher fluences. Consequently, increasing the turbulence inside the reactor is decisive for improving this reactor performance [78, 84, 138].

When applying AOPs, the degradation of products must be considered and carefully studied to ensure avoiding or minimizing the formation of potentially toxic by-products [139,140]. In this study, we evaluated the impact of VUV on the formation of THM and HAA precursors. In Lake A, a statistically significant THM formation increase of 20% in raw water was measured, in comparison to an increase of 8% in filtered water. For HAA, an average increase of 10% was estimated in raw water and 15% in filtered water. For both cases, $p < 0.05$ were obtained in the ANOVA test of raw water vs filtered water.

Another monitored parameter was BDOC, which is the biodegradable fraction of DOC. It can be assimilated and mineralized by the presence of bacteria in water. It is generally comprised of 10% to 20% of the DOC [140]. In Lake A raw water, we measured $BDOC_0 = 0.6$ mg C L^{-1} and average BDOC $= 0.5 \pm 0.04$ mg C L^{-1} for VUV treated water, while in filtered waters, the BDOC concentration was lower than the LOD (LOD $= 0.15$ mg C L^{-1}). In Lake B, an average BDOC increase of 20% was observed when waters were treated with VUV. These results shed light on the implementation of VUV technologies inside a drinking water treatment plant, suggesting that VUV reactor should be placed after DOC removal, where the negative impact on DBP formation is minimized.

4.5 Conclusions

The performance of VUV was tested using two water sources with different inorganic, NOM, and cyanobacterial contents. The main objective was to assess if VUV could simultaneously destroy MC-LR, MIB, and GSM. It was observed that although MC-LR, GSM, and MIB were

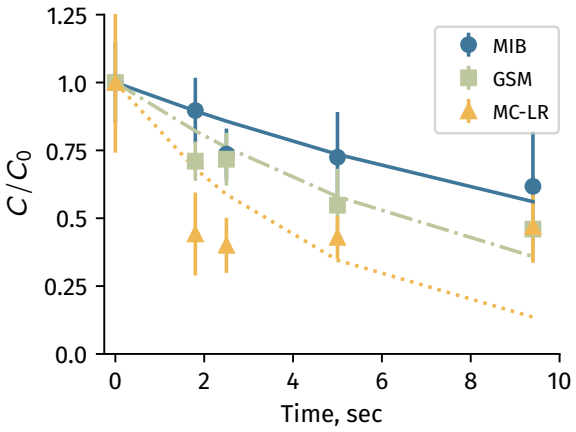

Figure 4.5: Degradation of micropollutants in the FTR for Lake A (Error bars denote standard deviation). Experiments conducted in duplicate using a lab-scale FTR UV/VUV reactor.

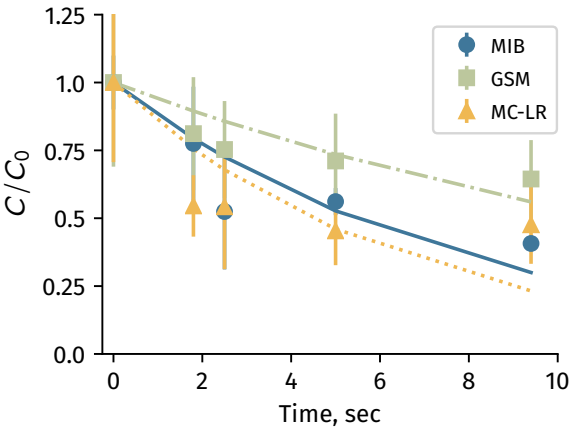

Figure 4.6: Degradation of micropollutants in the FTR for Lake B (Error bars denote standard deviation). Experiments conducted in duplicate using a lab-scale FTR UV/VUV reactor.

reduced following VUV treatment, the removals achieved may not be sufficient to completely eliminate toxicity and taste and odors. Under bloom conditions, removals of 40% to 60% of T&O compounds and MC-LR were achieved in a flow-through reactor. More importantly, the performance plateaued at higher fluences.

The impact of natural water source characteristics on the rate constants (developed in a collimated beam using UVA_{254}-adjusted fluences) was important. VUV performance was higher in the lake water with higher DOC/low mineral content compared to the lake with a low DOC/high mineral content.

The application of VUV led to a low ($< 10\%$) or moderate (up to 20%) average increase in the formation of either BDOC, THM, or HAA. Therefore, such negative impacts should be considered before using VUV technologies in driking water treatment plants. This process is a promising tool for applications in small and remote communities. However, further studies are warranted to discriminate the role of water matrix characteristics and the identification of the optimal VUV reactor location within a DWTP in order to optimize its performance and minimize the formation of oxidation by-products.

CHAPTER 5 Article 2 - Impact of vacuum UV on natural and algal organic matter from cyanobacterial impacted waters

Article authors

Flavia Visentin, Siddharth Bhartia, Madjid Mohseni, Sigrid Peldszus, Sarah Dorner and Benoit Barbeau

Journal and citation

Environmental Science: Water Research and Technology

F. Visentin, S. Bhartia, M. Mohseni, S. Peldszuz, S. Dorner and B. Barbeau, Environ. Sci.: Water Res. Technol., 2019, DOI: 10.1039/c9ew01068h.

5.1 Abstract

As mentioned in previous chapters, cyanobacterial blooms are a growing concern around the world. A feasible approach for treatment plants fed by sources contaminated with cyanobacteria is the incorporation of vacuum UV (VUV) technologies in their processes. VUV is a promising advanced oxidation process used to treat water impacted by cyanobacterial blooms, with potential applicability in small and remote communities because of its simplicity. In this work, water samples from three Canadian lakes periodically affected by cyanobacteria were used to assess the impact of natural and algal organic matter (NOM/AOM) on treatment with VUV. NOM and AOM were characterized before and after VUV treatment by size exclusion chromatography (SEC) and fluorescence emission-excitation matrix (FEEM). FEEM spectra were analyzed with the parallel factor analysis (PARAFAC) tool. As a result, we found seven principal components describing the whole dataset. Disinfection by-product (DBP) formation after VUV treatment was analyzed and trihalomethanes (THM) yield was calculated. THM yield increased by 15-20% after VUV treatment. Regarding DBP formation and NOM/AOM fractions from SEC, we found that humic substances are the most important fraction causing the increase in DBP formation with at least 3 higher yield than the other fractions: biopolymers, building blocks, low weight molecular acids and neutrals.

5.2 Introduction

Cyanobacteria affect freshwater resources from an esthetic perspective and are a health and safety concern. The World Health Organisation (WHO) has proposed two guideline alerts for managing drinking source waters containing cyanobacterial cells [141]. In Quebec (Canada) the Ministry of Environment developed a guidance manual for municipal drinking water treatment plant managers in which they suggest different actions ranging from: monitoring raw water quality, protective measures for the water intakes and implementation of treatment solutions [142]. The presence of cyanobacteria in the raw water could lead to toxins (cyanotoxins) in drinking water.

Amongst potential treatment options for cyanobacterial affected sources, advanced oxidation processes (AOP), such as ozone (O_3) + hydrogen peroxide (H_2O_2), ultraviolet light (UV) + O_3, UV + H_2O_2, are promising alternatives. AOP relies on hydroxyl radicals ($^{\bullet}OH$) to oxidize contaminants present in water and they have also been proposed to simultaneously control taste and odors (T&O) and cyanotoxins [111]. However, they can add complexity to drinking water treatment due to the need to rely on on-line chemical injection which may vary with water characteristics. In contrast, VUV is a robust and simpler AOP alternative that does not require chemical addition [92]. VUV relies on the use of a standard UVC lamp with a high purity quartz envelope and sleeve that enables a portion of short wavelength ($< 200\,nm$) photons to irradiate the water. These high energy photons react with water molecules to produce $^{\bullet}OH$ from the water itself [90]. This characteristic simplifies the operation of the system, and this process is deemed effective against pathogens (as most of the fluence is UVC) [143] and micropollutants [16]. Given its non-selective oxidant characteristic, $^{\bullet}OH$ will react with other compounds present in water, such as natural organic matter (NOM).

NOM is a complex mixture of organic substances in surface waters. Its presence adds color to water and may create aesthetic problems, such as T&O. In addition, NOM acts as a reservoir of precursors for the production of DBP following its reaction with free chlorine.

The main purpose of AOP is to degrade micropollutants but inevitably $^{\bullet}OH$ radical will oxidize NOM due to its non-selective nature. NOM degradation by AOP is site-specific as it is highly related to the water matrix. In theory, VUV can be efficient for NOM degradation because complete mineralization can be achieved [144] but the very high fluence needed makes this option costly. Hence, at the common fluences applied the reactions lead to a partial oxidation of NOM with an impact on DBP formation potential. In consequence, special attention must be given to DBP formation in VUV-treated waters as NOM oxidation may increase its reactivity with chlorine [144].

The NOM fraction originating from algal growth is known as algal organic matter (AOM). AOM extracted from algal cultures consists mainly of biopolymers (> 50%) while the remaining fractions are comprised of humic-like substances and/or low molecular weight (LMW) compounds [52]. AOM is composed of intracellular organic matter (IOM) and extracellular organic matter (EOM) [53]. During bloom season, EOM presence (its composition and concentration) affect water drinking treatment performance in a different way (in comparison when only background NOM is present) [145]. Thus, it can be useful to distinguish AOM from other background NOM to establish an appropriate water treatment strategy during bloom season. Henderson et al. (2008) demonstrates that AOM is of a very different character than NOM [53], which can, in turn, could be impacted differently by VUV.

The significant variety of compounds present in NOM makes impractical the determination of its exact composition. Therefore, there exists a wide range of characterization techniques. The denominated bulk parameters such as total, dissolved, biodegradable and assimilable organic carbon, UV absorbance at 254 nm (UVA_{254}), and specific UV-absorbance (SUVA) are used to determine the amount or characteristic of NOM within a sample [46]. These parameters are simple to measure and provide a general idea of what is present in the water. On the other hand, numerous methods are currently available for a more profound characterization, for example: hydrophobicity, size exclusion chromatography(SEC), nuclear magnetic resonance (NMR) spectroscopy, and fluorescence spectroscopy such as fluorescence emission-excitation matrix (FEEM). Among different techniques available for FEEM data processing, PARAllel FACtor analysis (PARAFAC) has received a lot of attention. PARAFAC is used to decompose trilinear multi-way data arrays. The decomposition allows to identify independent underlying signal components. According to Murphy et al. (2013) between 2011 and 2012, 70% of the studies where PARAFAC was applied were related to the study of NOM fluorescence [146]. Khan et al. (2019) applied PARAFAC to investigate the possibility of using fluorescence to characterise the AOM released by cyanobacterial and algal species. They observed that certain pairs of excitation-emission (Ex: Em) wavelengths could help for AOM monitoring in conjunction with cell pigments. For example, the fluorescence of amino acid-like material at (Ex:Em) = (290:345) nm dominated the AOM originating from Chlorella vulgaris, while that of Microcystis aeruginosa was dominated by fluorescence at (Ex:Em) = (355:475) nm (previously been associated only with terrestrially delivered substances). They proposed that fluorophores typically associated with "terrestrially-derived or humic-like" fluorescence ((335:438) nm, (355:475) nm and (300:390) nm) can also be produced by microorganisms [56]. Henderson et al. (2008) had reported a similar observation. They characterized AOM from algae and cyanobacteria species and found that tryptophan-like rather than humic/fulvic acid-like fluorescence dominated. In relationship with AOM

fluorescence from Microcystis aeruginosa, they noted that it was similar to that obtained for cyanobacteria in previous studies. However, additional fluorescence was detected in locations attributable to humic/fulvic-like [53].

Regarding SEC, carbon detection by chromatography is sometimes applied in drinking water to study NOM [46]. SEC coupled to three detectors (organic carbon, organic nitrogen and UV-absorbance), better known as LC-OCD-OND, allow to separate five NOM fractions: humic substances (HS), biopolymers (BP), building blocks (BB), LMW organic acids, and neutrals [147]. The OND provides information about the nitrogen content of the biopolymer and HS fractions [147].

Although the impact of AOP on NOM has been studied [78, 148], understanding the impact of AOM on VUV performance using algae-laden surface waters have yet to be reported. In order to understand how NOM and AOM characteristics were modified after VUV treatment, three Canadian lakes were selected with the objective of testing waters with dissimilar characteristics:

i. Lake A: low cyanobacteria concentration ($< 20{,}000\,\text{cells}\,\text{mL}^{-1}$) but high inorganic anion concentrations (chloride and alkalinity) as they are well known to impact negatively VUV performance

ii. Lake B: high total organic carbon (TOC) concentration ($14.7\,\text{mgC}\,\text{L}^{-1}$) during a cyanobacterial bloom condition ($195{,}000\,\text{cells}\,\text{mL}^{-1}$)

iii. Lake C: medium TOC concentration ($5.6\,\text{mgC}\,\text{L}^{-1}$) and low cyanobacteria concentration ($16{,}000\,\text{cells}\,\text{mL}^{-1}$)

iv. Lake C*: similar TOC concentration ($6.2\,\text{mgC}\,\text{L}^{-1}$) as earlier conditions for Lake C but with a higher cyanobacteria concentration ($33{,}000\,\text{cells}\,\text{mL}^{-1}$)

Natural cyanobacterial bloom conditions were tested because previous studies showed that cyanobacterial cells and toxins from environmental blooms were more resistant to oxidation compared to laboratory-cultured cells mixed with dissolved toxins [35].

5.3 Materials and methods

5.3.1 Source water location

To conduct this work, we sampled waters from three Canadian cyanobacteria-impacted lakes, identified as Lakes A, B, C and C* (Table 5.1). Lake A supplies drinking water to a community

with a bank filtration system and is located 40 km west of Montreal (Quebec, Canada). This lake, usually impacted by cyanobacterial blooms, was chosen due to its high chloride and alkalinity concentrations which reduce VUV performance. In Lake A, we sampled within the lake (raw water) and after the bank filtration (filtered water). Lake B is located 160 km east of Montreal (Quebec, Canada), and although it is used as a recreational water body, it is also under consideration as a source of drinking water for the area. Lake B was selected for this study because of its high cyanobacterial and organic carbon concentrations. In this case, only water from the lake was collected (raw water). Lake C is located 80 km southeast of Montreal (Quebec, Canada) and serves as a source of drinking water for several surrounding municipalities. Lake C experiences cyanobacterial blooms almost every summer. Lake C* describes a raw water collected during a severe cyanobacterial bloom. Samples from Lakes C and C* were collected in the drinking water treatment plant representing both raw and filtered water conditions.

Samples were collected from Lakes A and B on August 25, 2017 and September 7, 2017, respectively. Lake C and C* samples were collected on June 27, 2017 (no bloom present) and August 15, 2017 (cyanobacterial bloom present), respectively.

5.3.2 Source water characteristics

Source waters were characterized for total and dissolved organic carbon (TOC & DOC), and biodegradable dissolved organic carbon (BDOC) concentrations using a TOC analyzer (5310C Sievers Instruments Inc., USA). BDOC analysis was performed using the 30-d incubation batch method of Servais et al. [118]. The pH was measured with a Fisher Scientific pH-meter (Accumet, Fisher Scientific Instruments, USA), pre-calibrated with pH 4, 7 and 10 standard buffers (BDH VWR Analytical). Turbidity measurements (Hach 2100N turbidimeter) were assessed following Standard Methods #2130B [119]. Ions were measured by ionic chromatography ICS 5000 AS-DP DIONEX (Thermo Scientific) with an As18-4µm column. Alkalinity was measured by titration according to Standard Methods #2320 [119].

During field samplings, a YSI 6600 V2-4 water-quality multi-probe (YSI, Yellow Springs, Ohio, USA) equipped with a fluorescence 6131 phycocyanin, Blue Green Algae sensor was used to determine the dominance of cyanobacteria vs green algae in situ. The probe was located at the sampling point and samples were collected once the probe's measurements were stable. Cyanobacteria were assumed to be the predominant species when the phycocyanin level measured by the probe was higher than 2.4 RFU [149]. In addition, as a confirmation step, samples were preserved with Lugol's iodine for further taxonomic counts.

5.3.3 Vacuum UV experiments

A total of 4 sampling campaigns were conducted during the summer to autumn of 2017. For each campaign, lab-scale experiments were conducted in duplicate using a flow-through UV/VUV reactor (referred hereafter as FTR). The FTR is a 30-cm length annular photoreactor in a configuration similar to what could be installed for VUV treatment in a small drinking water treatment system. The FTR is equipped with an ozone generating low-pressure mercury lamp (Light Sources GPHVA357T5VH/4W, with a UV output at 254 nm equal to 110 µW cm^{-2} (11 W)) fitted in a dome-ended high purity quartz sleeve which was inserted in the center of a cylindrical Plexiglass® chamber. The applied fluence (H, mJ cm^{-2}) inside the FTR is controlled by adjusting the influent flow which feeds the 5-mm thick water inter-annular layer located between the inner reactive chamber and the outer sleeve [125].

A reference dose-response curve was established in a collimated beam reactor for MC-LR, geosmin and MIB [150]. Kinetics of VUV induced could be determined with more precision given that the pollutant concentrations and the local incident radiation are uniform in the reactor (see reference [124] for more details). This allows us to know the fluence (H) applied in each FTR experiment.

5.3.4 Natural organic matter characterization

FEEM spectra were measured with a spectrofluorophotometer RF-5301PC (Shimadzu, Japan) with a 4-mL macro quart, 10-mm path length cuvette (Fisherbrand). The excitation and emission wavelengths ranged between 250 nm to 380 nm and 350 nm to 600 nm, respectively. The slits for both excitation and emission were set to 10 nm with slow scanning speed. A dataset of 64 spectra were analyzed with the PARAFAC analysis decomposition routines for Excitation Emission Matrices (drEEM, version 0.2.0 toolbox [146] running on Matlab® R2018B software)

The dataset pre-processing was based on Murphy et al. (2010) and consisted of: (i) spectral corrections to account for the instrument systematic biases using the measured correction factors; (ii) correction of the inner filter effect with absorbance spectra for each sample; (iii) conversion to Raman units dividing the spectra by the Raman peak area between the emission wavelengths 381-426 nm at 350 nm excitation of MilliQ water; (iv) subtraction of the blank MilliQ water spectra. Samples that were diluted before measurements were corrected for the corresponding dilution factor. Finally, the Raman and Rayleigh scattering bands were excised from the spectra [151]. An example sample before/after processing is presented in the appendix (Figure A.4).

We developed a seven-components PARAFAC model to describe our dataset (64 spectra), where the number of components was selected after running preliminary tests and based on the sum of squared error indices (Figure A.1). Robustness of the models were tested by performing ten runs with random starting points under non-negativity constraint and 10^{-8} convergence criterion (Figure A.2). The selected final model was validated through split-half analysis where six different dataset "halves" are assembled to produce three validation tests [146, 152].

A size-exclusion chromatography system with organic carbon detection and organic nitrogen detection (LC-OCD-OND) was employed to characterize the samples. The system includes a weak cation exchange column (polymethacrylate based, TSK HW 50S, TOSOH, Japan) followed by three different detectors: organic carbon detector (OCD), organic nitrogen detector (OND), and UV (254 nm) detector (UVD) [147]. The organic carbon and organic nitrogen properties of various NOM components were characterized and quantified using a software program provided by the manufacturer (ChromCALC, DOC-LABOR, Karlsruhe, Germany). Prior to LC-OCD-OND analysis, all water samples were pre-filtered through a 0.45 µm polyethersulfone filter (Supor®, Pall Corporation). Details regarding the physical design and description of the LC-OCD-OND system can be found in Huber et al. (2011) [147]. Five NOM components, including biopolymers, humics, building blocks, LMW acids and LMW neutrals, were quantified using this technique.

5.3.5 Disinfection by product precursors

Samples were chlorinated under uniform formation conditions (1 ± 0.5 ppm Cl_2 at pH = 8.0 after 24 h incubation at 20 °C temperature) and free chlorine residual was quenched using ammonium sulphate ($2\,mg(NH_4)_2SO_4\ L^{-1}$). Samples were analyzed for trihalomethanes (THM) as described in USEPA 524-2 method (purge and trap (Aquatek 100 - Stratum 9800 de Teledyne Tekmar) coupled with GC-MicroECD (7890B Agilent)). Six HAAs (bromoacetic acid, bromochloroacetic acid, chloroacetic acid, dibromoacetic acid, dichloroacetic acid, and trichloroacetic acid) compounds were extracted by liquid/liquid extraction with methyl tertbutyl ether (MtBE) followed by derivatization with acidic methanol and analyzed by GC-ECD in accordance with USEPA Method 552.2 (GC-MicroECD, 7890B, Agilent).

5.3.6 Statistical analysis

Statistical analyses were realized using the Statistica 13 software package (Statsoft, OK, USA) with the level of significance set at $\alpha = 0.05$. Detected outliers were removed from the dataset prior to the statistical analysis. An ANOVA was conducted to identify the main

factors impacting DBP formation amongst the following variables: raw water, VUV treated raw water, filtered water and VUV treated filtered water.

5.4 Results and discussion

5.4.1 Source water characteristics

Table 5.1 presents the water quality characteristics of the three lakes representing four conditions. Lakes A and C had similar TOC (4.5 $\mathrm{mgC\,L^{-1}}$ to 5.6 $\mathrm{mgC\,L^{-1}}$) and were essentially composed of DOC as the total cell concentrations were moderate (less than 30,000 $\mathrm{cells\,mL^{-1}}$). In contrast, the TOC of Lake C* rose from 5.6 $\mathrm{mgC\,L^{-1}}$ to 6.2 $\mathrm{mgC\,L^{-1}}$ during the bloom event with 0.5 $\mathrm{mgC\,L^{-1}}$ being present as particulate organic matter.

Nevertheless, the most important cyanobacterial bloom was observed in Lake B, with 195,000 $\mathrm{cells\,mL^{-1}}$, and where TOC reached 14.7 $\mathrm{mgC\,L^{-1}}$, out which 2.5 $\mathrm{mgC\,L^{-1}}$ was particulate in nature. In Lake C, 16,000 cyanobacterial $\mathrm{cells\,mL^{-1}}$ were present indicating that WHO Alert Level 1 was not reached. On the other hand, Lake C* reached WHO Alert Level 1 with 33,000 cyanobacterial $\mathrm{cells\,mL^{-1}}$.

5.4.2 Vacuum UV experiments

A reference dose-response curve was established in a collimated beam reactor for which kinetics of VUV induced could be determined with more precision given that the pollutant concentrations and the local incident radiation are uniform in the reactor (see reference [124] or more details). This allowed us to know the equivalent fluence H applied in each FTR experiment.

For each source water, identical increased contact times were tested. Hence, different fluences were applied to every matrix water due to the variable UV absorbances (Table 5.2). For Lakes A, C and C* where cells concentrations were low ($<$ 20,000 $\mathrm{cells\,mL^{-1}}$, under WHO Alert Level 1) or moderate ($<$ 100,000 $\mathrm{cells\,mL^{-1}}$, under WHO Alert Level 2) [141], H ranged from 44 $\mathrm{mJ\,cm^{-2}}$ to 352 $\mathrm{mJ\,cm^{-2}}$. In Lake B, cells concentration was high ($>$ 100,000 $\mathrm{cells\,mL^{-1}}$, above WHO Alert Level 2) [141], therefore, the value of $\mathrm{UVA_{254}}$ was the highest measured during this work (0.296 $\mathrm{cm^{-1}}$, Table 5.1). As H is affected by water $\mathrm{UVA_{254}}$, in Lake B, H ranged from 20 $\mathrm{mJ\,cm^{-2}}$ to 160 $\mathrm{mJ\,cm^{-2}}$.

5.4.3 Natural organic matter characterisation by LC-OCD-OND

TOC and DOC are used to assess the performance of NOM removal in drinking water. For the ranges of fluence tested, DOC reductions after VUV treatment were never observed. Our results indicated an average decrease of UVA_{254} of 10% after 9.4 s of irradiation. Significant TOC degradation can be achieved only when high fluences are applied [78]. However, fractions measured by LC-OCD-OND (Figure 5.1) allow to observe how DOC composition was altered by VUV (Figure 5.1 and Figure 5.2). Regardless of the water matrix characteristics, the HMW fraction (BP, HS and BB) was reduced and the LMW increased. The largest variation of these two fractions is evident in Lake C* where the concentration of cyanobacteria is lower than in Lake B (Figure 5.2).

Correlation between HS aromaticity and HS molecular weight was reported several years

Table 5.1: Characteristics of the waters sampled from Lakes A, B, C and C*

	Lakes			
Parameters	**A**	**B**	**C**	**C***
TOC, $mgC\,L^{-1}$	4.5	14.7	5.6	6.2
DOC, $mgC\,L^{-1}$	4.5	12.2	5.5	5.7
BDOC, $mgC\,L^{-1}$	0.6	2.4	0.8	0.8
pH	8.4	7.7	7.4	7.1
Turbidity, NTU	0.9	15.7	3.0	9.7
UV absorbance @ 254 nm (UVA_{254}), cm^{-1}	0.085	0.296	0.144	0.171
Alkalinity, $mgCaCO_3\ L^{-1}$	170	14	49	54
Chloride, $mgCL^{-}\ L^{-1}$	94.0	12.0	7.90	8.20
Phycocyanin, RFU	-	7.70	0.05	0.15
Total cell count, $cells\,mL^{-1}$	30,000	220,000	29,000	35,500
Cyanobacteria cell count, $cells\,mL^{-1}$	20,000	195,000	16,000	33,000

Table 5.2: Fluence applied to waters samples from Lakes A, B, C and C*

	Lakes			
Fluence (H), $mJ\,cm^{-2}$	**A**	**B**	**C**	**C***
Minimum (retention time = 1.8 sec)	44	20	34	30
Maximun (retention time = 9.4 sec)	352	160	275	247

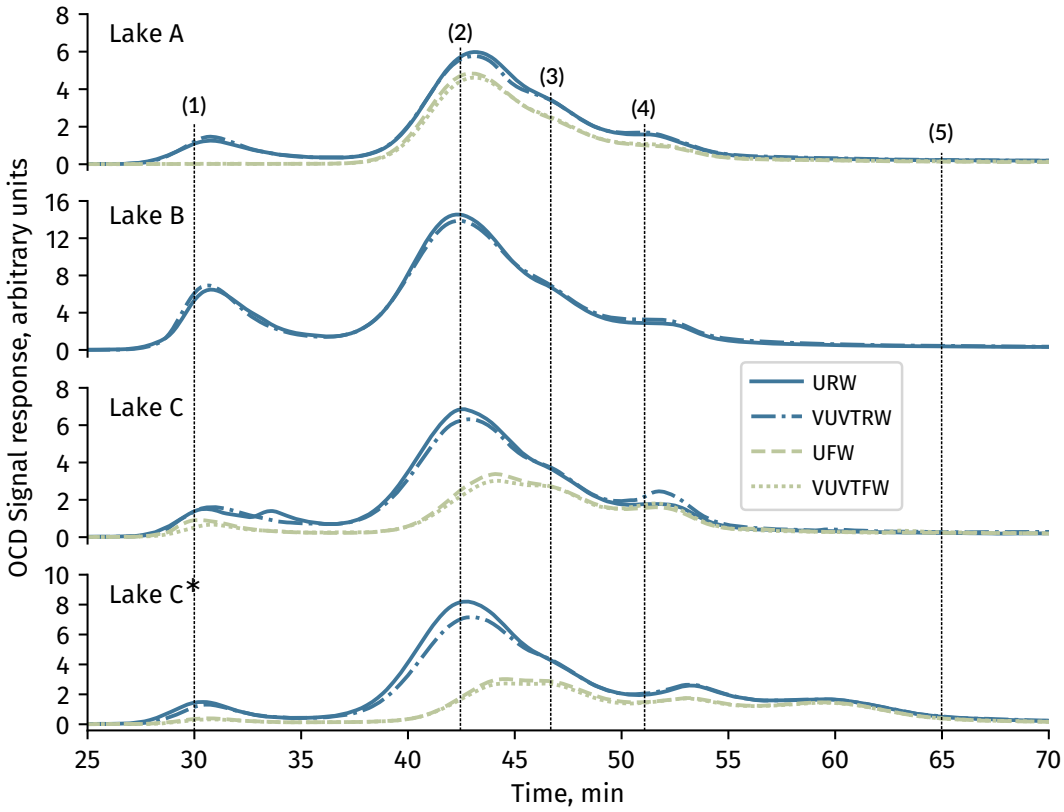

Figure 5.1: Five components of DOC measured by LC-OCD-ONC before and after (retention time equals to 9.4 s) VUV treatment. (1) biopolymers, (2) humic and fulvic acids, (3) building blocks, (4) LMW acids/humics and (5) LMW neutrals.

ago [153]. In 2011, Huber et al. presented an improved HS-diagram (Figure 5.3) [147]. After VUV treatment HS molecular weight and aromaticity decreased (except for raw water from Lake A and C, Figure 5.2) both in raw and filtered water. This means that VUV is breaking down larger molecules into smaller ones, as is also reflected in biodegradability. Biodegradability is observed through the increase of BDOC measurements, in our experiments BDOC increases from 20% to 35% were measured after VUV treatment (Figure A.2). These results are consistent with those of Imoberdorf and Mohseni (2014). Authors published a comparative study of the effect of VUV irradiation on NOM for different water sources. The authors also analyzed NOM by size exclusion chromatography and reported that HMW molecules were readily degraded (applied fluence in the study: up to 960 mJ cm^{-2}), and that LMW, which increases after irradiation, are formed through partial HMW degradation and are also partly degraded by hydroxyl radicals [154]. Similar trends were found in our experiments: HMW fraction decreases, and LMW fraction increases after VUV treatment (Figure 5.2).

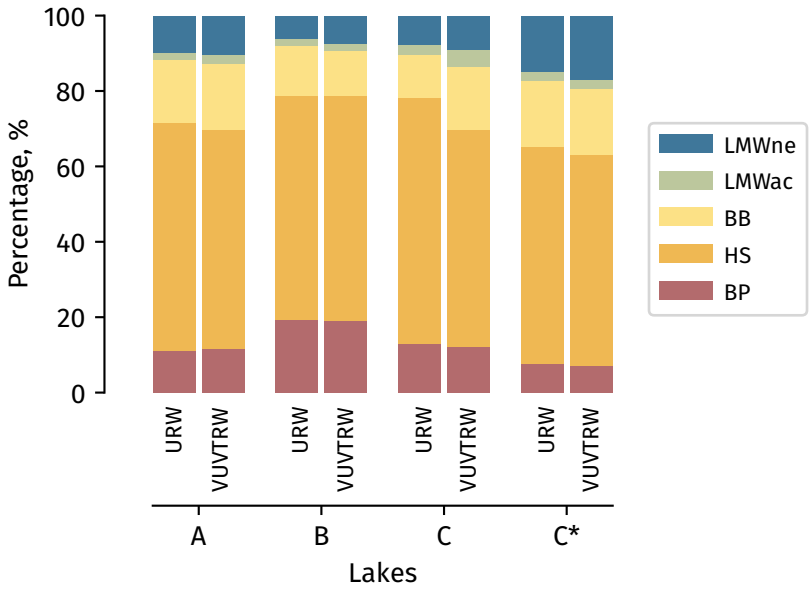

Figure 5.2: Five components of DOC measured by LC-OCD-ONC in raw water, before and after VUV treatment (retention time equals to 9.4 s). (BP) biopolymers, (HS) humics, (BB) building blocks, (LMWac) low-molecular weight acids, (LMWne) low-molecular weight neutrals.

The organic nitrogen (N) detector provides information about the subset of DOC that also contains N (including N content of biopolymer, biopolymer N/C ratio, N content of HS) (Figure A.1). N content of the biopolymer and the HS fraction can be used to calculate the N/C ratio in these fractions. The N content cannot be determined in the other fractions by LC-OCD-OND since the signals for nitrate and ammonia are masking them. The N content of biopolymer decreased slightly ($<$ 10% on average) in Lake C and C* after 9.4 s of VUV irradiation (fluence in Lake C and C* after 9.4 s, 275 mJ cm^{-2} and 247 mJ cm^{-2}, respectively). On the other hand, in Lake A and B this fraction increases 26% (fluence in Lake A after 9.4 s, 352 mJ cm^{-2}, while in Lake B for the same irradiation time the fluence was 160 mJ cm^{-2}). Lake B (Figure A.1(f)) showed the stronger changes in N composition before and after VUV irradiation. After 9.4 s of VUV irradiation N content of biopolymer increased by 35%. In filtered water, Lake C and C* had an 18% decrease of N concentration after 9.4 s irradiation (in Lake A, N content of biopolymer were below quantification limit. Fluence in Lake A, C and C* after 9.4 s, ranges from 247 mJ cm^{-2} to 352 mJ cm^{-2}).

N content of HS in irradiated raw waters (retention time of 9.4 s) increased in Lake A ($>$ 30%, with H = 352 mJ cm^{-2}) and decreased, 30% in Lakes B (H = 160 mJ cm^{-2}) and C

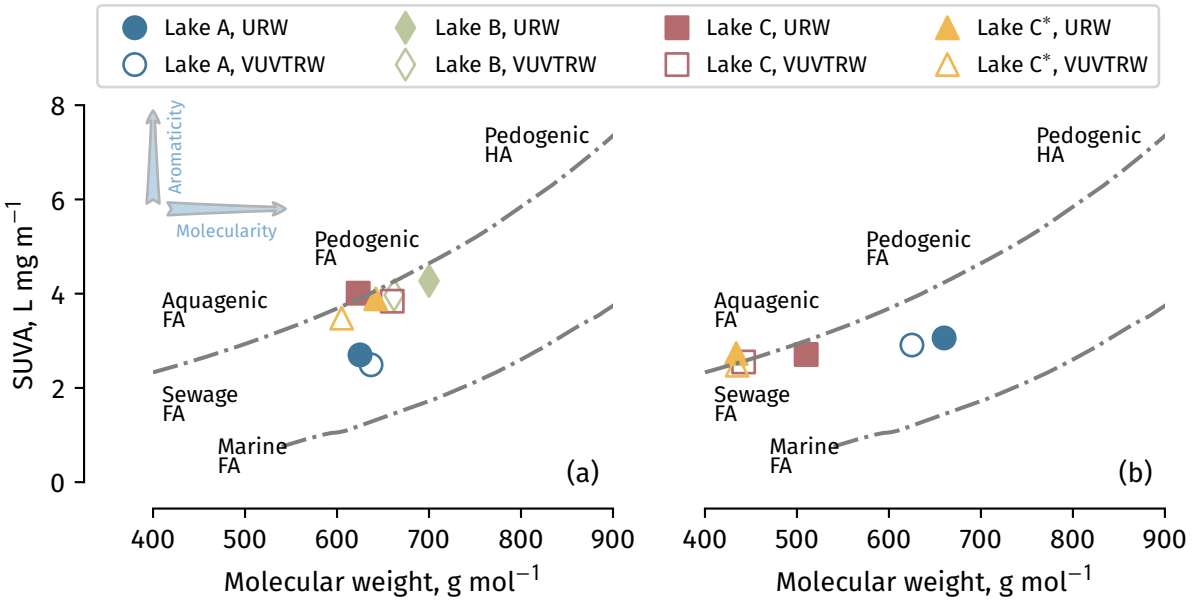

Figure 5.3: Humic substances diagram (HS-diagram) before and after (retention time equals to 9.4 s) VUV treatment. (a) Raw water: (URW) untreated raw water, (VUVTRW) VUV treated raw water. (b) Filtered water: (UFW) untreated filtered water, (VUVTFW) VUV treated filtered water. Based on [147].

($H = 275\,\mathrm{mJ\,cm^{-2}}$), and 16% in Lake C* ($H = 247\,\mathrm{mJ\,cm^{-2}}$). Regarding N/C biopolymer ratio, an increase on average more than 20% for all lakes was observed. The lower N/C biopolymer ratio was measured in raw water from Lake A (0.03) while Lake B, C and C* have on average an N/C biopolymer ratio of 0.05. Moradinejad et al. (2019) reported a similar trend when ozone was applied to two cyanobacterial cultured cells in a matrix of natural surface water. They reported an N/C ratio increase from 0.14 to 0.40 [155].

Understanding DON fraction and composition is useful to optimize the water treatment [156]. DON can react with oxidants to form nitrogenous DBPs and affect the speciation of regulated DBPs like THM and HAA [50, 157]. Algal events on drinking water sources may decrease the DOC/DON ratio. Consequently, DBP production could increase, especially if low DOC / DON ratios are observed [158]. In our study, N content of biopolymer had a significant and positive correlation with THM ($R^2 = 0.97$) and HAA ($R^2 = 0.74$) formation. DBP formation will be discussed in the following section.

5.4.4 FEEM and PARAFAC modeling

Online monitoring of cell pigments using probes facilitates the detection of cyanobacterial blooms. The measurement of cell pigments can be coupled with FEEM to better understand bloom's composition in order to improve the operation of drinking water treatment plants. Here, we measured FEEM in natural water samples (with and without blooms) before and after VUV treatment in order to assess the potential of FEEM for cyanobacterial bloom monitoring. PARAFAC helps to describe the data set (64 spectra) with a small number of (Ex:Em) pairs (7 PARAFAC's components). Overlapping PARAFAC with self-organising maps SOM allows to visualize which components are more relevant in each lake (more details can be found in the Appendix A).

The peaks of each component are shown in Figure 5.4, distributed in regions as proposed by Chen et al. (2003) [159]: C2(1) (fulvic acid-like), C1(1), C3(1), and C4(1) (humic acid-like), C5(1) and C7(1) (soluble microbial by-product-like) and C6(1) (aromatic protein II). The location of each peak is presented in Table 5.3. Given their strength and the protective characteristic of PARAFAC to overfitting [148], we also obtained, for each principal component, the secondary and tertiary (for component 1) peaks (Figure 5.4). In the fulvic acid-like regions there is one secondary peak, C2(2), associated to component 2. Three secondary peaks are located in the humic acid-like region, C1(2), C3(2) and C7(2), and tertiary peaks, C1(3). In the soluble microbial by-product like region includes the secondary peak, C6(2), while C2(2) lies in the region of aromatic protein II.

Based on Khan et al. [56], our peaks C7(1) and C5(1) are located in Chlorella vulgaris region, while, C1(2) peak is located in Microcystis aeruginosa region. It is important to note that we

Table 5.3: Peaks of PARAFAC components: emission and excitation primary peaks (in brackets, secondary and tertiary peaks)

Component	**(Ex:Em), (nm:nm)**
C1(1)	266:436, (338:436), (310:436)
C2(1)	238:408, (238:436)
C3(1)	310:400, (266:400)
C4(1)	330:412
C5(1)	298:372, (246:372)
C6(1)	238:336, (266:336)
C7(1)	282:356, (282:408)

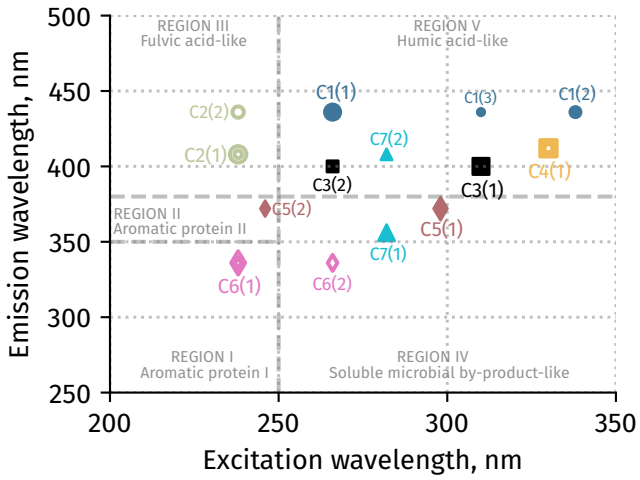

Figure 5.4: Location of the peaks of the seven-components resulted from the PARAFAC mode based on 64 spectral dataset (raw and filtered water from Lake A, C and C*, and raw water from Lake B). In brackets are indicated the primary (1), secondary (2), and tertiary (3) peaks. The distribution of the regions is after Chen et al. [159].

used natural cyanobacterial blooms and Microcystis aeruginosa was not the most abundant species in our samples. While Khan et al. used pure culture [56].

Further studies with natural cyanobacterial blooms in this field should be carried out to reach a stronger conclusion. Furthermore, location of C3(1) and C4(1) peaks, typically associated to humic acid-like, could be re-categorized as "microbial origin" as Khan et al. (2019) and Henderson et al. suggested [53, 56]. We found a secondary peak C1(2) located in that region suggesting that in natural cyanobacterial bloom it is possible to have a peak generated by cyanobacteria in the humic/fulvic-like region. We further investigate the correlation of peaks intensities in different regions. The maximum of fluorescence intensity ($F_{\max}$) in C1(2) is highly correlated with C3(1) and C4(1) ($R^2 > 0.90$). High correlations ($R^2 > 0.90$) were found between $F_{\max}$ of different components (Figure A.4). The component C5(1) (located in the soluble microbial by-product-like region) is highly correlated with C3(1) from humic acid-like region ($R^2 = 0.94$). At the same time, C3(1) has a high correlation with C1(1) ($R^2 = 0.97$) and C4(1) ($R^2 = 0.93$), all three are located in the humic acid-like region. C7(1) located in the soluble microbial by-product-like region is also correlated ($0.68 < R^2 < 0.71$) with components from humic acid-like region: C1(1) ($R^2 = 0.68$), C3(1) ($R^2 = 0.68$) and C5(1) ($R^2 = 0.71$). These correlations are useful to better understand fluorescence in humic acid-like region that could be generated by cyanobacterial blooms. As Henderson et al. (2008)

and Khan et al. (2019) suggested further work is required to elucidate current observations. Future work could focus on natural cyanobacterial blooms and their fluorescence in the region beyond (Ex:Em) = (250:300) nm. In terms of correlation between FEEM components and LC-OCD fractions, a high correlation ($R^2 > 0.80$) was found for C6(1) and C7(1) with BDOC and BP. A lower correlation ($0.59 < R^2 < 0.80$) was found for the same pair of components (C6(1) and C7(1)) and DOC and HS. On the other hand, no correlation was found between LC-OCD-OND fractions and peaks located in the humic acid-like region that are suspected from microbial origin (C3(1) and C4(1)).

5.4.5 DBP formation and yield after VUV treatment

In our study, humic substances, biopolymers and LMW all showed positive correlations with THM and HAA formation. LMW acid and neutral showed positive correlations with THM and HAA formation ($R^2_{\mathrm{THM}} = 0.74$ and $R^2_{\mathrm{HAA}} = 0.67$). A positive correlation was also found for humic substances ($R^2_{\mathrm{THM}} = 0.67$ and $R^2_{\mathrm{HAA}} = 0.84$). THM formation increased on average 12% (raw water) and 20% (filtered water) after 9.4 s of VUV irradiation (Figure 5.5). THM showed a positive correlation with $\mathrm{UV}_{254\,\mathrm{nm}}$ ($R^2 = 0.97$), SUVA ($R^2 = 0.75$), DOC ($R^2 = 0.95$) and DON ($R^2 = 0.97$). They also showed a positive correlation with components C7(1) ($R^2 = 0.82$) and C6(1) ($R^2 = 0.63$), i.e. the two PARAFAC components associated to microorganisms (more information about PARAFAC component correlation and THM is detailed in Figure A.9 in the Appendix).

Regarding HAA formation, 5% and 17% increases were measured on average after VUV treatment in raw and filtered water, respectively (fluence range from $20\,\mathrm{mJ\,cm^{-2}}$ to $352\,\mathrm{mJ\,cm^{-2}}$) (Figure 5.5). HAA also showed a positive correlation with $\mathrm{UV}_{254\,\mathrm{nm}}$ ($R^2 = 0.93$), SUVA ($R^2 = 0.87$), DOC ($R^2 = 0.97$) and DON ($R^2 = 0.74$). About PARAFAC, HAA showed negative correlations with components C7(1) ($R^2 = 0.56$) and C6(1) ($R^2 = 0.54$) (more details about the correlation between the PARAFAC components and HAA are presented in the Appendix (Figure A.9). Despite the positive correlations found between the different C fractions (HS, BP, BB, LWM acids and neutrals) and the formation of DBP, the fraction that was most important in the production of DBP was HS given that the waters had not been coagulated. Therefore, HS was the most abundant NOM fraction. This is the fraction that most contribute to the DBP production (slope values reported in Table A.3). We also calculated the THM yield (in $\mu\mathrm{gTHM\,mgTOC^{-1}}$, Table 5.4). Lake B showed the highest yield among all the raw water ($43\,\mu\mathrm{gTHM\,mgC^{-1}}$). However, Lake C* showed the highest yield after VUV treatment (27% higher than raw water). Even though Lake B had a 351 more intense bloom than Lake C*, it is likely that the background DOC was so high that it

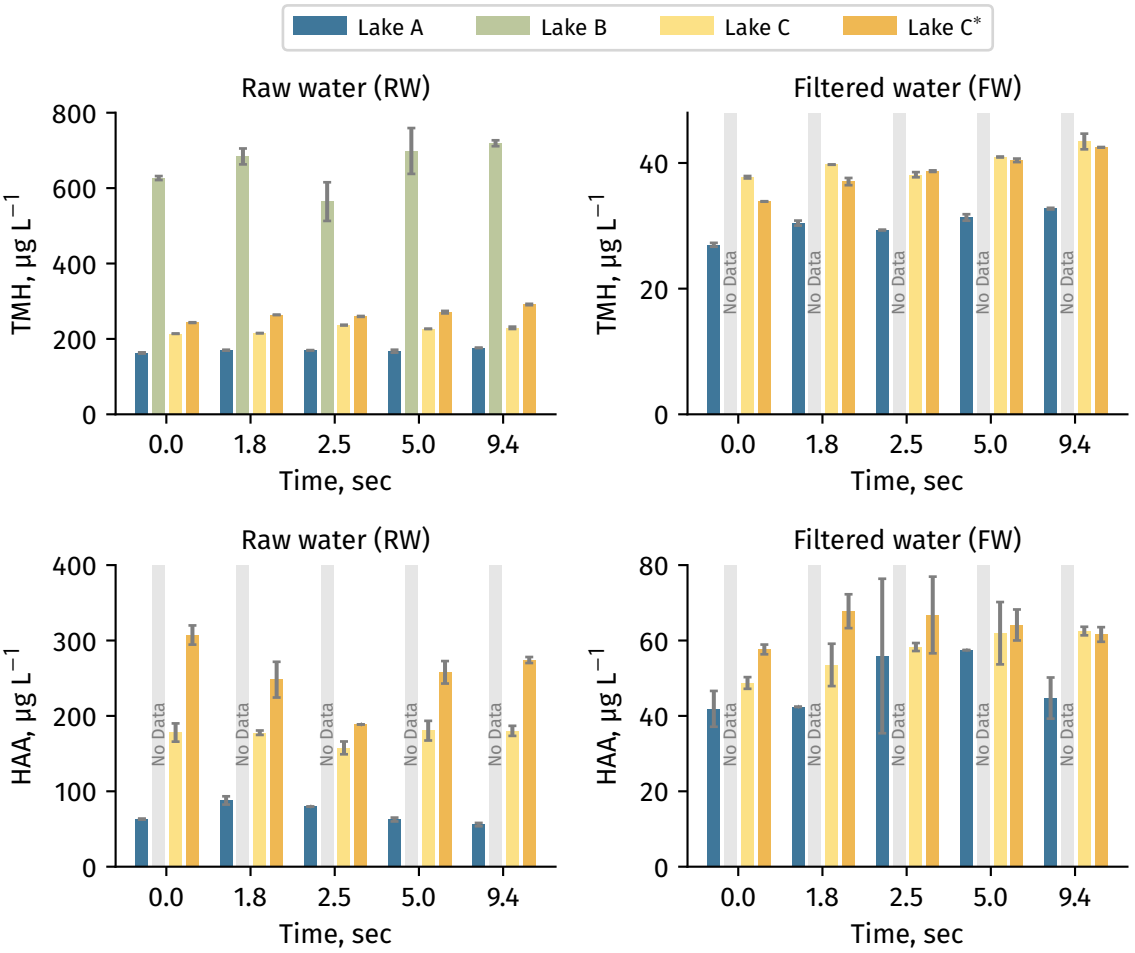

Figure 5.5: DBP formation (THM and HAA) in raw and filtered water, before and after VUV treatment. Error bars denote standard deviation.

reduced the oxidation and release of AOM from algae cells. Increased yield values are related to $^{\bullet}$OH exposure. $^{\bullet}$OH formation in VUV varies from lake to lake because it is related to the water matrix [150]. The $^{\bullet}$OH radical concentration would be producing hydroxylation of aromatics or the transformation to a more reactive form of NOM [160].

THM formation in Lake C and C* did not show any statistically significant difference. However, HAA formation in raw water from Lake C and C* were significantly different ($p < 0.05$), suggesting that AOM and not DOC background could be responsible for the HAA increase in Lake C*.

5.4.6 Effect of VUV treatment on contaminants degradation

During this work the performance of VUV was tested using tree different source waters with different inorganic, NOM, and cyanobacterial contents. Special focus on background NOM and AOM was done.

In a previous study, we assessed if VUV could simultaneously destroy MC-LR, MIB, and GSM in the same source waters. Under bloom conditions, removals of 40% to 60% of T&O compounds and MC-LR were achieved in the flow through reactor [150].

5.5 Conclusions

In this work, VUV was tested on three lakes with different inorganic, NOM, and AOM contents. The main objective was to assess how NOM and AOM were impacted by VUV treatment with respect to their characteristics as well as their propensity to form DBP.

In relation to the objectives set for this work, it can be summarized that:

1. **VUV impact on natural cyanobacterial blooms**. For the fluences investigated, minimal changes on the aggregate NOM measurement (DOC) were observed. However, LC-OCD-OND showed that the HMW fraction decreased while LMW increased after VUV treatment for all conditions tested (with and without natural cyanobacterial bloom). This observation was coherent with the slight reductions in UVA observed.

2. **FEEM as a tool to predict or identify cyanobacterial blooms**. FEEM is considered as a potential technique for online monitoring in drinking water. When cyanobacteria are present in raw water, attention should be given to Regions V and IV. Cyanobacterial blooms and their fluorescence in the region of excitation wavelengths

Table 5.4: Water yield, µgTHM mgC^{-1}, before (untreated) and after VUV irradiation (VUV treated, retention time equals to 9.4 s)

	Lakes			
	A	**B**	**C**	**C***
Untreated Raw Water (URW)	36	43	38	39
VUV Treated Raw Water (VUVTRW)	36	46	41	50
Untreated Filtered Water (UFW)	24	-	32	30
VUV Treated Filtered Water (VUVTFW)	28	-	37	38

larger than 250 nm and emission wavelengths larger than 300 nm need to be better evaluated.

3. **DBP formation after VUV**. In this work, in addition to analyzing the production of DBPs after VUV treatment, THM yield was calculated. In this way it was found that:

   a. While there are correlations between different carbon fractions and DBP formation, HS fraction is the one that causes the greatest increase in DBPs. The rate of change HS fraction with respect to DBPs (slope values reported in Table A.3) is at least 3 times higher than the rate of change from the rest of the fraction (BP, BB, LWM acids and neutrals).

   b. THM formation in raw and filtered water increased respectively by 12-20% after VUV treatment while HAA formation increased by 5% and 17%, respectively. These increases are coherent with the increased DBP reactivities (15-20%) calculated after VUV treatment in raw and filtered waters.

   c. PARAFAC components associated with cyanobacteria showed positive correlation with THM formation.

CHAPTER 6 Impact of Vacuum UV on cyanobacteria cell integrity and microcontaminants degradation

6.1 Introduction

In this chapter we present a study of the inactivation of cyanobacteria and the simultaneous degradation of cyanotoxins following VUV treatment. The objective was to validate the third hypothesis proposed in this thesis: VUV can simultaneously disinfect water and degrade organic trace contaminants. Algae are known to be quite resistant to UV disinfection. For example, Malayeri et al. (2017) summarized the literature on UV efficacy against various microorganisms [161]. Fluences in excess of $200\,\mathrm{mJ\,cm^{-2}}$ are needed to achieve more than 3 logs of inactivation of *M. aeruginosa*. Cyanobacteria are not considered *per se* as pathogenic but it is of interest to assess means to inactivate them given that they have been shown to regrow within water treatment plants [12]. Due to the release of $^{\bullet}$OH radicals, VUV is expected to provide an improved disinfection performance compared to UVC. For ozone applications, Cho et al. 2003 showed that the presence of free hydroxyl radicals could improved the inactivation of *B. subtilis* endospores by 40% [162]. With regards to VUV, Bai et al. (2019) recently studied the inactivation of natural cyanobacterial blooms and the concurrent degradation of cyanotoxins by $^{\bullet}$OH. They installed a plasma reactor that produce $^{\bullet}$OH to treat a coagulated-settled water from a drinking water treatment system in China. Authors conclude that $^{\bullet}$OH is an alternative for cyanobacterial inactivation and degradation without causing lysis [43]. However, other side reactions than $^{\bullet}$OH radicals oxidation may have caused the observed effects. To the best of our knowledge, not studies have reported up to now the impact of VUV on cyanobacteria inactivation.

To study whether the $^{\bullet}$OH produced by VUV can disinfect water while degrading cyanotoxins, we used two water matrices (buffered ultra-pure and surface water) in order to assess the role of NOM and mineralization. A mixture of cultured cyanobacterial cells (*Microcystis aeruginosa* and *Anabaena sp.*) that produced cyanotoxins were spiked to each water matrix. Both strains are hepatotoxins producers. A probe compound, carbamazepine (CBZ), was used to asses $^{\bullet}$OH radical formation during VUV treatment. CBZ is an antiepileptic drug very persistent in the aquatic environment resisting conventional water treatment. CBZ is a useful indicator because of its negligible direct photolysis at 254 nm relative to $^{\bullet}$OH oxidation under experimental conditions [163].

Two sets of experiments were carried out to treat water samples under $UV_{185\,nm}$ + $UV_{254\,nm}$ and $UV_{254\,nm}$ only. Algae inactivation was assessed by cytometry after staining the organisms.

6.2 Materials and methods

6.2.1 Preparation of spiked cyanobacteria samples

Microcystis aeruginosa (MA) strain CPCC 300 and Anabaena sp. (Ana) were cultured in Z8 and BG-11 medium, respectively. Cultures were incubated at 21 °C for 12 h light-darkness rotations at a photosynthetic photon flux density (PPFD) of 70 µmol s^{-1} m^{-2}. Cultures were harvested at stationary phase and spiked into buffered ultra-pure water (UPW, lightly buffered at a pH value of 7.0 with sodium phosphate. Final concentration of sodium phosphate = 2.5×10^{-3} M. This concentration allow us to simulate an alkalinity of 25 mg L^{-1} as $CaCO_3$) and in filtered surface water (SW) from Lake Champlain, southern Quebec (Canada), in order to reach a concentration of 10^6 cells mL^{-1} composed of 50% (in numbers) of each species (MA and Ana). The SW sample was collected from a water treatment plant intake in April and July 2019 (SF water quality parameters are summarized in Table 6.1) and filtered with a 0.45 µm membrane (Supor 45 µm, 47 m, PES PALL, Port Washington, NY, U.S.) prior to its use.

6.2.2 Cell counts, morphology and integrity

The cell count of MA was done with a Neubauer Chamber while Ana were counted with a Sedgewick Rafter counting cell. For flow cytometry, samples were stained with SYBR Green I (SG) and SG propidium iodide (PI) to determine total and compromised/dead cells [164]. The stains used both react with the nucleic acids but propidium iodide (as opposed to SYBR TM green) can only penetrate cells with compromised membranes. Use of PI to assess cells damaged by oxidation (e.g. chlorination or ozonation) has been commonly used in the past [165]. Cell integrity was determined using flow cytometry (BD Accuri C6 Flow Cytometer, San Jose, CA, USA) [155].

Table 6.1: Characteristics of the waters sampled.

Date	**DOC** mg C L^{-1}	**pH**	**UVA_{254}** cm^{-1}	**Alkalinity** mg $CaCO_3$ L^{-1}	**Chloride** mg Cl^- L^{-1}
Apr-2019	5.8	7.1	0.317	71	7.1
Jul-2019	5.2	7.8	0.153	89	7.1

6.2.3 Organic carbon characterization

Water samples were characterized for dissolved organic carbon (DOC) concentrations using a total organic carbon analyzer (5310C Sievers Instruments Inc., USA). A size-exclusion chromatography system with organic carbon detection and organic nitrogen detection (LC-OCD-OND) was also employed to characterize the samples. The system includes a weak cation exchange column (polymethacrylate based, TSK HW 50S, TOSOH, Japan) followed by three different detectors: organic carbon detector (OCD), organic nitrogen detector (OND), and UV (254 nm) detector (UVD) [166]. The organic carbon and organic nitrogen properties of various NOM components were characterized and quantified using a software provided by the manufacturer (ChromCALC, DOC-LABOR, Karlsruhe, Germany). DOC and LC-OCD-OND samples were filtered via pre-rinsed (with 1 L of ultra-pure water) 0.45 µm membrane (Supor 45 µm, 47 m, PES PALL, Port Washington, NY, U.S.) and stored in carbon free glass vials. Details regarding the physical design and description of the LC-OCD-OND system can be found in Huber et al. (2011) [166]. Five NOM components, including biopolymers, humics, building blocks, LMW acids and LMW neutrals, were quantified using this technique.

6.2.4 Characteristics of UV/VUV irradiation assays

Experiments were conducted in duplicate using a lab-scale collimated beam UV/ VUV reactor (referred hereafter as CBR). The stirred CBR setup allows the determination of the precise kinetics of VUV and UV induced reactions. Pollutant concentrations and the local incident radiation are uniform inside the CBR, allowing proper interpretation of the reaction kinetic. For VUV experiment, the CBR is equipped with an ozone-generating amalgam Hg lamp Light Sources GPHVA357T5VH/4W (UV output at 254 nm = 57 µW cm^{-2}) placed in a T-shape polyvinyl chloride (PVC) enclosure that is continuously purged with nitrogen to minimize the reaction of VUV radiation with the oxygen present in air (Figure 4.1) [123].

The water samples were contained in specially-designed cylindrical vessel made with regular quartz, except for the bottom part which is made of Suprasil quartz to allow 185 nm and 254 nm light to be efficiently transmitted. The vessel diameter and height are 4.8 cm (path length = 4.67 cm) and 1.5 cm, respectively. For experiments requiring 254 nm irradiation exclusively, the lamp was changed for a UVC amalgam germicidal lamp (Light Sources GPHVA357T6L/4W, UV output at 254 nm = 130 µW cm^{-2}).

6.2.5 Fluence calculations

The fluence applied in the CBR is calculated based on the following equation [143]:

$$H = E\,t \tag{6.1}$$

where H is the fluence in $\mathrm{mJ\,cm^{-2}}$, E is the irradiance in $\mathrm{mW\,cm^{-2}}$, and t is exposure time in s. Irradiance at 254 nm was measured through potassium iodide–potassium iodate (KI–KIO3) actinometry [117]. To obtain the applied fluence in the reactor, the fluence in (6.1) was multiplied by the correction factor, c_{F} [96, 123]:

$$H = c_{\mathrm{F}}\,E\,t = w_{\mathrm{F}}(\mathrm{UVA}_{254})\,r_{\mathrm{F}}\,p_{\mathrm{F}}\,d_{\mathrm{F}}\,E\,t \tag{6.2}$$

where $w_{\mathrm{F}}(\mathrm{UVA}_{254})$ is the water factor which is a function of UVA_{254} and source-water specific, r_{F} is the reflection factor (which considers the light reflected at the air-water interface), p_{F} is the petri factor (accounting for non-uniformity of irradiance), and d_{F} is the divergence factor of the beam. The values adopted were: $r_{\mathrm{F}} = 0.98$, $p_{\mathrm{F}} = 0.95$ and $d_{\mathrm{F}} = 0.73$ [124]. Knowing the irradiance ($E_{\mathrm{VUV}} = 0.87{\pm}0.13\ \mathrm{mW\,cm^{-2}}$ and $E_{\mathrm{UV\text{-}254nm}} = 1.03{\pm}0.10\ \mathrm{mW\,cm^{-2}}$) and the correction factors, the time for irradiation was adjusted to provide the targeted fluences, which ranged from $150\ \mathrm{mJ\,cm^{-2}}$ to $950\ \mathrm{mJ\,cm^{-2}}$ at 254 nm. The targeted fluences were selected to provide the expected treatment conditions needed to eliminate cyanotoxins.

6.2.6 Carbamazepine analysis

Samples were spiked with $100\ \mathrm{\mu g\,L^{-1}}$ of CBZ. CBZ initial concentration was selected based on literature review that suggest that $k_{\bullet\mathrm{OH\text{-}CBZ}}\,[\mathrm{CBZ}] >> k_{\bullet\mathrm{OH\text{-}Si}}\,[\mathrm{Si}]$ of all other scavengers [99]. CBZ was analyzed by ultra-high performance liquid chromatography coupled to tandem mass spectrometry (UHPLC-MS/MS) through a heated electrospray ionization source (heated-ESI). The system consists of a HTC thermopal autosampler (CTC analytics AG, Zwingen, Switzerland) with a 50 µL sample loop, a quaternary pump Accela 1250 (Thermo Finnigan, San Jose, CA) and a TSQ Quantiva mass spectrometer (Thermo Fisher 125 Scientific, Waltham, MA). The chromatographic separation was performed with a Hypersil Gold C18 column (100 mm × 2.1 mm, 1.9 µm particle size). The column temperature was set at 50 °C in a thermostated compartment [167]. The limit of detection (LOD) was $10\ \mathrm{ng\,L^{-1}}$.

6.2.7 Toxins analysis

A multi-toxin method based on on-line solid-phase extraction ultra-high performance liquid chromatography high-resolution mass spectrometry (SPE-UHPLC-HRMS) was applied during this work [168]. Chromatographic separation was done with a Thermo Scientific Dionex UltiMate 3000 RS pump and column compartment. A Dionex UltiMate 3000 pump was coupled to the system used for on-line solid phase extraction. Pumps were controlled by a Chromeleon 7.2 Software (Thermo Fisher Scientific, Waltham, MA and Dionex Softron GMbH part of Thermo Fisher Scientific, Germany). Sample injection was done with a PAL system RTC autosampler (Zwingen, Switzerland). A Hypersil Gold aQ ($20 \times 2\,\text{mm}$, $12\,\mu\text{m}$ particle size, $175\,\text{Å}$ pore size) column was used for on-line SPE. Chromatographic separation was performed with a Hypersil Gold C18 column ($100\,\text{mm} \times 2.1\,\text{mm}$, $1.9\,\mu\text{m}$ particle size, $175\,\text{Å}$ pore size) kept at $55\,^{\circ}\text{C}$. A Q-Exactive mass spectrometer was controlled by the X-Calibur 3.0 software (Thermo Fisher Scientific, Waltham, MA) [168, 169]. Table 6.2 summarizes the cyanotoxins analyzed along with the limit of detection (LOD) and the limit of quantification (LOQ) for each toxin.

6.3 Results

6.3.1 $^{\bullet}$OH radical formation

CBZ was used as a probe to assess VUV performance in comparison with $\text{UV}_{254\,\text{nm}}$. During our experiments CBZ degraded, in average, twice faster under VUV irradiation at 185 nm than at $\text{UV}_{254\,\text{nm}}$ irradiation (Figure 6.1 and Table 6.3). As expected, CBZ degradation was more efficient in buffered ultra-pure water than in surface water due to the low presence of NOM and other inorganic compounds that act as $^{\bullet}$OH scavengers [163]. It is worth highlighting the similar values of the rate constants k' for ultra-pure water under $\text{UV}_{254\,\text{nm}}$ and surface water under VUV. Later on, the energy consumption of each assay will be discussed, but we can anticipate that the UV lamp consumed 3 times more energy than the VUV lamp.

VUV irradiation of CBZ allowed determining the $R_{\bullet\text{OH,UV}}$ which can be defined as the free radical activity as described in Rosenfeldt and Linden (2007) [137] and described in Eq. (6.3):

$$R_{\bullet\text{OH,UV}} = \frac{1}{H} \int_0^t [^{\bullet}\text{OH}]\,\text{d}t = \frac{k'^{\text{D}}_{\text{T}} - k'^{\text{D}}_{\text{d}}}{k_{\bullet\text{OH-CBZ}}} \tag{6.3}$$

where the $R_{\bullet\text{OH,UV}}$ concept is defined as the experimentally determined $^{\bullet}$OH radical exposure per UV fluence in $\text{M}\,\text{s}\,\text{cm}^2\,\text{mJ}^{-1}$, H is the fluence in $\text{mJ}\,\text{cm}^{-2}$, k'^{D}_{T} is the rate constant obtained

VUV irradiation, $k'^{\mathrm{D}}_{\mathrm{d}}$ is that rate constant obtained under $\mathrm{UV}_{254\,\mathrm{nm}}$ irradiation and $k_{\bullet\text{OH-CBZ}}$ is the rate constant of CBZ under $^{\bullet}$OH oxidation. The $R_{\bullet\mathrm{OH,UV}}$ was 2.4 times higher in ultra-pure water than in surface water (Table 6.3).

Our results agree with previous studies on CBZ degradation by VUV and $\mathrm{UV}_{254\,\mathrm{nm}}$. In ultra-pure water, our pseudo-first order rate constants for CBZ degradation (obtained as k' values from Table 6.3 multiplied by E, irradiance in $\mathrm{mW\,cm^{-2}}$ for VUV and $\mathrm{UV}_{254\,\mathrm{nm}}$

Table 6.2: List of cyanotoxins analyzed, LOD ($\mathrm{ng\,L^{-1}}$) and LOQ ($\mathrm{ng\,L^{-1}}$)

Cyanotoxins	**Acronyms**	**LOD,** $\mathrm{ng\,L^{-1}}$	**LOQ,** $\mathrm{ng\,L^{-1}}$
Anatoxie-a	ANA-a	18	59
Cylindrospermopsin	CYN	41	135
Microcystin Total	MCtot	5	15
Microcystin-RR	MC-RR	11	37
[$\mathrm{Asp_3}$] Microcystin-RR	dmMC-RR	5	17
Microcystin-YR	MC-YR	10	34
Microcystin-HtyR	MC-HtyR	26	88
Microcystin-LR	MC-LR	15	49
[$\mathrm{Asp_3}$] Microcystin-LR	dmMC-LR	9	30
Microcystin-HilR	MC-HilR	14	45
Microcystin-WR	MC-WR	37	123
Microcystin-LA	MC-LA	9	32
Microcystin-LY	MC-LY	29	97
Microcystin-LW	MC-LW	8	27
Homoanatoxin-a	HANA-a	12	39
Anabaenopeptin-a	AP-A	20	67
Anabaenopeptin-b	APB	6	19

Table 6.3: CBZ rate constants and $R_{\bullet\mathrm{OH,UV}}$ (R-square fitting result is reported for each case)

	$k' \times 10^{-3}$, $\mathrm{cm^2\,mJ^{-1}}$		$R_{\bullet\mathrm{OH,UV}} \times 10^{-13}$, $\mathrm{M\,s\,cm^2\,mJ^{-1}}$
	VUV	$\mathbf{UV}_{254\,\mathrm{nm}}$	
Ultra-pure Buffered Water	8.7 ± 2.9 ($R^2 = 0.98$)	4.0 ± 0.0 ($R^2 = 0.95$)	3.9 ± 0.7
Surface Water	3.3 ± 0.5 ($R^2 = 0.96$)	2.0 ± 0.0 ($R^2 = 0.98$)	1.6 ± 0.6

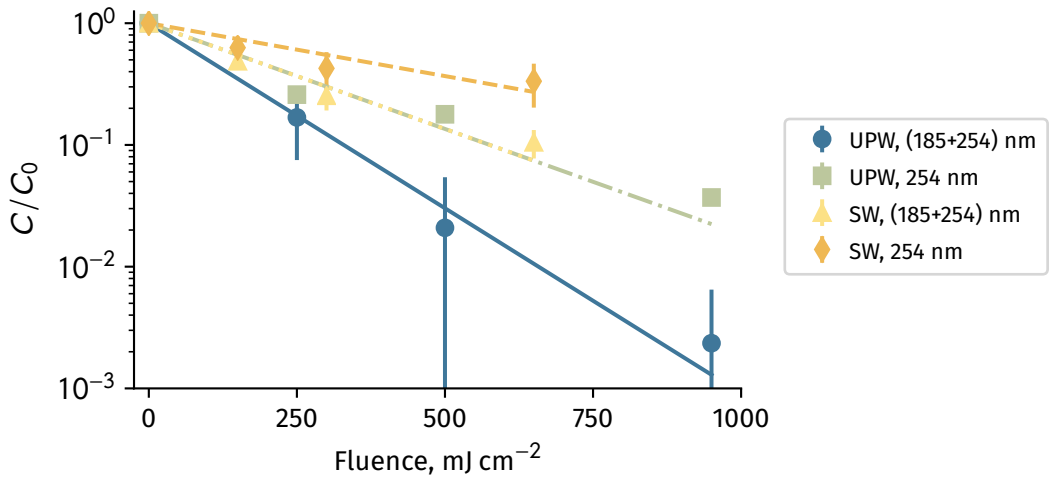

Figure 6.1: CBZ degradation by VUV in ultra-pure and surface water. Error bars denote standard deviation.

informed in Material & Methods section), are $7.6\times10^{-3}\,s^{-1}$ (under VUV irradiation) and $4.1\times10^{-3}\,s^{-1}$(under $UV_{254\,nm}$ irradiation). In surface water, values are $2.8\times10^{-3}\,s^{-1}$ (under VUV irradiation) and $2.1\times10^{-3}\,s^{-1}$ (under $UV_{254\,nm}$ irradiation). Matrix water highly affect VUV performance, in ultra-pure water under VUV irradiation CBZ degradation was 2.6 faster than in surface water.

Zhu et al. (2019) studied the degradation of CBZ under VUV and $UV_{254\,nm}$ irradiation in synthetic water (ultra-pure water with NOM from Suwannee River, International Humic Substances Society, USA). The pseudo-first order rate constants for CBZ degradation in their experiments under VUV treatment were: $6.3\times10^{9}\,M^{-1}\,s^{-1}$ without NOM and $1.5\times10^{9}\,M^{-1}\,s^{-1}$ with $4\,mgC\,L^{-1}$ of added NOM. They affirmed that CBZ was not significantly removed under $UV_{254\,nm}$ irradiation during their experiments (CBZ rate constant under $UV_{254\,nm}$ obtained from a graph in their article $= 1.7\times10^{-4}\,s^{-1}$). However, under VUV irradiation, 97.6% of CBZ degradation was achieved (with a second-order rate constant of the reaction between CBZ and $^{\bullet}OH$ of $1.4\times10^{9}\,M^{-1}\,s^{-1}$, and an optimal VUV intensity estimated by the authors as 7.5×10^{-8} Einstein s^{-1}, based on the electrical energy per order calculation). Although partially CBZ degradation could be caused by photolysis since the lamp used emits in simultaneous 254 nm and 185 nm, the authors concluded that CBZ degradation could be attributed to oxidation caused by reactive radicals formed during VUV irradiation. They arrived to this conclusion based on the fact that photons emitted at 185 nm are completely absorbed by water molecules (molar absorption coefficient, ε, of H_2O at 185 nm $= 1.8\,cm^{-1}$ [131]).

Consequently, no photon acts directly on CBZ degradation [163].

6.3.2 Cell inactivation assessment using flow cytometry

FCM technique allows us to monitoring cell integrity before and after treatment. Figure 6.2 presents FCM results before and after ($H = 250\,\mathrm{mJ\,cm^{-2}}$) VUV and $UV_{254\,nm}$ treatment. At that fluence, cell lysis was not observed (more details in the following section). Higher fluence ($> 500\,\mathrm{mJ\,cm^{-2}}$) may reflect the inability of the dye to properly stain the damaged DNA after the UV treatments, rather than an actual lysis of the cyanobacterial cells. On the mentioned figure is possible to observe viable (green delimited area) and dead (red delimited area) cells. In ultra-pure water 99.1% and 99.6% of cells added ([MA] = $5{\times}10^5\,\mathrm{cells\,mL^{-1}}$ + [Ana] = $5{\times}10^5\,\mathrm{cells\,mL^{-1}}$) were viable. For the same conditions, VUV was more effective in cell inactivation than $UV_{254\,nm}$. Cells inactivation under VUV were 1.5 faster than under $UV_{254\,nm}$ exclusively (Table 6.4). These results show that the concentration of $^{\bullet}$OH present influences cell viability. In 2019, Bai et al. reported the inactivation of natural cyanobacterial blooms by $^{\bullet}$OH. Authors also used FCM to evaluate cell inactivation and they affirmed that the $^{\bullet}$OH inactivation is caused by the breakage of DNA strands.

In terms of water matrix effect on cell inactivation, not influence was observed (either in VUV and $UV_{254\,nm}$), since k' values in ultra-pure and surface water are similar.

To achieve 3-log of inactivation, a fluence of $500\,\mathrm{mJ\,cm^{-2}}$ of VUV irradiation were needed. Regarding $UV_{254\,nm}$, more than $600\,\mathrm{mJ\,cm^{-2}}$ should be applied to get the same log inactivation.

6.3.3 Cyanotoxin degradation

Cyanotoxin analysis showed that concentrations of CYN, ANA-a, dmMC-RR, MC-RR, MC-YR, MC-WR, MC-LA, MC-LY, MC-LW were below the LOD. The other toxins have been detected (mostly different structural variants of MC) but in this chapter only MCtot data are presented.

Table 6.4: Cell inactivation rate constants (R-square fitting result is reported for each case)

	$k' \times 10^{-3}$, $\mathrm{cm^2\,mJ^{-1}}$	
	VUV	**$UV_{254\,nm}$**
Ultra-pure Buffered Water	13.0 ± 1.4 ($R^2 = 0.94$)	9.5 ± 2.1 ($R^2 = 0.93$)
Surface Water	13.0 ± 0.7 ($R^2 = 0.87$)	9.0 ± 2.8 ($R^2 = 0.77$)

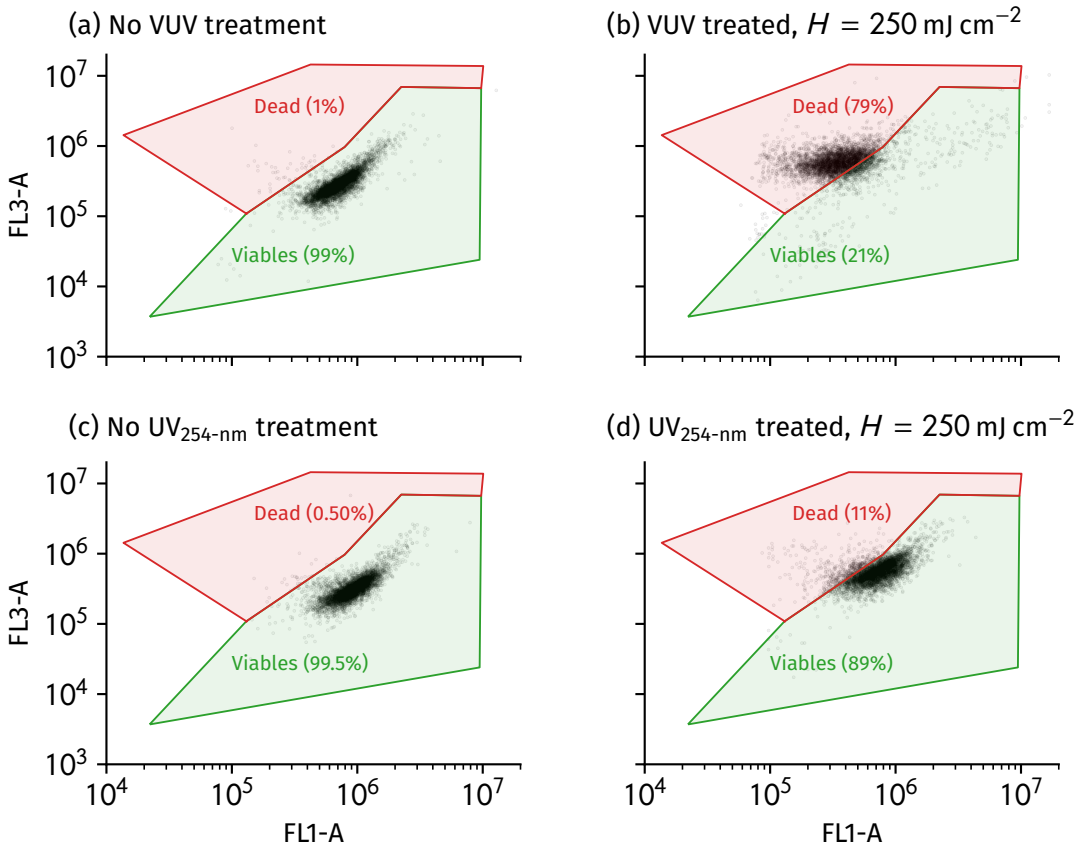

Figure 6.2: Cell integrity measured by FCM in ultra-pure water with MA + Ana: a) before VUV treatment, b) treated with VUV, $H = 250\,\mathrm{mJ\,cm^{-2}}$; c) before $\mathrm{UV_{254\,nm}}$ treatment, b) treated with $\mathrm{UV_{254\,nm}}$, $H = 250\,\mathrm{mJ\,cm^{-2}}$.

The first attempt was conducted exclusively with MA ($10^6\,\mathrm{cells\,mL^{-1}}$) to observe the response to VUV treatment and analyzing the MC total (Figure 6.4). The extracellular and total fractions were measured (the intracellular fraction was obtained as the difference between these two). In the untreated samples, the concentration of MC total was $C_0 = 64\,\mathrm{\mu g\,L^{-1}}$ (Figure 6.4). After applying the first fluence of VUV ($250\,\mathrm{mJ\,cm^{-2}}$) a reduction of only 10% was obtained. Although the reduction seems relatively small, the most important point to note here is that, at this fluence, there was no intracellular cyanotoxin release. The release of intracellular cyanotoxin becomes noticeable at a fluence of $500\,\mathrm{mJ\,cm^{-2}}$, reaching a full release at the maximum fluence tested ($950\,\mathrm{mJ\,cm^{-2}}$) (Figure 6.4). When analyzing the total fraction (intracellular + extracellular) altogether we observed between 40% to 50% degradation at the highest fluence. These results are consistent with those obtained by Visentin et al. 2019, where the effect of the water matrix on the degradation of MC-LR was studied [150]. Their

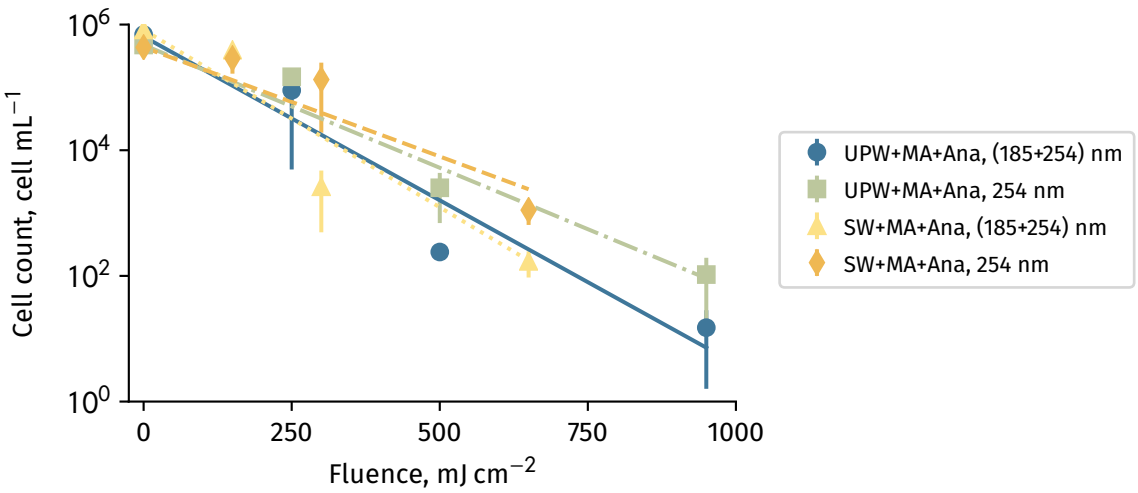

Figure 6.3: Removal after VUV and $UV_{254\,nm}$ in ultra-pure & surface water with MA + Ana.

results showed higher removal (up to 80%), at lower cell and initial cyanotoxin concentrations (1.95×10^5 cells mL^{-1} and $C_0 = 10\,\mu g\,L^{-1}$ of MC-LR). Moreover, in that case (Chapter 4) only MC-LR was spiked, while here, the data is for a mix of MC and the initial concentration is 6 times higher ($C_0 = 64\,\mu g\,L^{-1}$ of MCtot vs. $C_0 = 10\,\mu g\,L^{-1}$ of MC-LR). Higher initial concentration and a mix of cyanotoxin could explain why less degradation could be achieved in this section (in comparison with Chapter 4).

6.3.4 Electrical Energy Consumption per Order

The concept of electrical energy per order (EEO) was introduced by Bolton & Cater (1996) to benchmark the relative performance of different AOPs. It is defined as the number of kWh of electrical energy required to reduce the concentration of a pollutant by 1 order of magnitude (90%) in 1 m^3 of contaminated water. The EEO can be estimated as follow [170]:

$$\mathrm{EEO} = \frac{P\,t}{V\,\log\left(C_\mathrm{i}/C_\mathrm{f}\right)} \tag{6.4}$$

where EEO is the kWh m^{-3} order^{-1}, P is the energy input from UV light in kW, t is the irradiation time in h, V is the reaction volume in m^3, C_i is the initial concentration of CBZ in mol L^{-1} and C_f is the final concentration of CBZ in mol L^{-1}.

In both ultra-pure and surface waters, EEO in $UV_{254\,nm}$ was, on average, 3 times higher than

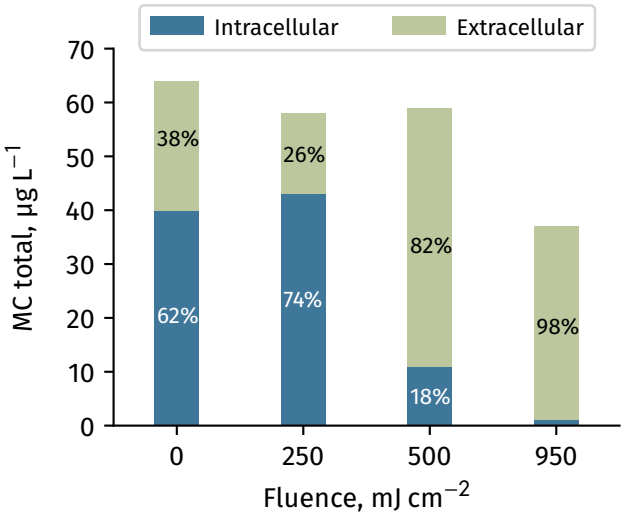

Figure 6.4: MCtot (intra and extracellular) degradation in ultra-pure water with MA treated by VUV.

for VUV (Table 6.5 and Table 6.6). This means that to obtain a similar degradation with $UV_{254\,nm}$, a larger amount of energy is required than when applying VUV. This estimation does not consider the cost of H_2O_2 required by $UV_{254\,nm}$ for the production of $^{\bullet}OH$ radicals that could improve the performance of $UV_{254\,nm}$. VUV, without needing to aggravate any chemical product would be, for the conditions tested in this case, more economical in terms of energy consumption.

6.4 Conclusions

In this chapter cyanobacteria cell integrity and cyanotoxin degradation by VUV were studied. Ultra-pure (pH = 7) and surface waters were spiked with MA and Ana (total cell concen-

Table 6.5: EEO in ultra-pure water

Fluence	**EEO, kWh m^{-3}**		
mJ cm^{-2}	**VUV**	**$UV_{254\,nm}$**	**$UV_{254\,nm}$/VUV**
250	11	29	2.6
500	10	45	4.4
950	14	47	3.4

Table 6.6: EEO in surface water

Fluence	**EEO, kWh m^{-3}**		
mJ cm^{-2}	**VUV**	**$UV_{254\,nm}$**	**$UV_{254\,nm}$/VUV**
150	40	100	2.5
300	43	117	2.7
650	52	182	3.5

tration added of 10^6 cells mL^{-1}, both strains were cyanotoxin producers) and treated under $UV_{254\,nm}$ and VUV irradiation. For that purpose, two UV lamps were used in a CBR: one that emits UV light at wavelength of 254 nm and another one that emits at (185+254) nm (VUV). The use of CBZ as a probe allows us evaluating the $^{\bullet}OH$ concentration produced by VUV. With regards to whether VUV can disinfect water contaminated by cyanobacteria and degrade cyanotoxins at the same time, we outlined the following conclusions:

6.4.1 $^{\bullet}OH$ radical formation

The $R_{\bullet OH,UV}$ increased 2.4-folds (3.9×10^{-13} M s cm^2 mJ^{-1} in ultra-pure water and 1.6×10^{-13} M s cm^2 mJ^{-1} in surface water). This is expected since the absence of NOM (which acts as a scavenger) allows $UV_{185\,nm}$ to break more H_2O molecules and increase the [$^{\bullet}OH$].

6.4.2 Cell inactivation

The reduction in cells integrity achieved was:

1. 5-logs in ultra-pure water ($H = 250\,mJ\,cm^{-2}$) by VUV irradiation
2. 4-logs in surface water ($H = 150\,mJ\,cm^{-2}$) by VUV irradiation
3. 3-log of inactivation were achieved at $500\,mJ\,cm^{-2}$ by VUV irradiation
4. 3-log of inactivation were achieved at $600\,mJ\,cm^{-2}$ by $UV_{254\,nm}$ irradiation

Cells integrity was measured by staining the genetic material of the cyanobacterial suspension. We suspect that these very high fluences are reflecting the inability of the dye to properly stain the damaged DNA after the UV treatments, rather than an actual lysis of the cyanobacterial cells.

6.4.3 MCtot degradation

1. For fluences $< 250\,mJ\,cm^{-2}$, intracellular MCtot was not released, and thus, preventing the production of intracellular MC degradation.
2. In average, 45% of MCtot was degraded after VUV irradiation ($C_0 = 64\,\mu g\,L^{-1}$ for an average fluence of $H = 800\,mJ\,cm^{-2}$).

6.4.4 Energy consumption

1. For CBZ degradation, VUV consumes less energy than $UV_{254\,nm}$ for the same removal.
2. In average, the EEO was 3 times lower under VUV irradiation that $UV_{254\,nm}$.

CHAPTER 7 GENERAL DISCUSSION

This chapter highlights the main findings from this research project. The overall objective was to analyze the effectiveness of VUV in surface waters affected by natural cyanobacterial blooms. The increasing frequency with which cyanobacterial blooms are affecting sources of drinking water is a growing concern worldwide. Small and remote communities exposed to this problem need a practical and simple solution because of the limited technical and financial resources they have at their disposal. The interest of VUV lies in its simplicity since it does not require the addition of chemicals to simultaneously disinfect and degrade contaminants .

Throughout this work, we examined the performance of VUV for the degradation of cyanotoxin and of T&O compounds. The disinfection was also analyzed based on the inactivation of cyanobacterial obtained after the VUV irradiation.

To achieve the objectives set out in Chapter 1, two different types of reactors were used: a collimated beam reactor (CBR) and flow-through reactor (FTR).

The CBR allowed us to study the reactions of pollutants of interest and to understand the degradation mechanisms that occur during the treatments. To verify the efficiency of $UV_{185\,nm}$ with respect to $UV_{254\,nm}$, two lamps were used in this reactor (Chapter 6). The first lamp emits energy at two wavelengths: 185 nm and 254 nm. The $UV_{185\,nm}$ fraction produces $^{\bullet}OH$ radicals, known for their non-selective oxidation capacity. The other lamp emits energy at 254 nm. This energy disinfects and degrades certain contaminants via photolysis, such as MC-LR, but is inefficient for the degradation of others, such as GSM, MIB and CBZ. Exchanging the lamps, one for the other, allowed as to assess the effect of $^{\bullet}OH$ radicals on the disinfection and degradation of pollutants.

The FTR was used to reproduce real conditions in a drinking water treatment plant (Chapter 4 and (Chapter 5). This allowed us to determine the performance of $UV_{185\,nm}$ in similar conditions to those found in the treatment of raw water affected by cyanobacteria.

VUV performance has been previously tested in the treatment of drinking water. The effects of temperature, inorganic compounds and NOM have been reported. In ultra-pure water with CBZ as a probe, from temperatures ranging 5 °C to 35 °C, VUV was less sensitive than $UV_{254\,nm}$+H_2O_2 [126]. In regard to NOM mineralization, these studies showed VUV performance depended on the nature of the NOM and on the presence of inorganic compounds, such as alkalinity, in the water matrix [78]. Concerning inorganic compounds, such as Cl^-,

experiments conducted in ultra-pure water with NOM from Suwannee River (International Humic Substances Society) showed that when the Cl^- concentration is higher than $20\,mg\,L^{-1}$, becomes the major 185 nm photon absorber rather than the water and chlorine atom radical ($^{\bullet}Cl$) is produced. $^{\bullet}Cl$ and $^{\bullet}OH$ both contribute to contaminant degradation [130]. The impact of Cl^- on the performance of VUV is directly related to the contaminant to be degraded and the water matrix to be treated. The impact, therefore, is site-specific and difficult to predict, because it depends on the reactivity of Cl^- with the compounds present in water [130]. Therefore, tests should be done in each case, especially if the concentration of Cl^- is greater than $20\,mg\,L^{-1}$. Bicarbonate, meanwhile, was found to be a radical scavenger as well as a 185 nm photon absorber (HCO_3^-, $\varepsilon_{185\,nm} = 290\,M^{-1}\,cm^{-1}$) [99].

Based on these previous findings, a lake with high natural contents of Cl^- and alkalinity (HCO_3^-) was selected for this project. The second lake had a low concentration of Cl^- and HCO_3^-, but a high concentration of DOC due to a cyanobacterial bloom. In this way, the interaction of NOM/AOM and inorganic ions could be evaluated against VUV treatment (Chapter 4). Our results showed that VUV performance was higher in the lake water with a high DOC/low mineral content compared to the lake with a low DOC/high mineral content.

Regarding cyanotoxin degradation MC-LR can be substantially degraded by $UV_{254\,nm}$ [73]. In combination with $UV_{185\,nm}$, greater degradation rates can be achieved. Chintalapati and Mohseni (2019) reported 90% MC-LR degradation in unfiltered bloom water at high cell densities ($230{,}000\,cells\,mL^{-1}$) by VUV ($UV_{185\,nm}$ + $UV_{254\,nm}$) [88].

Originally, the idea of this project was based on the treatment of natural blooms and toxins. Natural cyanobacterial bloom conditions were selected, because previous studies showed that cyanobacterial cells and toxins from environmental blooms were more resistant to oxidation as compared to laboratory-cultured cells mixed with dissolved toxins [35]. To better understand the performance of VUV, it is preferable to test toxins arising from natural blooms. Unfortunately, this is a bit difficult to accomplish since, so far, it is not possible to predict when a bloom will be toxic. Regrettably, natural cyanotoxins were not produced during our first batch of experiments so we decide to spike our samples with a commercial MC-LR (Chapter 4). While MC-LR is the most commonly cyanotoxin found, the effect of VUV was evaluated on a single toxin instead of a mix. Our results show MC-LR degradations that vary between 60 and 80% for a cyanobacterial bloom with similar cell concentrations as the one tested by Chintalapati and Mohseni (2019) (our sample contained $200{,}000\,cells\,mL^{-1}$, 88% of cells were *Cyanophyceae* class and 83% of the cyanobacterial cells corresponded to *Planktothrix agardhii*) but for a DOC 3.5 times higher. However, the lower performance in our tests may be due to the scavenger effect of the DOC. Having used raw water with a

high concentration of cells meant that the degradation of contaminants did not reach the recommended limits (total MC-LR (free plus cell-bound) is $1\,\mu g\,L^{-1}$ in drinking water [104]).

In the second part of the work (Chapter 6), a mix of cyanotoxins was treated by VUV, but they were produced by a laboratory-cultured cells. Despite being a mixture of cyanotoxins, most of them were MC. In this case, we observed between 40% and 50% degradation of MC-LR for a cell concentration of 1,000,000 cells mL^{-1}. Once again, the weaker performance may be related to the high concentration of carbon in the sample.

The effect of VUV on the degradation of other toxins such as CYN, saxitoxin and ANA-a were not assessed throughout this project. It is important to evaluate the degradation of a wide range of cyanotoxins because a robust treatment is required in the presence of cyanobacterial bloom. Not all oxidants are effective for all cyanotoxins, for example O_3 is efficient for the oxidation of MC, CYN and ANA-a but not for saxitoxin. Cl_2 is effective for the oxidation of MC, CYN, and saxitoxin, but not for ANA-a. $^{\bullet}OH$ radical is effective by oxidizing MC, ANA-a and CNY, but no data has been found regarding its effectiveness in degrading saxitoxin [171]. Verifying if VUV ($UV_{185\,nm}$ + $UV_{254\,nm}$) is effective for the degradation of all toxins would be very advantageous.

Another point to note that may explain the lower performance of our tests in FTR is related to reactor hydraulics. During the experiments, the flow inside the reactor was laminar (Reynolds from 320 to 1700). The reactor design is key to the effective operation of VUV. The 185nm photons are expected to be absorbed in the 0.3 cm layer close to the lamp [15]. This means that under a laminar regime, there is distinct probability a particle enters and leaves the reactor without having come into contact with this thin layer and consequently, the chances of being oxidized by the $^{\bullet}OH$ located within that layer are minimal. Increasing the turbulence of the reactor would increase the chances that the particles come into contact with the $^{\bullet}OH$ and thus be oxidized. Incorporating buffers into the reactor would favor an increase in the Reynolds [84].

The great advantage of VUV lies in the formation of $^{\bullet}OH$ from the photolysis of water directly without adding any chemicals by $UV_{185\,nm}$. In addition, being a wavelength that is always accompanied by another ($UV_{254\,nm}$) with a disinfection potential, it is extremely advantageous to be able to achieve simultaneous disinfection and degradation of a wide range of pollutants due to the character of oxidant non-selective $^{\bullet}OH$. VUV is simple to operate, has no toxic sorbents, backwash concentrates or cleaning chemicals which must later be disposed off. This is certainly appropriate for rural and remote community settings. However, the possibility of employing these new technologies at competitive costs and of integrating them into a pre-exixting treatment system remain unknown.

Another significant issue is the use of mercury lamps in UV drinking water treatment. In case of lamp breakage, it is the plant operators and the cleaning staff who are exposed to greater risks than the consumers [172]. A correct management and ultimate disposal in case of lamp breakage, implies training and cost that some small communities assume. At this point, the advances that have been made in UV-light emitting diode (LED) are very encouraging. UV-LED has the same advantage as the UV of mercury lamps, it does not require the addition of chemicals to photolyze contaminates and to disinfect. In addition they are also mercury free and more robust. Moreover, they feature virtually instantaneous start-ups and tunable wavelengths which gives great flexibility for reactor design [173].

7.1 Were the project hypotheses validated?

In Chapter 1 we defined the objectives and hypothesis for the project. The results obtained during this work can be summarized as follow.

i. **Cyanotoxin and T&O degradation from natural matrix water can be achieved by VUV**

   We found that VUV degrades all three contaminants. Although the maximum acceptable concentration (MAC) for MC-LR was not reached (this will be discussed below) and T&O concentrations are greater than $10\,\mathrm{ng\,L^{-1}}$ (also discussed below), it was possible to degrade the contaminants between 40% and 80% from their initial concentrations. The degree of influence of different compounds (organic or inorganic) affecting the VUV efficiency in each water matrix was also determined. (Article 1, Environ. Sci.: Water Res. Technol., 2019,5, 2048-2058)

   The impact of natural source water characteristics on the rate constants (developed in a collimated beam using $UV_{254\,nm}$-adjusted fluences) was important. VUV performance was higher in the lake water with a high DOC/low mineral content compared to the lake with a low DOC/high mineral content.

   Application of VUV led to a low ($< 10\%$) or moderate (up to 20%) average increase in the formation of either BDOC, THM, or HAA. Therefore, such negative impacts should be considered before applying VUV if chlorination is used as final disinfection.

   VUV is a promising option for application in small and remote communities affected by cyanobacterial blooms. However, further studies are warranted to discriminate the role of water matrix characteristics and the identification of the optimal VUV reactor location within a drinking water treatment plant in order to optimize its performance and minimize the formation of oxidation byproducts.

ii. **AOM has a greater impact on VUV performance than NOM**

In contrast to what was initially stated, NOM background seems to have greater influence on the formation of DBP after the chlorination of water treated by VUV. The C fractions determined by SEC and a correlation analysis with DBP show that the humic acid (HS) fraction is responsible for the increase in DBP formation. While there are correlations between different carbon fractions and DBP formation, HS fraction is the one that causes the greatest increase in DBPs. The rate of change HS fraction with respect to DBPs (slope values reported in Supplementary information, Article 2, Environ. Sci.: Water Res. Technol., X, Y, Z) is at least 3 times higher than the rate of change from the rest of the fraction (BP, BB, LWM acids and neutrals)

iii. **VUV can disinfect and degrade organic trace contaminants simultaneous**

We found that VUV can disinfect water contaminated by cyanobacteria and degrade organic trace such as CBZ and cyanotoxins. (Article 3)

7.2 MC-LR degradation from surface water

The MC-LR degradation achieved was 50% in the FTR reactor, which simulates the real working conditions. These results were published in the first article (Environ. Sci.: Water Res. Technol., 2019,5, 2048-2058): for Lake A, the initial concentration was $C_0 = 5.5\,\mu g\,L^{-1}$, and the final concentration obtained reached $C_f = 2.2\,\mu g\,L^{-1}$; for Lake B, the initial condition $C_0 = 11.5\,\mu g\,L^{-1}$ was degraded down to $C_f = 5.2\,\mu g\,L^{-1}$. The final concentration obtained in this work (Article 1) after degradation does not comply with the MAC of $1.5\,\mu g\,L^{-1}$ for MC-LR in drinking water, proposed by Health Canada. A possible explanation for these could be that the experiments were carried out in raw water without pre-treatment. The presence of particulate fractions of NOM and AOM and inorganic compounds highly affect VUV efficacy. Lake A contained high concentration of Cl^- ($94\,mg\,L^{-1}$) and alkalinity ($170\,mg\,L^{-1}$ as $CaCO_3$), both interfere with of VUV performance. Lake B contained a high carbon concentration mainly from a cyanobacterial bloom, leading to a high absorption of 185 nm and 254 nm radiation, directly interfering with the performance of the VUV treatment.

7.3 T&O degradation from surface water

Under bloom conditions, removals of 40% to 60% of T&O compounds were achieved in the FTR. The degradation obtained is not sufficient to allow a proper mitigation of a T&O event which can reach, for example, $40\,ng\,L^{-1}$ in St. Lawrence River. It should be noted that a

human can detect these compounds with a sensitivity as low as $10\,\mathrm{ng\,L^{-1}}$ [174]. Therefore, any treatment for their degradation must be highly efficient. For the degradation of pollutants to be optimal, the production of $^{\bullet}OH$ must be optimized, as discussed below. As suggested in the previous section, carrying out a pre-treatment (coagulation-settling-filtration) on the water affected by cyanobacteria could help to achieved the optimum conditions.

7.4 Influence of inorganic components from surface water on VUV performance

DOC and the major solutes, Cl^- and $HCO_3{}^-$, of a water matrix are expected to interfere with the elimination of contaminants under VUV treatment. Throughout this work, the use of different water matrices allowed evaluating the influence of these compounds on the effectiveness of VUV. For example, Lake A was chosen due to its high concentration of Cl^- ($94\,\mathrm{mg\,L^{-1}}$) and alkalinity (170 mg CaCO3 $\mathrm{L^{-1}}$) (Article 2).

Analyzing the fraction of absorbed photons ($f_{\mathrm{Si}} = \alpha_{\mathrm{Si}}/\alpha_{\mathrm{Total}}$) in Lake A, we found that Cl^- absorbed 75% of the 185 nm photons while H_2O absorbed 15%, and the remaining 10% is absorbed by $HCO_3{}^-$ and NOM. The way Cl^- acts on VUV performance is specific to each location [130]. For Lake A, it would appear to be responsible for the low efficiency in the degradation of contaminants due to the estimated high absorption. In contrast, for Lake B (where $[Cl^-] < 20\,\mathrm{mg\,L^{-1}}$), we determined that H_2O is the dominant 185 nm light absorber, since 50% of these photons are absorbed by water and 35% by Cl^-. In this case the absorption of NOM is almost 10%. Then the efficiency is clearly affected in Lake B by the high concentration of NOM and AOM, rather than $HCO_3{}^-$. Due to the important impact of Cl^- on VUV performance, water utilities should consider using a sulfate-based rather than a chloride-based coagulant for their physico-chemical treatment as the carryover of chloride to filtered water (the most probable location of the VUV step) would negatively impact its performance. (Article 1, Environ. Sci.: Water Res. Technol., 2019,5, 2048-2058).

7.5 NOM and AOM impact on VUV performance and DBP formation

Using chlorination as a disinfection method lead to chlorinated DBP formation. The interaction of chlorine with the NOM is the main route of production of DBP. In this project, water samples from three Canadian lakes periodically affected by cyanobacteria were used to assess the characteristics of NOM and AOM upon VUV treatment. NOM and AOM were characterized before and after VUV treatment by size exclusion chromatography and fluorescence emission-excitation matrix. DBP formation after VUV treatment was analyzed and trihalomethanes (THM) yields ((in $\mu\mathrm{gTHM\,mgC^{-1}}$) were calculated. The THM yields

increased by 15% to 20% after VUV treatment. Humic substances were found as the most important fraction causing the DBP formation to increase, with a yield at least 3 times higher than the other fractions: biopolymers, building blocks, low weight molecular acids and neutrals (Article 2). An appropriate NOM removal pre-treatment, like for example filtration, seems to be the best strategy to minimize DBP.

7.6 $^{\bullet}$OH production in ultra-pure and surface water

$^{\bullet}$OH production was estimated by using CBZ as a probe during experiments carried out with VUV and $UV_{245\,nm}$. CBZ was partially degraded by photolysis. Under VUV irraditation (185 + 254 nm) $^{\bullet}$OH is the main responsible for CBZ degradation [43]. Since $^{\bullet}$OH is a non-selective oxidant it reacts with CBZ as well as with other components present in the irradiated water. $^{\bullet}$OH production in ultra-pure water was 5 times higher than in surface waters. This can be explained due to the lack of competing NOM and inorganic compounds in ultra-pure water. Thus, more 185 nm photons are available to react with water molecules and produce more $^{\bullet}$OH radicals. Larger concentration of $^{\bullet}$OH radicals available leads to more efficient contaminant's degradation and disinfection in ultra-pure water.

7.7 Simultaneous cyanobacteria inactivation and cyanotoxin degradation by VUV

The degradation of cyanotoxins and T&O compounds through the application of VUV was demonstrated during this work. The use of different water matrices allowed us evaluating which NOM and AOM fractions have a greater impact on VUV efficiency. Among the carbon fractions identified by SEC, humic substances are the one that have the greatest influence on VUV performance (Article 2).

The formation of $^{\bullet}$OH was crucial not only for the degradation of cyanotoxins but also for the inactivation of cyanobacteria. These results encourage a strategy to considering VUV technology as a feasible and efficient drinking water treatment.

Particularly, due to its simplicity and high efficiency, the simultaneous disinfection and degradation of contaminants without injection of on-line chemicals, make VUV technology a smart and green option for small and remote locations.

7.8 Operating costs of VUV ($UV_{185\,nm}$+$UV_{254\,nm}$) vs. UV-C ($UV_{254\,nm}$)

Two different reactors were used to understand how VUV perform in cyanobacterial bloom contaminated water. The CBR allows studying the reactions at laboratory scale, while the FTR reproduces real working conditions using a lab scale reactor.

The performance of the UV treatments were compared using two different lamps, VUV ($UV_{185\,nm}$+$UV_{254\,nm}$) and UV-C ($UV_{254\,nm}$). An estimation of the electrical energy per order (Chapter 6) was also made.

To reach acceptable contaminants removal efficiencies with UV-C ($UV_{254\,nm}$) it needs to be combined with H_2O_2. The H_2O_2 reacts with $UV_{254\,nm}$ light to produce $^{\bullet}OH$. One of the disadvantages of this method is its inefficient use of H_2O_2. It requires an injection of a high dose of H_2O_2, when only a minimum fraction actually reacts with $UV_{254\,nm}$ to produce OH radicals. Consequently, at the end of treatment there is a high concentration of H_2O_2 unused that must be removed [175]. This adds extra cost and complexity to the process by the inefficient use of H_2O_2 and its subsequent removal step.

In Chapter 6 we showed that VUV ($UV_{185\,nm}$+$UV_{254\,nm}$) has a lower electrical energy per order than UV-C ($UV_{254\,nm}$) under the conditions studied. Previous works, for the same contaminants (atrazine, carbamazepine, diclofenac and sulfamethoxazole), showed that the electrical energy per order could be 2 to 7 times higher when using VUV in comparison with UV-C ($UV_{254\,nm}$) + H_2O_2 [125, 176]. The energy consumption of UV-C ($UV_{254\,nm}$) could be lower but requires the injection of H_2O_2 and its removal in the final step.

7.9 Benefits of using VUV to treat drinking water

UV light was used for the first time in Marseille (France) in 1910 for water disinfection. Since then, the conventional low pressure mercury lamp has become a mature technology and a method of choice for disinfection of chlorine-resistant pathogens. However, the presence of a heavy metal inside the lamp represents a possible mercury hazard [72]. Lamps that contain mercury (and the special management thus incurred) can be replaced by cleaner and more efficient ones, such as LED [177].

The possibility of changing traditional UV lamps for UV-LED has many advantages, for example: they are mercury free, compact, more durable and reach full power faster [173].The recent advances made in the application of the UV-LED for water disinfection are very promising. In lab tests, UV-LED is as efficient as the conventional low pressure UV lamps for microbe inactivation in water [178]. Recently, Jarvis et al. (2019) published an article

with data of a full-scale UV-LED reactor for disinfection of pathogenic microorganisms in drinking water treatment. The authors affirm that the full-scale UV-LED reactor was at least as effective as conventional mercury UV reactors for the inactivation of *Cryptosporidium spp.*. In a similar vein, the validation of a UV-LED reactor for the disinfection of municipal drinking water was published by Austin et al. (2019) [177]. This type of validation is necessary because current UV disinfection standards and protocols were developed exclusively for UV mercury lamps. But, they do not necessarily represent UV-LED disinfection performance [173].

The fact that the VUV technology is simple to operate without the on-line addition of chemicals in the process, makes it an "eco-friendly" solution. If this is added to the possibility of using mercury-free lamps, then VUV is even more interesting. Unfortunately, so far no published information related to VUV and LED has been found which leaves the door open for future work in this field.

7.10 Disadvantages of VUV in drinking water treatment

There is the possibility, as in any oxidation process, that a compound degraded by VUV produces a new compound (intermediates or products) even more toxic than the original. Zhu et al. (2019) studied CBZ degradation after VUV and toxicity of identified intermediates or products [163]. They found that VUV reduces CBZ ecotoxicity but also generates products with higher toxicity. This must undoubtedly be studied in depth before a real-scale application is designed.

7.10.1 Indirect impact of VUV

Although in most countries chlorination of drinking water is a common practice, it is known to produce DBP [48,64]. DBP levels in drinking water are usually regulated. In Quebec, the *"Règlement sur la qualité de l'eau potable"*, requires a maximum annual average concentration of total THM to be $80\,\mu g\,L^{-1}$. It also suggest a guideline of $60\,\mu g\,L^{-1}$ for HAA5. Meeting the local DBP standard is of utmost importance since DBP are considered potentially carcinogenic. Since the use of Cl_2 as residual disinfectant combined with VUV increases the DBP formation (Article 2). The use of any treatment option lowering NOM concentration prior to VUV treatment (e.g. a carbon filter) should be an effective solution. In the cases where the use of a free chlorine residual disinfectant is not required, VUV could be the last treatment step. However, under this scenario, the formation of BDOC should be considered as more important regrowth could be favoured by the effect of VUV on NOM which leads to increase in its biodegradability.

CHAPTER 8 CONCLUSION

8.1 Summary of Works

Cyanobacterial bloom occurrences are becoming more frequent around the world. In Canada, many small systems are supplied by lake waters which are prone to cyanobacterial blooms. In this study, VUV was demonstrated to be a potential treatment option for achieving chemical-free direct photolysis and advanced oxidation of one of the most common and toxic cyanobacterial toxins (MC-LR) and algae-derived T&O metabolites (MIB and GSM). The influence of NOM (background NOM and AOM) on VUV performance was evaluated. In the last part of the work, the influence of VUV on the cellular integrity of two cultured cyanobacterial (*Microcystis Aeruginsoa* and *Anabaena Sp.*) .) was studied, as well as their cyanotoxin degradation. A probe, carbamazepine, was used to better establish the role of $^{\bullet}$OH radicals. The conclusions of this study and recommendations for future work are discussed below.

i. **NOM from cyanobacterial-impacted water and its influence on VUV performance**

   NOM and AOM composition changed after VUV treatment according $UV_{254\,nm}$ and SUVA values. Even though minimal changes in DOC were observed, LC-OCD-OND fractions after VUV treatment were altered. The HMW fraction decreased while LMW increased after VUV treatment for all conditions tested (with and without natural cyanobacterial bloom).

   Recent publications based on the study of certain cultured cyanobacterial species have pointed toward FEEM as a useful tool to predict or identify cyanobacterial blooms. In this work, we performed FEEM analysis on natural blooms before and after VUV treatment. In congruence with the data discovered during the literature review, it was found that cyanobacterial bloom and its fluorescence need to be carefully evaluated to ensure that FEEM coupled with pigment online monitoring, can serve as a good cyanobacterial predictor. A closer study is required because it seems that certain species of cyanobacteria emit fluorescence in regions typically associated to humic substances.

ii. **Contaminant degradation achieved during this project: MC-LR, GSM, MIB and CBZ**

   Under bloom conditions, removals of 40% to 60% of T&O compounds and MC-LR were achieved in a flow-through reactor. MC-LR was reduced following VUV treatment.

However, for an $C_0 = 15\,\mu g\,L^{-1}$ the WHO and Canadian guideline of $1\,\mu g\,L^{-1}$ was not achieved (in Article 1: for Lake A, the initial concentration was $C_0 = 5.5\,\mu g\,L^{-1}$, and the final concentration obtained reached $C_f = 2.2\,\mu g\,L^{-1}$; for Lake B, the initial condition $C_0 = 11.5\,\mu g\,L^{-1}$ was degraded down to $C_f = 5.2\,\mu g\,L^{-1}$). The performance plateaued at higher fluences, due to matrix water influence (NOM, AOM and Cl^-, alkalinity, etc.) and the pilot reactor's hydrodynamic design. Given the limited depth of penetration of $UV_{185\,nm}$, the reactor's hydrodynamic design, ideally, should be designed to generate turbulence in order to increase the probability of exposure to the radiation present mostly near the sleeve wall. The low Reynold numbers achieved in our flow-through reactor (320 to 1700) were not favorable to achieve this objective.

iii. **Water quality impacts on VUV performance**

Water quality highly impacts VUV performance. NOM, AOM and inorganic components (such as Cl^- and HCO_3) interfere with contaminant degradation. The interference of these compounds and their effect on the efficacy of VUV is therefore highly site-specific. For example, MR-LR, GMS and MIB degradation in matrix water with higher DOC/low mineral content was more efficient when compared to the matrix water with a low DOC/high mineral content, suggesting that a high alkalinity/chloride concentration is more detrimental than a high DOC.

Regarding major solutes, Cl^- plays a significant role on VUV performance. The strong absorption of Cl^- at $UV_{185\,nm}$ concentrations higher than $20\,mg\,L^{-1}$ had already been shown to produce a decrease in performance [130]. However, Cl^- reacts with $UV_{185\,nm}$ to produce $^{\bullet}Cl$ and $^{\bullet}Cl_2^-$ radicals so they can be expected to react with the background water matrix to produce $^{\bullet}OH$. This $^{\bullet}OH$ radicals can also degrade targeted contaminants. However, the net effect is to reduce the performance of VUV. The impact, therefore, is site-specific and difficult to predict, because it depends on the reactivity of Cl^- with the compounds present in water [130].During this work, VUV performance decreased in the presence of high Cl^- concentration ($> 90\,mg\,L^{-1}$).

iv. **DBP formation after VUV treatment in cyanobacterial affected water**

The application of VUV led to a low ($< 10\%$) or moderate (up to 20%) average increase in the formation of either BDOC, THM, or HAA. Therefore, such negative impacts should be considered before using VUV technologies in drinking water treatment plants. This process is a promising tool for applications in small and remote communities. However, further studies are warranted to determine the role of water matrix characteristics and to identify the optimal VUV reactor location within a drinking water treatment plant in

order to optimize its performance and minimize the formation of oxidation by-products. Our results suggest that providing for a biological filtration post-treatment would be a good solution, given the fact that LMW compounds generated by VUV are in part biodegradable, as shown by the increase in BDOC concentrations (BDOC measured in mg C L^{-1} before and after $UV_{185\,nm}$, 2.4 millig/L to 3.1 millig/L).

v. **Cyanobacterial cell integrity after VUV treatment** (data not yet published)

In the case of the analysis of cell integrity two UV lamps were used: one that emits UV light at a wavelength of 254 nm and another one that emits at (254 + 185)nm (VUV). In this way, the effect of $^{\bullet}OH$ radicals on disinfection could be evaluated. $UV_{185\,nm}$ was more efficient than $UV_{254\,nm}$ in ultra-pure (buffer at pH 7 with sodium phosphate) and surface water. Reduction in cell integrity of 5 and 4-logs in ultra-pure and surface water, respectively, were achieved. 3-log of inactivation were achieved at 500 mJ cm^{-1} by VUV irradiation. To obtain the same inactivation with $UV_{254\,nm}$ it was necessary 600 mJ cm^{-1}.

Cells integrity was measured by staining the genetic material of the cyanobacterial suspension. We suspect that these very high effects reflect the inability of the dye to properly stain the damaged DNA after the UV treatments, rather than actual lysis of the cyanobacterial cells.

vi. **CBZ as a probe and $^{\bullet}OH$ concentration produced by VUV**

The use of CBZ as a probe in the last part of the work allowed us to estimate the concentration of $^{\bullet}OH$ present during $UV_{185\,nm}$ treatment. The same tests performed with ultra-pure water (buffer at pH 7 with sodium phosphate) and surface water showed that in the first matrix, the $R_{^{\bullet}OH,UV}$ is increased 2.43-folds (3.86×10^{-13} cm^2 M s mJ^{-1} in ultra-pure water and 1.59×10^{-13} cm^2 M s mJ^{-1} in surface water). This is expected because the absence of NOM (which acts as a scavenger) allows $UV_{185\,nm}$ to break up more H_2O molecules and give rise to more $^{\bullet}OH$.

8.2 Limitations

i. **Fluence applied throughout this project and energy consumption**

From the point of view of disinfection (fluence tipicaly applied on disinfection of parasites in Quebec 40 mJ cm^{-2}), the fluences (doses) applied throughout this work are higher than usual (20 mJ cm^{-2} to 352 mJ cm^{-2}). Nevertheless, it should be considered that the main objective was the degradation of cyanotoxins and and to achieve this, a larger dose was needed than for disinfection. It is clear that a higher fluence (dose) implies more energy

expenditure, and consequently VUV would be more costly to operate than a standard UVC process.

ii. **Cyanotoxin**

Initially, it was the intent to use cyanotoxins from a natural cyanobacterial bloom because it is known that these are more resistant than purified cyanotoxins produced by cells grown in laboratories or synthetic ones. Unfortunately, this was not possible in the first part of the work as the sampled natural bloom contained minimal concentrations of cyanotoxins. Therefore, purified MC-LR was spiked in the natural cyanobacteria bloom. Despite this, the use of natural cyanobacterial bloom allowed us to better understand the influence of NOM and AOM on VUV treatment.

8.3 Future Research

i. **New products or daughter component formation**

Undoubtedly, a point worth analyzing before applying a process of oxidation of contaminants in drinking water in real scale is the formation of new products / contaminants.

Throughout this work, the degradation of toxins, T&O components and a probe was observed and large reductions in their concentrations (from 40% to 99%) were noted.

However, a toxicity test was not carried out to evaluate the possibility of the formation of new products that could be even more toxic than the original ones. Further studies should address this issue.

ii. **Reactor design in large scale treatment**

During this project, two reactors were used, one on a laboratory scale and the other on a pilot scale. The design of a full-scale reactor that allows the use of $UV_{185\,nm}$ in a thin layer of a few millimeters will be a great challenge. Improved hydrodynamic design is needed to achieve high oxidation performance using $UV_{185\,nm}$.

iii. **Use of LED lamps**

The use of mercury lamps within the drinking water industry is a risk that needs to be managed. In future, the use of an LED lamp could avoid this risk. Since currently there are advances in the field of disinfection with LED at $UV_{254\,nm}$, the next step could be LED $UV_{185\,nm}$ for degradation of pollutants and simultaneous disinfection.

iv. **Energy consumption and costs**

Linked to the issue of reactor design, energy consumption and costs must also be considered.

REFERENCES

[1] W. Kardinaal and P. Visser, "Dynamics of Cyanobacterial Toxins," in *Harmful Cyanobacteria*, J. Huisman, H. Matthijs, and P. Visser, Eds. Springer, 2005, pp. 41–63.

[2] M. J. Codd G, Morrison L, "Cyanobacterial toxins: Risk management for health protection," *Toxicology and Applied Pharmacology*, vol. 203, no. 3 SPEC. ISS., pp. 264–272, 2005.

[3] S. U. Dow C, "Cyanotoxins," in *The Ecology of Cyanobacteria. Their Diversity in Time and Space*, B. Whitton and M. Potts, Eds. Kluwer Academic Publishers, 2002, pp. 613–632.

[4] J. O'Keeffe, "Cyanobacteria and drinking water- occurrence risks management and knowledge gaps for public health," National Collaborating Centre for Environmental Health, Report, 2019.

[5] A. Zamyadi, L. A. Coral, B. Barbeau, S. Dorner, F. R. Lapolli, and M. Prevost, "Fate of toxic cyanobacterial genera from natural bloom events during ozonation," *Water Research*, vol. 73, pp. 204–15, 2015. [Online]. Available: https://www.ncbi.nlm.nih.gov/pubmed/25682048

[6] J. M. O'Neil, T. W. Davis, M. A. Burford, and C. J. Gobler, "The rise of harmful cyanobacteria blooms: The potential roles of eutrophication and climate change," *Harmful Algae*, vol. 14, pp. 313–334, 2012. [Online]. Available: http://dx.doi.org/10.1016/j.hal.2011.10.027

[7] L. A. Coral, A. Zamyadi, B. Barbeau, F. J. Bassetti, F. R. Lapolli, and M. Prevost, "Oxidation of microcystis aeruginosa and anabaena flos-aquae by ozone: impacts on cell integrity and chlorination by-product formation," *Water Research*, vol. 47, no. 9, pp. 2983–94, 2013. [Online]. Available: https://www.ncbi.nlm.nih.gov/pubmed/23561505

[8] W. Kardinaal and P. Visser, *Dynamic of Cyanobacterial Toxins.* Springer, Eds., 2005, pp. 41–63.

[9] S. Wood, P. Holland, D. Stirling, L. Briggs, J. Sprosen, J. Ruck, and R. Wear, "Survey of cyanotoxins in new zealand water bodies between 2001 and 2004," *New Zealand Journal of Marine and Freshwater Research*, vol. 40, pp. 585–597, 2006.

[10] K. Sivonen, *Toxic Cyanobacteria*. Elsevier, 2009, pp. 290–[307].

[11] A. Zamyadi, S. Dorner, S. Sauve, D. Ellis, A. Bolduc, C. Bastien, and M. Prevost, "Species-dependence of cyanobacteria removal efficiency by different drinking water treatment processes," *Water Research*, vol. 47, no. 8, pp. 2689–700, 2013. [Online]. Available: https://www.ncbi.nlm.nih.gov/pubmed/23515107

[12] A. Zamyadi, S. Dorner, M. Ndong, D. Ellis, A. Bolduc, C. Bastien, and M. Prévost, "Low-risk cyanobacterial bloom sources: Cell accumulation within full-scale treatment plants," *Journal - American Water Works Association*, vol. 105, no. 11, pp. E651–E663, 2013.

[13] J. Westrick, D. Szlag, B. Southwell, and J. Sinclair, "A review of cyanobacteria and cyanotoxins removal/inactivation in drinking water treatment," *Analytical and Bioanalytical Chemistry*, vol. 397, no. 5, pp. 1705–1714, 2010. [Online]. Available: https://doi.org/10.1007/s00216-010-3709-5

[14] J. Crittenden, D. Trussell, D. Hand, H. K, and G. Tchobanoglous, *MWH ' s Water Treatment: Principles and Design*, 2012.

[15] G. Imoberdorf and M. Mohseni, "Modeling and experimental evaluation of vacuum-UV photoreactors for water treatment," *Chemical Engineering Science*, vol. 66, no. 6, pp. 1159–1167, 2011.

[16] M. Li, M. Hao, L. Yang, H. Yao, J. R. Bolton, E. Blatchley, and Z. Qiang, "Trace organic pollutant removal by VUV/UV/chlorine process: feasibility investigation for drinking water treatment on a mini-fluidic VUV/UV photoreaction system and a pilot photoreactor," *Environmental Science & Technology*, vol. 52, no. 13, pp. 7426–7433, 2018. [Online]. Available: https://www.ncbi.nlm.nih.gov/pubmed/29792423

[17] L. Yang, M. Li, W. Li, Y. Jiang, and Z. Qiang, "Bench- and pilot-scale studies on the removal of pesticides from water by VUV/UV process," *Chemical Engineering Journal*, vol. 342, pp. 155–162, 2018.

[18] O. T. Paerl H, "Harmful Cyanobacterial Blooms: Causes, Consequences, and Controls," *Microbial Ecology*, vol. 65, no. 4, pp. 995–1010, 2013.

[19] B. Whitton and M. Potts, "Introduction to the cyanobacteria," in *The Ecology of Cyanobacteria. Their Diversity in Time and Space*, B. Whitton and M. Potts, Eds. Kluwer Academic Publishers, 2002, ch. 1, pp. 1–11.

[20] C. Quiblier, S. Wood, I. Echenique-Subiabre, M. Heath, A. Villeneuve, and J.-F. Humbert, "A review of current knowledge on toxic benthic freshwater cyanobacteria e Ecology, toxin production and risk management," *Water Research*, vol. 47, pp. 5464–5479, 2013.

[21] B. Whitton and M. Potts, "Introduction to the Cyanobacteria," in *Ecology of Cyanobacteria II. Their Diversity in Space and Time*, B. Whitton, Ed. Springer, 2012, pp. 1–13.

[22] O. Roderick and G. Ganf, "Freshwater Blooms," in *The Ecology of Cyanobacteria. Their Diversity in Time and Sspace*, B. Whitton and M. Potts, Eds. Kluwer Academic Publishers, 2002, ch. 6, pp. 149–194.

[23] N. Jakubowska and E. Szeląg-Wasielewska, "Toxic Picoplanktonic Cyanobacteria—Review," *Marine Drugs*, vol. 13, no. 3, pp. 1497–1518, 2015.

[24] D. Anderson, P. Glibert, and J. Burkholder, "Harmful algal blooms and eutrophication: nutrient sources, compositions, and consequences," *Estuaries*, vol. 25, no. 4, pp. 704–726, 2002.

[25] C. Zhao, N. Shao, S. Yang, H. Ren, Y. G. P., Feng, B. Dong, and Y. Zhao, "Predicting cyanobacteria bloom occurrence in lakes and reservoirs before blooms occur," *Science of The Total Environment*, vol. 670, pp. 837–848, 2018.

[26] N. Tromas, N. Fortin, L. Bedrani, Y. Terrat, P. Cardoso, D. Bird, C. Greer, and J. Shapiro, "Characterising and predicting cyanobacterial blooms in an 8-year amplicon sequencing time course," *International Society for Microbial Ecology*, vol. 11, p. 1746–1763, 2017.

[27] A. Bukowska, T. Kaliński, M. Koper, I. Kostrzewska-Szlakowska, J. Kwiatowski, H. Mazur-Marzec, and I. Jasser, "Predicting blooms of toxic cyanobacteria in eutrophic lakes with diverse cyanobacterial communities," *Nature. Scientific Reports*, vol. 7, p. 8342–1763, 2017.

[28] WHO, "Guidelines for Drinking-Water Quality. Surveillance and Control of Community Supplies. Second edition," Geneva, 1997, accessed: 01.04.2019.

[29] B. Whitton and M. Potts, "Introduction to the cyanibacteria," in *Ecology of Cyanobacteria II. Their Diversity in Space and Time*, B. Whitton and M. Potts, Eds. Springer, 2012, ch. 1, pp. 1–11.

[30] A. Herrero and E. Flores, *The Cyanobacteria: Molecular Biology, Genomics and Evolution / Book*, 2008. [Online]. Available: http://www.horizonpress.com/cyan

[31] M. Welker and H. von Dohren, "Cyanobacterial peptides: Nature's own combinatorial biosynthesis," *6 Federation of European Microbiological Societies*, vol. 30, pp. 530–563, 2006.

[32] WHO, "Cyanobacterial toxins: Microcystin-LR in Drinking-water. Background document for development of WHO Guidelines for Drinking-water Quality," 2009.

[33] ——, "Guidelines for safe recreational water. Coastal and fresh waters." *Risk Management*, vol. 1, p. 253, Geneva, 2003.

[34] D. R. De Figueiredo, U. M. Azeiteiro, S. M. Esteves, F. J. M. Gonccalves, and M. J. Pereira, "Microcystin-producing blooms - A serious global public health issue," *Ecotoxicology and Environmental Safety*, vol. 59, no. 2, pp. 151–163, 2004.

[35] A. Zamyadi, S. L. MacLeod, Y. Fan, N. McQuaid, S. Dorner, S. Sauve, and M. Prevost, "Toxic cyanobacterial breakthrough and accumulation in a drinking water plant: a monitoring and treatment challenge," *Water Research*, vol. 46, no. 5, pp. 1511–23, 2012. [Online]. Available: https://www.ncbi.nlm.nih.gov/pubmed/22137293

[36] A. Zamyadi, N. McQuaid, M. Prévost, and S. Dorner, "Monitoring of potentially toxic cyanobacteria using an online multi-probe in drinking water sources," *Environmental Monitoring and Assessment*, vol. 14, no. 2, pp. 579–588, 2012.

[37] S. Kommineni, K. Amante, B. Karnik, and M. Sommerfeld, "Strategies for Controlling and Mitigating Algal Growth within Water Treatment Plants," *Water Research Foundation*, 2009.

[38] G. Joh and J. Lee, "Cyanobacterial biofilms on sedimentation basins in a water treatment plant in South Korea," *Journal of Applied Phycology*, vol. 24, no. 2, pp. 285–293, 2012. [Online]. Available: http://dx.doi.org/10.1007/s10811-011-9678-z

[39] A. Zamyadi, S. MacLeod, Y. Fan, N. McQuaid, S. Dorner, S. Sauvé, and M. Prévost, "Toxic cyanobacterial breakthrough and accumulation in a drinking water plant: A monitoring and treatment challenge," *Water Research*, vol. 46, no. 5, pp. 1511–1523, 2012.

[40] P. Pazouki, M. Prévost, N. McQuaid, B. Barbeau, M. L. de Boutray, A. Zamyadi, and S. Dorner, "Breakthrough of cyanobacteria in bank filtration," *Water Research*, vol. 102, pp. 170–179, 2016.

[41] T. Bartram, J., Burch, M., Falconer, I.R., Jones, G., Kuiper-Goodman, "Situation assessment, planning and management," in *Toxic Cyanobacteria in Water*, I. Chorus and J. Bartram, Eds. London: E&FN Spon, 1999, ch. Chapter 6, pp. 183–210.

[42] A. Z. Husein Almuhtaram, Yijing Cui and R. Hofmann, "Cyanotoxins and cyanobacteria cell accumulations in drinking water treatment plants with a low risk of bloom formation at the source," *Toxins*, no. 10:11, p. 430, 2002.

[43] M. Bai, Q. Zheng, W. Zheng, H. Li, S. Lin, L. Huang, and Z. Zhang, "$^{\bullet}$OH Inactivation of cyanobacterial blooms and degradation of toxins in drinking water treatment system," *Water Research*, vol. 154, pp. 144–152, 2019.

[44] J. Edzwald and T. John, *Chemincal Principles, Source Water Composition and Watershed Protection.* American Water Works Association, 2011, book section 3, pp. 3.58–3.67.

[45] D. Hendricks, *Organic Carbon as a Contaminant*, 1st ed. CRC Press, 2006, book section Appedix 2A, pp. 47–49.

[46] A. Matilainen, E. Gjessing, T. Lahtinen, L. Hed, A. Bhatnagar, and M. Sillanpää, "An overview of the methods used in the characterisation of natural organic matter (NOM) in relation to drinking water treatment," *Chemosphere*, vol. 83, no. 11, pp. 1431–42, 2011. [Online]. Available: https://www.ncbi.nlm.nih.gov/pubmed/21316073

[47] S. Krasner, H. Weinberg, S. Richardson, P. S., R. Chinn, J. Michael, Sclimenti, G. Onstad, and A. Thruston, "Occurrence of a new generation of disinfection byproducts," *Environmental Science and Technology*, vol. 40, no. 23, pp. 7175–7185, 2006.

[48] J. Rook, *Formation of Haloforms during Chlorination of Natural Water. Water Treatment and Examination*, 1974, vol. 23.

[49] USEPA, "Alternative Disinfectants and Oxidants Guidance Manual. EPA 815-R-99-014," Geneva, 1999.

[50] S. Richardson, "Disinfection by-products and other emerging contaminants in drinking water," *TrAC Trends in Analytical Chemistry*, vol. 22, no. 10, pp. 666–684, 2003.

[51] J. Lewis WM, W. Wurtsbaugh, and H. Paerl, "Rationale for control of anthropogenic nitrogen and phosphorus in inland waters," *Environmental Science & Technology*, no. 45, p. 10030–10035, 2011.

[52] L. Villacorte, Y. Ekowati, T. Neu, J. Kleijn, H. Winters, G. Amy, J. Schippers, and K. M, "Characterisation of algal organic matter produced by bloom-forming marine and freshwater algae," *Water Research*, vol. 73, pp. 216–30, 2015. [Online]. Available: https://www.ncbi.nlm.nih.gov/pubmed/25682049

[53] R. K. Henderson, A. Baker, S. A. Parsons, and B. Jefferson, "Characterisation of algogenic organic matter extracted from cyanobacteria, green algae and diatoms," *Water Research*, vol. 42, no. 13, pp. 3435–45, 2008. [Online]. Available: https://www.ncbi.nlm.nih.gov/pubmed/18499215

[54] L. Wang, F. Wu, Zhangr, W. Li, and H. Liao, "Characterization of dissolved organic matter fractions from lake hongfeng, southwestern china plateau," *Journal of Environmental Sciences*, vol. 21, no. 5, pp. 581–588, 2009. [Online]. Available: http://dx.doi.org/10.1016/S1001-0742(08)62311-6

[55] M. Leloup, R. Nicolau, V. Pallier, C. Yéprémian, and G. Feuillade-Cathalifaud, "Organic matter produced by algae and cyanobacteria: Quantitative and qualitative characterization," *Journal of Environmental Sciences*, vol. 25, no. 6, pp. 1089–1097, 2013.

[56] S. Khan, A. Zamyadi, N. R. H. Rao, X. Li, R. M. Stuetz, and R. K. Henderson, "Fluorescence spectroscopic characterisation of algal organic matter: towards improved in situ fluorometer development," *Environmental Science: Water Research & Technology*, vol. 5, no. 2, pp. 417–432, 2019.

[57] R. Henderson, S. Parsons, and B. Jefferson, "Successful Removal of Algae through the Control of Zeta Potential," *Separation Science and Technology*, vol. 43, no. 7, pp. 1653–1666, 2008. [Online]. Available: http://www.tandfonline.com/doi/abs/10.1080/01496390801973771

[58] N. Her, N. Gary, J. Sohn, and U. Gunten, "Uv absorbance ratio index with size exclusion chromatography (uri-sec) as an nom property indicator," *Journal of Water Supply: Research and Technology - AQUA*, vol. 57, no. 1, pp. 35–44, 2008.

[59] C. Chow, M. Drikas, J. House, M. Burch, and R. Velzeboer, "The impact of conventional water treatment processes on cells of the cyanobacterium microcystis aeruginosa," *Water Research*, vol. 33, no. 15, pp. 3253–3262, 1999.

[60] P. E. Stackelberg, J. Gibs, E. T. Furlong, M. T. Meyer, S. D. Zaugg, and R. L. Lippincott, "Efficiency of conventional drinking-water-treatment processes in removal of pharmaceuticals and other organic compounds," *Science of the*

Total Environment, vol. 377, no. 2-3, pp. 255–72, 2007. [Online]. Available: https://www.ncbi.nlm.nih.gov/pubmed/17363035

[61] P. Kumar, K. Hegde, S. K. Brar, M. Cledon, and A. Kermanshahi pour, "Physico-chemical treatment for the degradation of cyanotoxins with emphasis on drinking water treatment—how far have we come?" *Journal of Environmental Chemical Engineering*, vol. 6, no. 4, pp. 5369–5388, 2018.

[62] E. Rodríguez, G. D. Onstad, T. P. Kull, J. S. Metcalf, J. L. Acero, and U. von Gunten, "Oxidative elimination of cyanotoxins: Comparison of ozone, chlorine, chlorine dioxide and permanganate," *Water Research*, vol. 41, no. 15, pp. 3381 – 3393, 2007.

[63] M. A. Laszakovits J, "Removal of cyanotoxins by potassium permanganate: Incorporating competition from natural water constituents," *Water Research*, no. 155, pp. 86–95, 20019.

[64] B. . V. Corporation, Ed., *White'S Handbook of Chlorination and Alternative Disinfectants*, 5th ed., 2010.

[65] A. Zamyadi, Y. Fan, R. Daly, and M. Prevost, "Chlorination of microcystis aeruginosa: toxin release and oxidation, cellular chlorine demand and disinfection by-products formation," *Water Research*, vol. 47, no. 3, pp. 1080–90, 2013.

[66] USEPA, accessed: 2019-05-03. [Online]. Available: https://www.epa.gov/dwreginfo/chloramines-drinking-water

[67] E. Rodriguez, M. Najado, J. Meriluoto, and L. Acero, "Oxidation of microcystins by permanganate: Reaction kinetics and implications for water treatment," *Water Research*, vol. 41, pp. 102–110, 2007.

[68] J.-A. Park, B. Yang, J.-H. Kim, J.-W. Choi, H.-D. Park, and S.-H. Lee, "Removal of microcystin-LR using UV-assisted advanced oxidation processes and optimization of photo-fenton-like process for treating nak-dong river water, south korea," *Chemical Engineering Journal*, vol. 348, pp. 125–134, 2018.

[69] H. J. von Gunten U, "Bromate formation during ozonization of bromide-containing waters: Interaction of ozone and hydroxyl radical reactions," *Environmental Science & Technology*, vol. 28 (7), pp. 1234–1242, 1994.

[70] G. Onstad, S. Strauch, J. Meriluoto, G. Codd, and von Gunten U, "Selective oxidation of key functional groups in cyanotoxins during drinking water ozonation," *Environmental Science & Technology*, vol. 41 (12), pp. 4397–4404, 2007.

[71] N. B. Newcombe G, "Treatment options for the saxitoxin class of cyanotoxins," *Water Supply*, vol. 2 (5-6), pp. 271–275, 2002.

[72] J. Bolton and C. Cotton, *The Ultraviolet Disinfection Handbook*, 1st ed. American Water Works Association, Denver, CO, 2008.

[73] X. He, A. A. de la Cruz, A. Hiskia, T. Kaloudis, K. O'Shea, and D. D. Dionysiou, "Destruction of microcystins (cyanotoxins) by UV-254 nm-based direct photolysis and advanced oxidation processes (AOPs): influence of variable amino acids on the degradation kinetics and reaction mechanisms," *Water Research*, vol. 74, pp. 227–38, 2015. [Online]. Available: https://www.ncbi.nlm.nih.gov/pubmed/25744186

[74] X. He, M. Pelaez, J. A. Westrick, K. E. O'Shea, A. Hiskia, T. Triantis, T. Kaloudis, M. I. Stefan, A. A. de la Cruz, and D. D. Dionysiou, "Efficient removal of microcystin-LR by UV-C/H_2O_2 in synthetic and natural water samples," *Water Research*, vol. 46, no. 5, pp. 1501–10, 2012. [Online]. Available: https://www.ncbi.nlm.nih.gov/pubmed/22177771

[75] X. Liu, Z. Chen, N. Zhou, J. Shen, and M. Ye, "Degradation and detoxification of microcystin-LR in drinking water by sequential use of UV and ozone," *Journal of Environmental Sciences*, vol. 22, no. 12, pp. 1897–1902, 2010.

[76] X. Zhang, J. He, S. Xiao, and X. Yang, "Elimination kinetics and detoxification mechanisms of microcystin-lr during uv/chlorine process," *Chemosphere*, vol. 214, pp. 702 – 709, 2019.

[77] S. Zhou, Y. Shao, N. Gao, S. Zhu, L. Li, J. Deng, and M. Zhu, "Removal of microcystis aeruginosa by potassium ferrate (VI): Impacts on cells integrity, intracellular organic matter release and disinfection by-products formation," *Chemical Engineering Journal*, vol. 251, pp. 304–309, 2014.

[78] G. Imoberdorf and M. Mohseni, "Degradation of natural organic matter in surface water using vacuum-UV irradiation," *Journal of Hazardous Materials*, vol. 186, no. 1, pp. 240–6, 2011. [Online]. Available: https://www.ncbi.nlm.nih.gov/pubmed/21122985

[79] A. Serrano Mora and M. Mohseni, "Temperature dependence of the absorbance of 185 nm photons by water and commonly occurring solutes and its influence on the VUV advanced oxidation process," *Environmental Science Water Research & Technology*, vol. 4, pp. 1303–1309, 2018.

[80] A. Braun, H. Pintori, H. Popp, Y. Wakahata, and W. M, "Technical development of uv-c- and vuv-photochemically induced oxidative degradation processes," *Water Science & Technology*, vol. 49(4), pp. 235–240, 2014.

[81] W. Buchanan, F. Roddick, N. Porter, and M. Drikas, "Fractionation of uv and vuv pretreated nom from drinking water," *Environmental Science & Technology*, vol. 39, no. 12, pp. 4647–4654, 2005.

[82] A. Serrano Mora, "UV/vacuum-UV advanced oxidation process for the treatment of micropollutants from drinking water sources under common operational temperatures," Ph.D. dissertation, The University of British Columbia, 2016. [Online]. Available: http://hdl.handle.net/10012/7123

[83] M. Bagheri and M. Mohseni, "Computational fluid dynamics (CFD) modeling of VUV/UV photoreactors for water treatment," *Chemical Engineering Journal*, vol. 256, pp. 51–60, 2014.

[84] ——, "Impact of hydrodynamics on pollutant degradation and energy efficiency of VUV/UV and H_2O_2/UV oxidation processes," *Journal of Environmental Management*, vol. 164, pp. 114 – 120, 2015.

[85] ——, "A study of enhanced performance of VUV/UV process for the degradation of micropollutants from contaminated water," *Journal of Hazardous Materials*, vol. 294, pp. 1 – 8, 2015.

[86] W. Buchanan, F. Roddick, and N. Porter, "Formation of hazardous by-products resulting from the irradiation of natural organic matter: comparison between uv and vuv irradiation," *Chemosphere*, vol. 63, no. 7, pp. 1130–41, 2006. [Online]. Available: https://www.ncbi.nlm.nih.gov/pubmed/16297432

[87] ——, "Removal of VUV pre-treated natural organic matter by biologically activated carbon columns," *Water Research*, vol. 42, no. 13, pp. 3335–42, 2008. [Online]. Available: https://www.ncbi.nlm.nih.gov/pubmed/18502470

[88] P. Chintalapati and M. Mohseni, "Degradation of cyanotoxin microcystin-LR in synthetic and natural waters by chemical-free UV/VUV radiation," *Journal of Hazardous Materials*, vol. 381, p. 120921, 2019. [Online]. Available: https://www.ncbi.nlm.nih.gov/pubmed/31374374

[89] K. Linden and M. Mohseni, *Advanced Oxidation Processes: Applications in Drinking Water Treatment*. Elsevier, 2014, vol. 2, pp. 148–172.

[90] M. Gonzalez, E. Oliveros, M. Worner, and A. Braun, "Vacuum-ultraviolet photolysis of aqueous reaction systems," *Journal of Photochemistry and Photobiology C: Photochemistry Reviews*, vol. 5, no. 3, pp. 225–246, 2004.

[91] G. V. Buxton, C. L. Greenstock, W. P. Helman, and A. B. Ross, "Critical review of rate constants for reactions of hydrated electrons, hydrogen atoms and hydroxyl radicals in aqueous solution," *Journal of Physical and Chemical Reference Data*, vol. 17, no. 2, pp. 513–886, 1988.

[92] K. Zoschke, H. Bornick, and E. Worch, "Vacuum-UV radiation at 185 nm in water treatment–a review," *Water Research*, vol. 52, pp. 131–45, 2014. [Online]. Available: https://www.ncbi.nlm.nih.gov/pubmed/24463177

[93] S. Liu, X. Hu, W. Jiang, L. Ma, M. Cai, H. Xu, m. Wu, and F. Ma, "Degradation of microcystins from microcystis aeruginosa by 185-nm UV irradiation," *Water, Air, & Soil Pollution*, vol. 227, no. 4, 2016.

[94] A. Afzal, T. Oppenlander, J. R. Bolton, and M. G. El-Din, "Anatoxin-a degradation by advanced oxidation processes: vacuum-uv at 172 nm, photolysis using medium pressure uv and uv/h(2)o(2)," *Water Research*, vol. 44, no. 1, pp. 278–86, 2010. [Online]. Available: https://www.ncbi.nlm.nih.gov/pubmed/19818467

[95] S. R. Kuhn H, Braslavsky S, "Chemical actinometry," New England River Basins Commission, Technical Report. IUPAC, 2004.

[96] K. Bolton, J.; Linden, "Standardization of methods for fluence (UV dose) determination in bench-scale uv experiments," *Journal of Environmental Engineering*, vol. 129, no. (3), pp. 209–215, 2003.

[97] O. Rahn, "Potassium iodide as a chemical actinometer for 254 nm radiation: use of Iodate as an electron scavenger," *Photochemistry and Photobiology*, vol. 64, no. (4), pp. 450–455, 1997.

[98] O. Rahn, M. Stefan, J. Bolton, E. Goren, P. Shaw, and K. Lykke, "Quantum yield of the iodideiodate chemical actinometer. dependence on wavelength and concentration," *Photochemistry and Photobiology*, vol. 78, no. (2), pp. 146–152, 2003.

[99] F. Laith, "The use of 185 nm radiation for drinking water treatment. influence of temperature and major solutes on the degradation of trace organic contaminants." PhD Thesis, The University of British Columbia, 2017.

[100] H. Morowitz, "Absorption effects in volume irradiation dosimetry," *Science*, vol. 111, pp. 229–230, 1950.

[101] M. Lurling and I. Roessink, "On the way to cyanobacterial blooms: impact of the herbicide metribuzin on the competition between a green alga (scenedesmus) and a cyanobacterium (microcystis)," *Chemosphere*, vol. 65, no. 4, pp. 618–26, 2006. [Online]. Available: https://www.ncbi.nlm.nih.gov/pubmed/16540149

[102] G. A. Codd, L. F. Morrison, and J. S. Metcalf, "Cyanobacterial toxins: Risk management for health protection," *Toxicology and Applied Pharmacology*, vol. 203, no. 3, pp. 264–272, 2005.

[103] WHO, "Cyanobacterial toxins: Microcystin-LR in drinking-water. background document for development of
(WHO) guidelines for drinking-water quality," Geneva, 1998.

[104] Health Canada, "Guidelines for Canadian Drinking Water Quality: Supporting Documentation. Cyanobacterial Toxins – Microcystin-LR," Canda, 2002.

[105] B. Whitton and M. Potts, *Introduction to the Cyanobacteria.* Kluwer Academic Publishers, 2002, pp. 1–11.

[106] USEPA, "Drinking water health advisory for the cyanobacterial microcystin toxins," Washington, DC, 2015.

[107] J. Mallevialle, *Identification and treatment of tastes and odors in drinking water.* Denver, CO,: American Water Works Association, 1987.

[108] J. Fan, P. Hobson, L. Ho, R. Daly, and J. Brookes, "The effects of various control and water treatment processes on the membrane integrity and toxin fate of cyanobacteria," *Journal of Hazardous Materials*, vol. 264, pp. 313–22, 2014. [Online]. Available: https://www.ncbi.nlm.nih.gov/pubmed/24316803

[109] J. Naceradska, M. Pivokonsky, L. Pivokonska, M. Baresova, R. K. Henderson, A. Zamyadi, and V. Janda, "The impact of pre-oxidation with potassium permanganate on cyanobacterial organic matter removal by coagulation," *Water Research*, vol. 114, pp. 42–49, 2017. [Online]. Available: https://www.ncbi.nlm.nih.gov/pubmed/28226248

[110] V. K. Sharma, T. M. Triantis, M. G. Antoniou, X. He, M. Pelaez, C. Han, W. Song, K. E. O'Shea, A. A. de la Cruz, T. Kaloudis, A. Hiskia, and D. D. Dionysiou, "Destruction of microcystins by conventional and advanced oxidation processes: A review," *Separation and Purification Technology*, vol. 91, pp. 3–17, 2012.

[111] F. Al Momani, D. W. Smith, and M. Gamal El-Din, "Degradation of cyanobacteria toxin by advanced oxidation processes," *J Hazard Mater*, vol. 150, no. 2, pp. 238–49, 2008. [Online]. Available: https://www.ncbi.nlm.nih.gov/pubmed/17560023https://ac.els-cdn.com/S0304389407005936/1-s2.0-S0304389407005936-main.pdf?_tid=3e600ddb-8e4a-4d91-8775-5b78ebed13cd&acdnat=1538578568_4b6ff672cdca495e7927fd9b75ddae66

[112] T. K. Kim, B. R. Moon, T. Kim, M. K. Kim, and K. D. Zoh, "Degradation mechanisms of geosmin and 2-MIB during UV photolysis and UV/chlorine reactions," *Chemosphere*, vol. 162, pp. 157–64, 2016. [Online]. Available: https://www.ncbi.nlm.nih.gov/pubmed/27494316

[113] W. Schmidt, H. Willmitzer, K. Bornmann, and J. Pietsch, "Production of drinking water from raw water containing cyanobacteria–pilot plant studies for assessing the risk of microcystin breakthrough," *Environmental Toxicology*, vol. 17, no. 4, pp. 375–85, 2002. [Online]. Available: https://www.ncbi.nlm.nih.gov/pubmed/12203960

[114] E. C. Wert, J. A. Korak, R. A. Trenholm, and F. L. Rosario-Ortiz, "Effect of oxidant exposure on the release of intracellular microcystin, MIB, and geosmin from three cyanobacteria species," *Water Research*, vol. 52, pp. 251–9, 2014. [Online]. Available: https://www.ncbi.nlm.nih.gov/pubmed/24289950

[115] K. Zoschke, N. Dietrich, H. Bornick, and E. Worch, "UV-based advanced oxidation processes for the treatment of odour compounds: efficiency and by-product formation," *Water Research*, vol. 46, no. 16, pp. 5365–73, 2012. [Online]. Available: https://www.ncbi.nlm.nih.gov/pubmed/22858230

[116] K. Kutschera, H. Bornick, and E. Worch, "Photoinitiated oxidation of geosmin and 2-methylisoborneol by irradiation with 254 nm and 185 nm UV light," *Water Research*, vol. 43, no. 8, pp. 2224–32, 2009. [Online]. Available: https://www.ncbi.nlm.nih.gov/pubmed/19303132

[117] R. O. Rahn, J. Bolton, and M. I. Stefan, "The iodide/iodate actinometer in UV disinfection: determination of the fluence rate distribution in UV reactors," *Photochemistry and Photobiology*, vol. 82, no. 2, pp. 611–5, 2006. [Online]. Available: https://www.ncbi.nlm.nih.gov/pubmed/16613521

[118] P. Servais, A. Barillier, and J. Garnier, "Determination of the biodegradable fraction of dissolved and particulate organic carbon," *International Journal of Limnology*, vol. 31, no. 1, pp. 78–80, 1995.

[119] E. A. Clescheri L, Greenberg AE, *Standard Methods for the Examination of Water and Wastewater*, 20th ed. American Public Health Association (APHA), American Water Works Association (AWWA) and the Water Environment Federation, 1998.

[120] N. McQuaid, A. Zamyadi, M. Prevost, D. F. Bird, and S. Dorner, "Use of in vivo phycocyanin fluorescence to monitor potential microcystin-producing cyanobacterial biovolume in a drinking water source," *J Environ Monit*, vol. 13, no. 2, pp. 455–63, 2011. [Online]. Available: https://www.ncbi.nlm.nih.gov/pubmed/21157617

[121] Q. Sun, T. Zhang, F. Wang, C. Liu, C. Wu, R. R. Xie, and Y. Zheng, "Ultraviolet photosensitized transformation mechanism of microcystin-LR by natural organic matter in raw water," *Chemosphere*, vol. 209, pp. 96–103, 2018. [Online]. Available: https://www.ncbi.nlm.nih.gov/pubmed/29913404

[122] P. B. Fayad, A. Roy-Lachapelle, S. V. Duy, M. Prevost, and S. Sauve, "On-line solid-phase extraction coupled to liquid chromatography tandem mass spectrometry for the analysis of cyanotoxins in algal blooms," *Toxicon*, vol. 108, pp. 167–75, 2015. [Online]. Available: https://www.ncbi.nlm.nih.gov/pubmed/26494036

[123] C. Duca, G. Imoberdorf, and M. Mohseni, "Novel Collimated Beam Setup to Study the Kinetics of VUV-Induced Reactions Normalized radiation intensity," *Photochemistry and Photobiology*, pp. 238–240, 2014.

[124] ——, "Novel collimated beam setup to study the kinetics of vuv-induced reactions," *Photochem Photobiol*, vol. 90, no. 1, pp. 238–40, 2014. [Online]. Available: https://www.ncbi.nlm.nih.gov/pubmed/23952050

[125] A. Serrano Mora, "UV/vacuum-UV advanced oxidation process for the treatment of micropollutants from drinking water sources under common operational temperatures," Ph.D. dissertation, The University of British Columbia, 2016. [Online]. Available: http://hdl.handle.net/10012/7123

[126] L. Furatian and M. Mohseni, "Temperature dependence of 185nm photochemical water treatment. the photolysis of water," *Journal of Photochemistry and Photobiology A: Chemistry*, vol. 356, pp. 364–369, 2018.

[127] A. Cabaj, R. Sommer, and M. Kundi, "The influence of dose distributions in the result of UV-biosodimetry," in *IRPA9. International congress on radiation protection*, vol. 3, 1996, Conference Proceedings.

[128] A. Cabaj, R. Sommer, and D. Schoenen, "Biodosimetry: Model calculation for UV water disidention devices with regard to dose distributins," *Water Research*, vol. 30, no. 4, pp. 1003–1009, 1996.

[129] S. Jin, A. A. Mofidi, and K. G. Linden, "Polychromatic UV fluence measurement using chemical actinometry, biodosimetry, and mathematical techniques," *Journal of Environmental Engineering*, vol. 132, no. 8, pp. 831–841, 2006.

[130] L. Furatian and M. Mohseni, "Influence of chloride on the 185 nm advanced oxidation process," *Chemosphere*, vol. 199, pp. 263–268, 2018. [Online]. Available: https://www.ncbi.nlm.nih.gov/pubmed/29448193

[131] J. WEEKS, G. MEABURN, and S. GORDON, "Absorption coefficients of liquid water and aqueous solution in the far ultraviolet," *Radiation Research*, vol. 19, pp. 559–567, 1963.

[132] K. Hasegawa and P. Neta, "Rate constants and mechanisms of reaction of chloride (Cl_2^-) radicals." *The Journal of Physical Chemistry*, vol. 82, pp. 854–857, 1978.

[133] B. Langlais, D. A. Reckhow, and D. R. Brink, *Ozone in Water Treatment: Application and Engineering*. American Water Works Association Research Foundation: Compagnie Générale Eaux, 1991.

[134] C. Duca, G. Imoberdorf, and M. Mohseni, "Effects of inorganics on the degradation of micropollutants with vacuum UV (VUV) advanced oxidation," *Journal of Environmental Science and Health, Part A*, vol. 52, no. 6, pp. 524–532, 2017. [Online]. Available: https://www.ncbi.nlm.nih.gov/pubmed/28276889

[135] P. Xie, S. Yue, J. Ding, Y. Wan, X. Li, J. Ma, and Z. Wang, "Degradation of organic pollutants by vacuum-ultraviolet (VUV): Kinetic model and efficiency," *Water Research*, vol. 133, pp. 69–78, 2018. [Online]. Available: https://www.ncbi.nlm.nih.gov/pubmed/29367049

[136] J. Goldstone, M. Pullin, S. Bertilsson, and B. Voelker, "Reactions of hydroxyl radical with humic substances: bleaching, mineralization, and production of bioavailable carbon substrates," *Environmental Science & Technology*, vol. 36, pp. 362–372, 2002.

[137] E. Rosenfeldt and K. Linden, "The $R_{\bullet OH,UV}$ concept to characterize and the model UV/H_2O_2 process in natural waters," *Environmental Science & Technology*, vol. 41, no. 7, pp. 2548–2553, 2007.

[138] S. Dobrovic, H. Juretic, and N. Ruzinski, "Photodegradation of natural organic matter in water with UV irradiation at 185 and 254 nm: importance of hydrodynamic conditions on the decomposition rate," *Separation Science and Technology*, vol. 42, p. 1421–1432, 2007.

[139] U. Von Gunten, "Ozonation of drinking water: Part i. oxidation kinetics and product formation," *Water Research*, vol. 37, pp. 1443–1467, 2003.

[140] I. Escobar and A. Randall, "Assimilable organic carbon (AOC) and biodegradable dissolved organic carbon (BDOC): Complementary measurements," *Water Research*, vol. 35, no. 18, p. 4444–4454, 2001.

[141] WHO, "Guidelines for safe recreational water environments. coastal and fresh waters," Geneva, 2003.

[142] D. Ellis, "Guide d'intervention pour les propirétaires, les exploitants ou les conceptieurs de stations de production d'eau potable municipales prises avec une prblématique de fleurs d'eau de cyanobactéries," Ministère du développement durable, de l'environnement et parcs Québec, Guidelines, Canada, 2009.

[143] J. R. Bolton, *The Ultraviolet Disinfection Handbook*, first edition ed. American Water Works Association, Denver, CO, 2008.

[144] M. Sillanpää and A. Matilainen, "Chapter 6 - nom removal by advanced oxidation processes," in *Natural Organic Matter in Water*, M. Sillanpaa, Ed. Butterworth-Heinemann, 2015, pp. 159 – 211.

[145] R. Henderson, S. Parsons, and B. Jefferson, "The impact of algal properties and pre-oxidation on solid–liquid separation of algae," *Water Research*, vol. 42, no. 8-9, pp. 1827–1845, 2008. [Online]. Available: http://linkinghub.elsevier.com/retrieve/pii/S004313540700704X

[146] K. R. Murphy, C. A. Stedmon, D. Graeber, and R. Bro, "Fluorescence spectroscopy and multi-way techniques. PARAFAC," *Analytical Methods*, vol. 5, no. 23, 2013.

[147] S. A. Huber, A. Balz, M. Abert, and W. Pronk, "Characterisation of aquatic humic and non-humic matter with size-exclusion chromatography - organic carbon detection - organic nitrogen detection (LC-OCD-OND)," *Water Research*, vol. 45, no. 2, pp. 879–885, 2011. [Online]. Available: http://dx.doi.org/10.1016/j.watres.2010.09.023

[148] A. Matilainen and M. Sillanpää, "Removal of natural organic matter from drinking water by advanced oxidation processes," *Chemosphere*, vol. 80, no. 4, pp. 351–365, 2010. [Online]. Available: http://dx.doi.org/10.1016/j.chemosphere.2010.04.067

[149] N. McQuaid, a. Zamyadi, M. Prévost, D. F. Bird, and S. Dorner, "Use of in vivo phycocyanin fluorescence to monitor potential microcystin-producing cyanobacterial biovolume in a drinking water source." *Journal of Environmental Monitoring : JEM*, vol. 13, no. 2, pp. 455–463, 2011.

[150] F. Visentin, S. Bhartia, M. Mohseni, S. Dorner, and B. Barbeau, "Performance of vacuum uv (vuv) for the degradation of mc-lr, geosmin, and mib from cyanobacteria-impacted waters," *Environmental Science: Water Research & Technology*, vol. 5, pp. 2048–2058, 2019.

[151] K. Murphy, K. Butler, R. Spencer, C. Stedmon, J. Boehme, and G. Aiken, "Measurement of DOM fluorescence in aquaticenvironments: An interlaboratory comparison," *Environmental Science & Technology*, vol. 44, p. 9405–9412, 2010.

[152] C. A. Stedmon and R. Bro, "Characterizing dissolved organic matter fluorescence with parallel factor analysis: a tutorial," *Limnology and Oceanography: Methods*, vol. 6, p. 572–579, 2008.

[153] Y.-P. Chin, G. Aiken, and E. O'Loughlin, "Molecular weight, polydispersity, and spectroscopic properties of aquatic humic substances," *Environmental Science & Technology*, vol. 28, no. 11, pp. 1853–1858, 1994.

[154] G. Imoberdorf and M. Mohseni, "Comparative study of the effect of vacuum-ultraviolet irradiation on natural organic matter of different sources," *Journal of Environmental Engineering*, vol. 140, no. 3, 2014.

[155] S. Moradinejad, C. M. Glover, J. Mailly, T. Z. Seighalani, S. Peldszus, B. Barbeau, S. Dorner, M. Prevost, and A. Zamyadi, "Using advanced spectroscopy and organic matter characterization to evaluate the impact of oxidation on cyanobacteria," *Toxins (Basel)*, vol. 11, no. 5, 2019. [Online]. Available: https://www.ncbi.nlm.nih.gov/pubmed/31108999

[156] J. A. Leenheer and J.-P. Croué, "Characterizing aquatic dissolved organic matter," *Environmental Science & Technology*, vol. 37, pp. 18A–26A, 2003.

[157] R. J. Peters, E. W. de Leer, and L. de Galan, "Dihaloacetonitriles in dutch drinking waters," *Water Research*, vol. 24, no. 6, pp. 797 – 800, 1990.

[158] A. Dotson, P. Westerhoff, and S. W. Krasner, "Nitrogen enriched dissolved organic matter (DOM) isolates and their affinity to form emerging disinfection by-products," *Water Science and Technology*, vol. 60, no. 1, pp. 135–143, 07 2009.

[159] W. Chen, P. Westerhoff, J. Leenheer, and K. Booksh, "Fluorescence excitation-emission matrix regional integration to quantify for dissolved organic matter," *Environmental Science & Technology*, no. 37, pp. 5701–5710, 2003.

[160] A. D. Dotson, V. O. S. Keen, D. Metz, and K. G. Linden, "Uv/h2o2 treatment of drinking water increases post-chlorination dbp formation," *Water Research*, vol. 44, no. 12, pp. 3703 – 3713, 2010.

[161] A. H. Malayeri, M. Mohseni, B. Cairns, and J. R. Bolton, "Fluence (UV Dose) required to achieve incremental log inactivation of bacteria, protozoa, viruses and algae," *IUVA News. The Official Publication of International Ultraviolet Association*, vol. 3, no. 18, pp. 4–6, 2017. [Online]. Available: https://www.iuvanews.com/stories/pdf/archives/180301_UVSensitivityReview_full.pdf

[162] M. Cho, H. Chung, and J. Yoon, "Disinfection of water containing natural organic matter by using ozone-initiated radical reactions," *Applied and Environmental Microbiology*, vol. 69, no. 4, pp. 2284–2291, 2003. [Online]. Available: https://aem.asm.org/content/69/4/2284

[163] S. Zhu, B. Dong, Y. Wu, L. Bu, and S. Zhou, "Degradation of carbamazepine by vacuum-uv oxidation process: Kinetics modeling and energy efficiency," *Journal of Hazardous Materials*, no. 368, pp. 178–185, 2019.

[164] E. C. Wert, M. M. Dong, and F. L. Rosario-Ortiz, "Using digital flow cytometry to assess the degradation of three cyanobacteria species after oxidation processes," *Water Research*, vol. 47, no. 11, pp. 3752–61, 2013. [Online]. Available: https://www.ncbi.nlm.nih.gov/pubmed/23726712

[165] M. K. Ramseier, U. von Gunten, P. Freihofer, and F. Hammes, "Kinetics of membrane damage to high (HNA) and low (LNA) nucleic acid bacterial clusters in drinking water by ozone, chlorine, chlorine dioxide, monochloramine, ferrate(VI), and permanganate," *Water Research*, vol. 45, no. 3, pp. 1490 – 1500, 2011. [Online]. Available: http://www.sciencedirect.com/science/article/pii/S0043135410007803

[166] S. A. Huber, A. Balz, M. Abert, and W. Pronk, "Characterisation of aquatic humic and non-humic matter with size-exclusion chromatography–organic carbon detection–

organic nitrogen detection (LC-OCD-OND)," *Water Research*, vol. 45, no. 2, pp. 879–85, 2011. [Online]. Available: https://www.ncbi.nlm.nih.gov/pubmed/20937513

[167] M.-F. Morissette, S. Vo Duy, H. P. H. Arp, and S. Sauvé, "Sorption and desorption of diverse contaminants of varying polarity in wastewater sludge with and without alum," *Environmental Science.: Processes Impacts*, vol. 17, pp. 674–682, 2015. [Online]. Available: http://dx.doi.org/10.1039/C4EM00620H

[168] A. Roy-Lachapelle, S. Vo Duy, G. Munoz, Q. T. Dinh, E. Bahl, D. F. Simon, and S. Sauvé, "Analysis of multiclass cyanotoxins (microcystins, anabaenopeptins, cylindrospermopsin and anatoxins) in lake waters using on-line spe liquid chromatography high-resolution orbitrap mass spectrometry," *Anal. Methods*, vol. 11, pp. 5289–5300, 2019. [Online]. Available: http://dx.doi.org/10.1039/C9AY01132C

[169] G. Munoz, S. V. Duy, A. Roy-Lachapelle, B. Husk, and S. Sauvé, "Analysis of individual and total microcystins in surface water by on-line preconcentration and desalting coupled to liquid chromatography tandem mass spectrometry," *Journal of Chromatography A*, vol. 1516, pp. 9 – 20, 2017. [Online]. Available: http://www.sciencedirect.com/science/article/pii/S0021967317311408

[170] J. R. Bolton and S. R. Cater, *Homogeneous Photodegradation of Pollutants in Contaminated Water: An Introduction.* CRC Press, 1994, pp. 467–490.

[171] J. Westrick, D. Szlag, B. Southwell, and J. Sinclair, "A review of cyanobacteria and cyanotoxins removal/inactivation in drinking water treatment," *Analytical and Bioanalytical Chemistry*, vol. 397, no. 5, pp. 1705–1714, Jul 2010. [Online]. Available: https://doi.org/10.1007/s00216-010-3709-5

[172] J. A. Westrick, A. Fuller, and J. P. Malley, "Assessing the risk of mercury in drinking water after uv lamp breaks," New England Water Treatment Technology Assistance Center. University of New Hampshire, Report, 2008.

[173] P. Jarvis, O. Autin, E. H. Goslan, and F. Hassard, "Application of ultraviolet light-emitting diodes (uv-led) to full-scale drinking-water disinfection," *Water*, vol. 11, no. 9, 2019. [Online]. Available: https://www.mdpi.com/2073-4441/11/9/1894

[174] F. Hammes, S. Meylan, E. Salhi, O. Köster, T. Egli, and U. von Gunten, "Formation of assimilable organic carbon (AOC) and specific natural organic matter (NOM) fractions during ozonation of phytoplankton," *Water Research*, vol. 41, no. 7, pp. 1447–1454, 2007.

[175] G. Matafonova and V. Batoev, "Recent advances in application of uv light-emitting diodes for degrading organic pollutants in water through advanced oxidation processes: A review," *Water Research*, vol. 132, pp. 177 – 189, 2018. [Online]. Available: http://www.sciencedirect.com/science/article/pii/S0043135417310941

[176] G. IJpelaar, D. Harmsen, E. Beerendonk, R. van Leerdam, D. Metz, A. Knol, A. Fulmer, and S. Krijnen, "Comparison of low pressure and medium pressure UV lamps for UV/H_2O_2 treatment of natural waters containing micro pollutants," *Ozone: Science & Engineering,*, vol. 32, pp. 329–337, 2010.

[177] O. Autin and J. Bolton, "Validation of a reactor containing UV leds for the disinfection of municipal drinking water," *UV Solutions*, vol. 2019, p. 17, 09 2019.

[178] K. A. Sholtes, K. Lowe, G. W. Walters, M. D. Sobsey, K. G. Linden, and L. M. Casanova, "Comparison of ultraviolet light-emitting diodes and low-pressure mercury-arc lamps for disinfection of water," *Environmental Technology*, vol. 37, no. 17, pp. 2183–2188, 2016, pMID: 26888599.

[179] J. K. Edzwald and J. E. Tobiason, "Enhanced coagulation: US requirements and a broader view," *Water Science and Technology*, vol. 40, no. 9, pp. 63 – 70, 1999.

[180] E. Ejarque-Gonzalez and A. Butturini, "Self-organising maps and correlation analysis as a tool to explore patterns in excitation-emission matrix data sets and to discriminate dissolved organic matter fluorescence components," *PLoS One*, vol. 9, no. 6, p. e99618, 2014. [Online]. Available: https://www.ncbi.nlm.nih.gov/pubmed/24906009

[181] T. Vatanen, T. Osmala, T. Raiko, K. Lagus, M. Sysi-Aho, M. Orešič, T. Honkela, and H. Lähdesmäki, "Self-organization and missing values in SOM and GTM," *Neurocomputing*, vol. 147, pp. 60–70, 2015.

APPENDIX A IMPACT OF NATURAL NOM AND AOM IN VACUUM UV TREATMENT

SUVA values before and after VUV treatment

SUVA, defined as UVA 254 normalized to DOC, is a good predictor of the aromaticity of NOM. In 1999, Edzwald and Tobiason proposed that a SUVA value greater than 4 indicates the predominance of aquatic humic matter, highly aromatic and hydrophobic character, and high molecular weight. While SUVA values between 2 and 4, are composed by a mixture of aquatic humic and non-humic matter, with a mix of aromatic and aliphatic character and low to high molecular weight. When SUVA lower than 2, then a high fraction of non-humic matter is present, aliphatic and hydrophobic character and low molecular weight [179].

Table A.1: SUVA, L m^{-1} mgC^{-1}, values before and after VUV treatment

	Lakes			
	A	**B**	**C**	**C***
Untreated Raw Water (URW), retention time = 0 s	2.70	4.27	4.01	3.89
VUV Treated Raw Water (VUVTRW), retention time = 9.4 s	2.49	3.97	3.84	3.48
Untreated Filtered Water (UFW), retention time = 0 s	3.06	-	2.71	2.73
VUV Treated Filtered Water (VUVTFW), retention time = 9.4 s	2.91	-	2.55	2.48

LC-OCD-OND chromatograph

Figure A.1 (a, d, g and j) shows the ultraviolet detector (UVD) signal from the LC-OCD-OND for the four lakes. Without VUV treatment, in Lake A (where a bank filtration water system is responsible for NOM removal), the UVD signal in filtered water is 25% lower than in raw water. Among the four lakes, Lake B shows the higher UVD signal due to the high cell concentration (almost 4 times higher than Lake A and two times Lake C and C*). DOC measurement was stable and UVD declined, thus modest reductions of SUVA were obtained (about 0.2-0.4 units) (Table A.1). In terms of TOC in Lake C and C*, it also remained stable (reductions: 1% to 6%). This was expected given the low fluence applied. DOC characterization by LC-OCD-OND are depicted in Figure A.1 (b, e, h, and k). The figure revealed a change in the molecular weight of NOM components after VUV treatment. While the overall reduction in DOC was small, humics were strongly bleached (strong reduction in $UV_{254\,nm}$ response). An increase in biodegradability is observed through the increase in BDOC measurements (from 20% to 35%). Figure A.2 as the HMW fraction decreases.

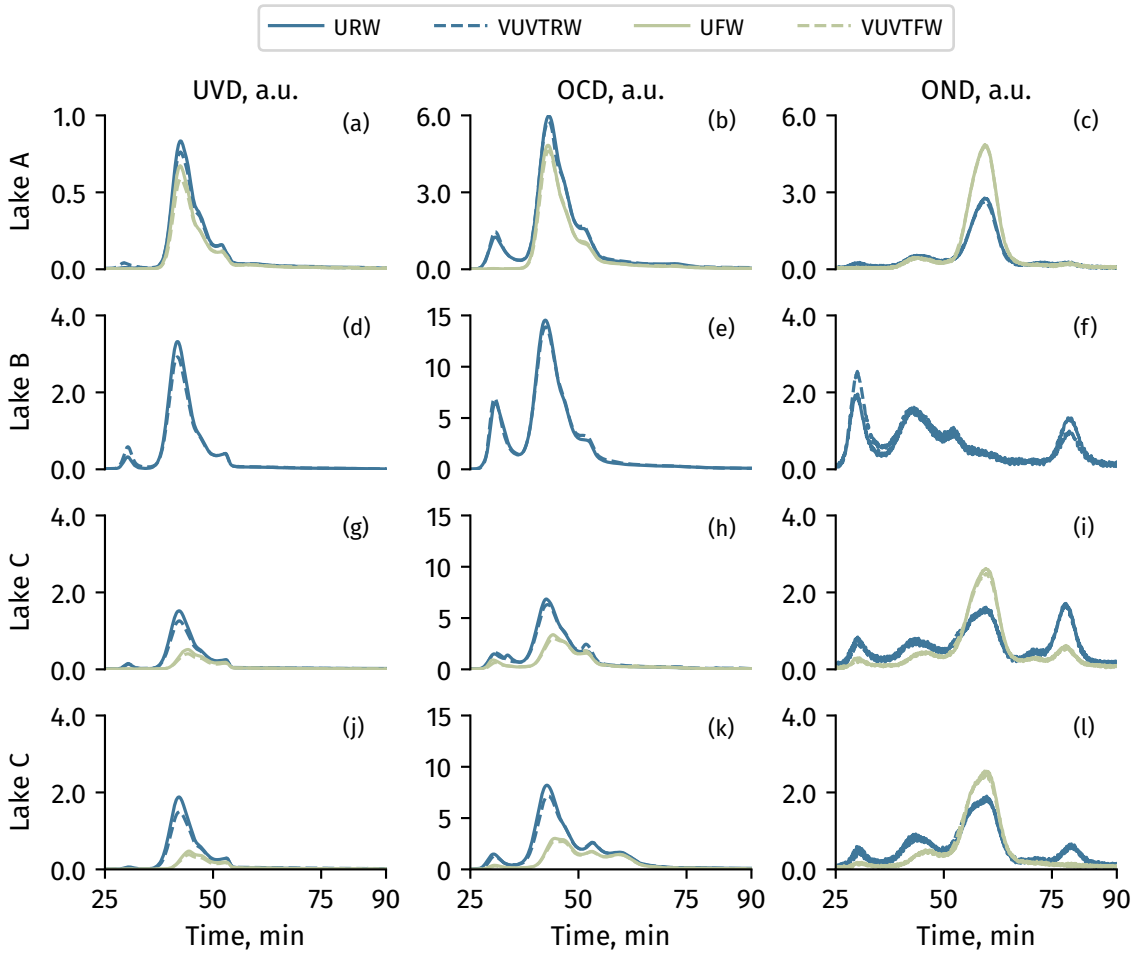

Figure A.1: LC-OCD-OND spectra (URW = Untreated Raw Water, VUVTRW = VUV Treated Raw Water, UFW = Untreated Filtered Water, UVTFW = VUV Treated Filtered Water; a.u. denotes arbitrary units).

Biodegradability though biological dissolved organic carbon (BDOC) measurements

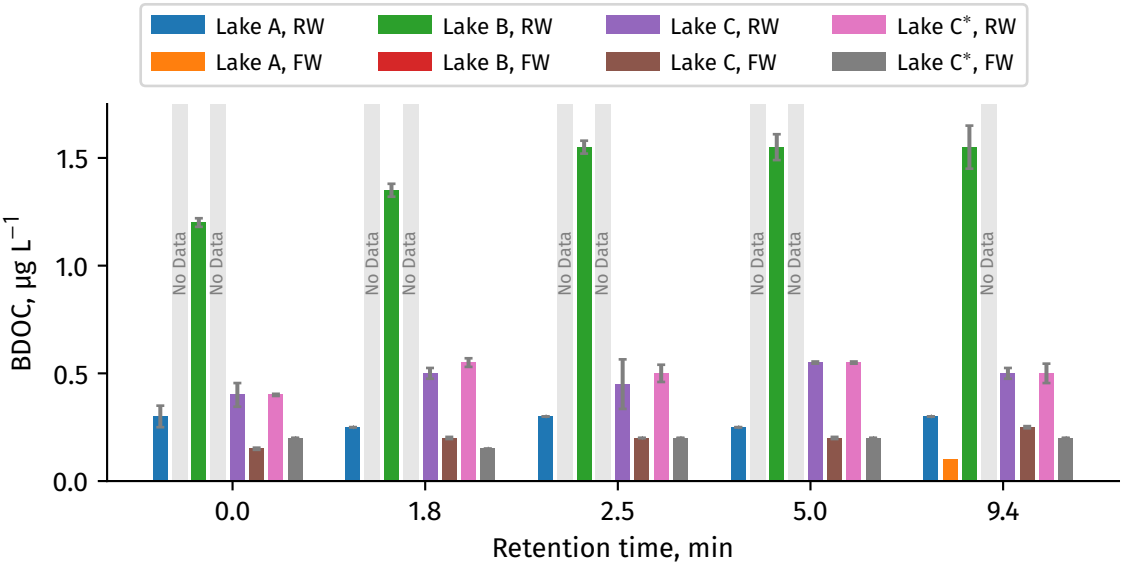

Figure A.2: BDOC before and after VUV treatment. RW = Raw Water, FW = Filtered Water.

PARAFAC modeling

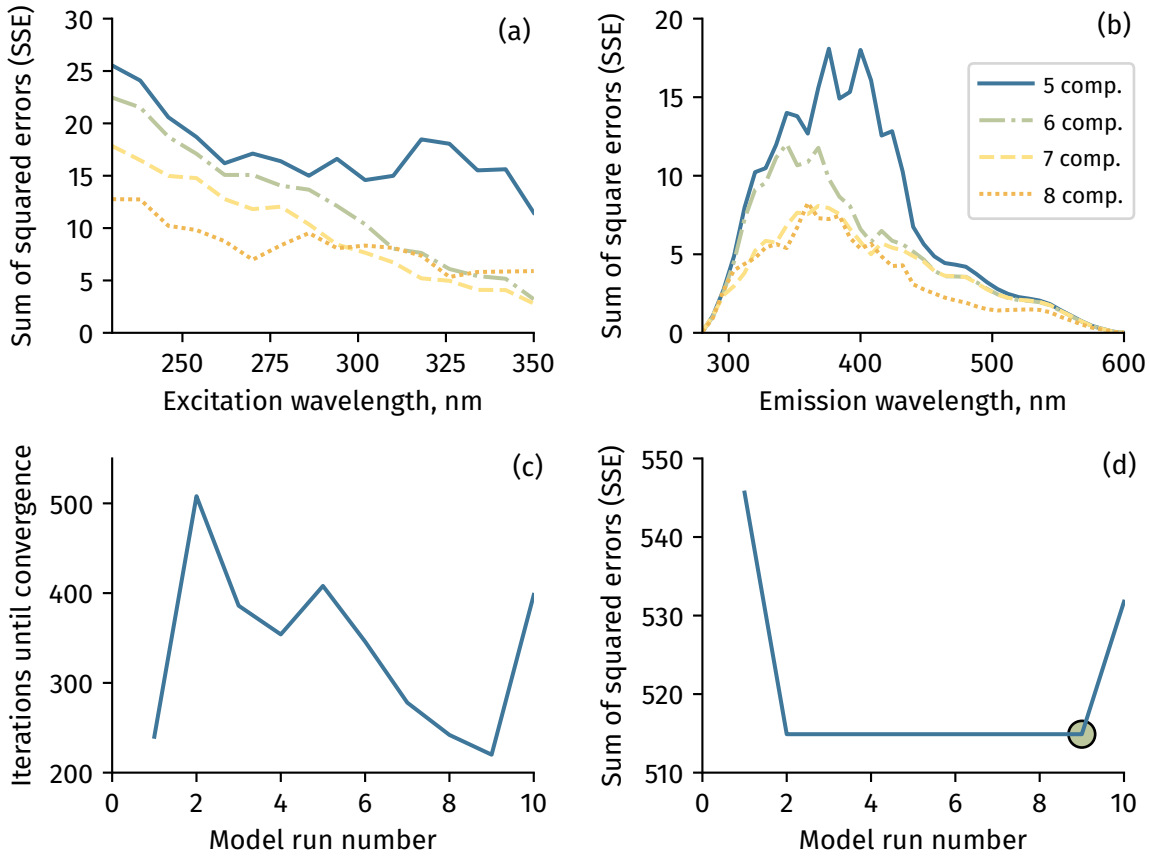

Figure A.3: (a-b) SSE of PARAFAC models with different number of component. (c-d) Robustness of the 7-components PARAFAC model. Ten runs with random starting points.

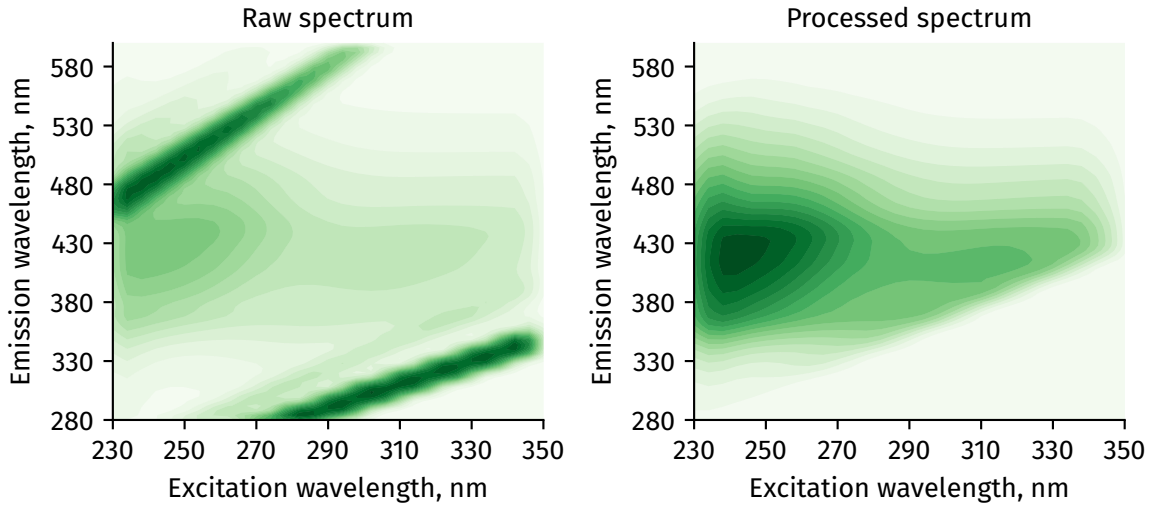

Figure A.4: Example comparing a raw and processed FEEM spectrum input in the PARAFAC models.

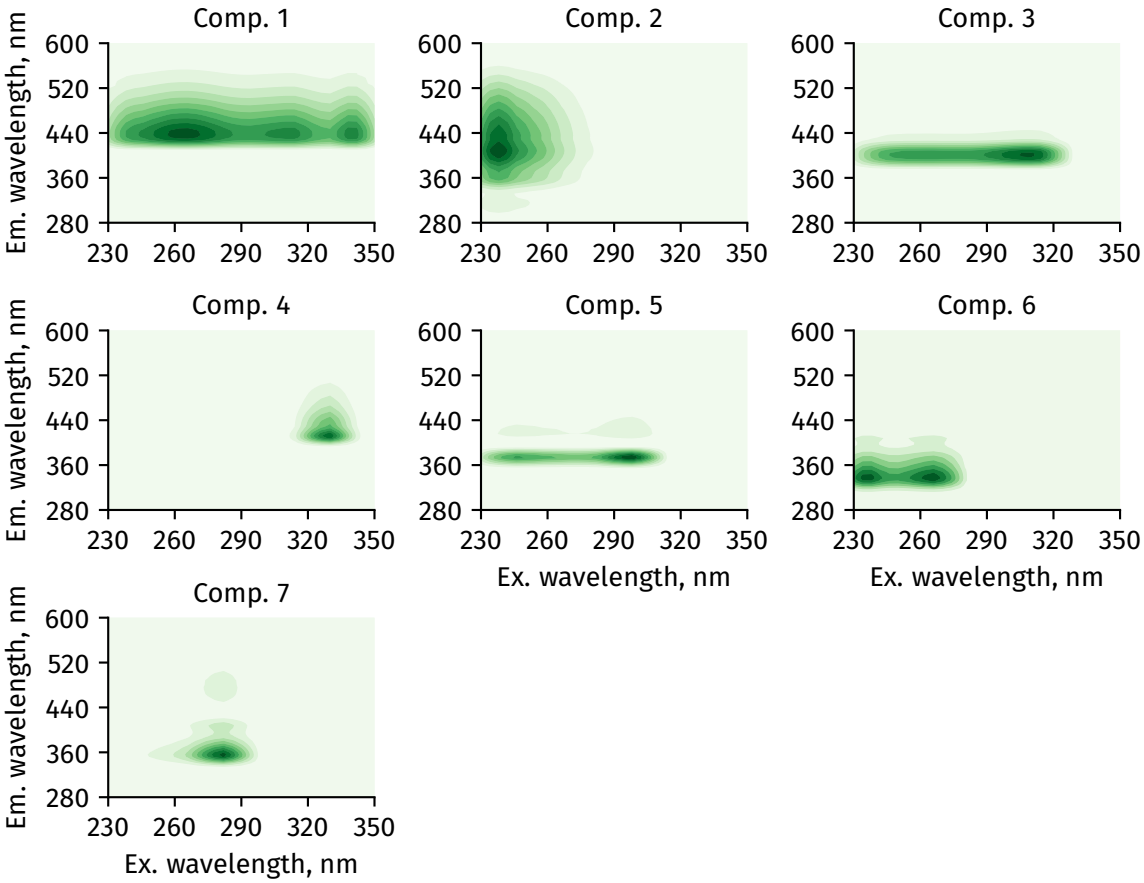

Figure A.5: Components obtained from PARAFAC modeling.

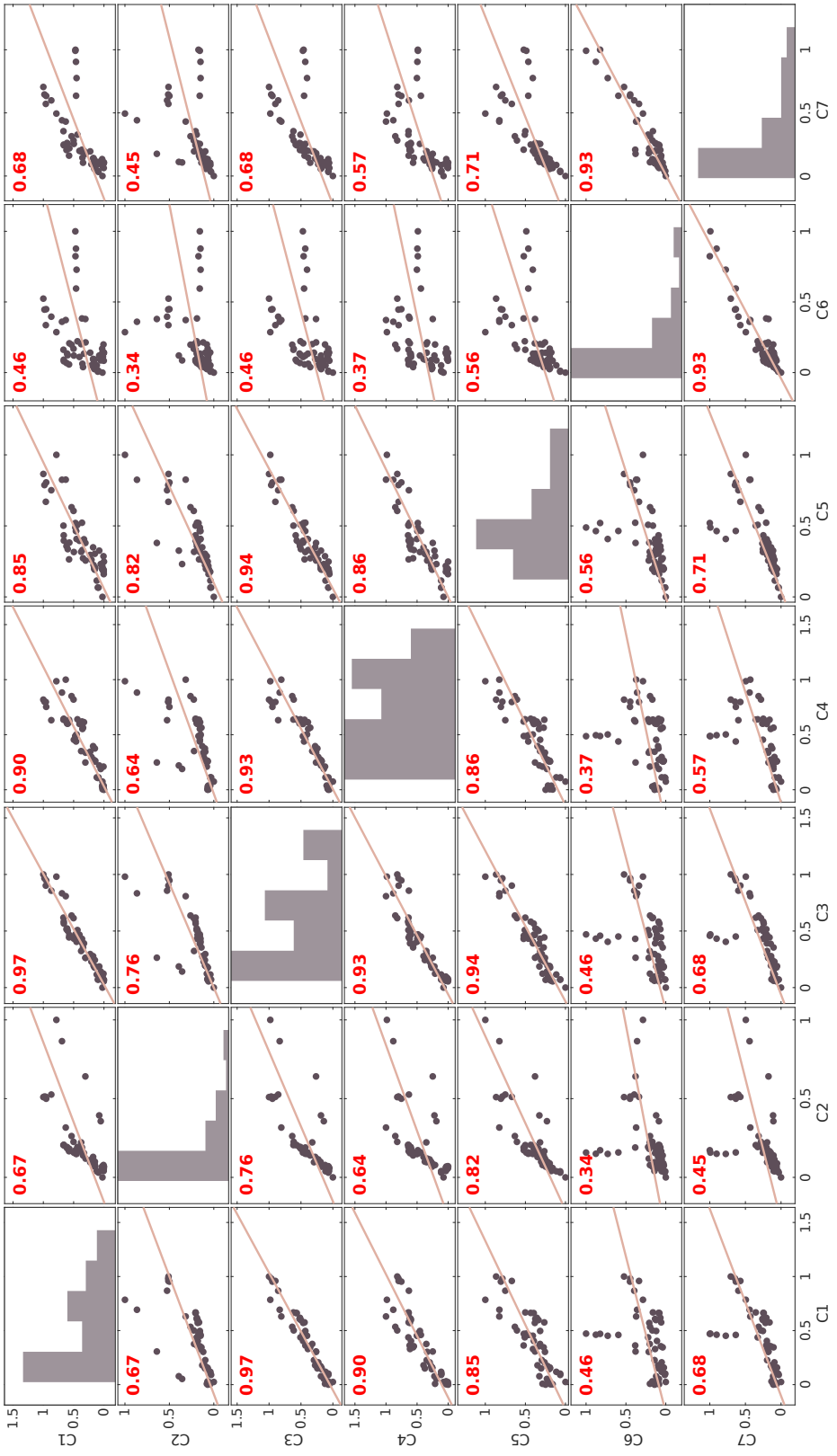

Figure A.6: Correlation plot of the $F_{\max}$ values between each PARAFAC component.

SOM modeling

SOM is a pattern recognition method. It clusterizes and reduces the dimensionality of input FEEM without make assumption about the data structure [180]. A dataset of 64 spectra were analyzed with the PARAllel FACtor analysis (PARAFAC) decomposition routines for Excitation Emission Matrices (drEEM, version 0.2.0 toolbox [146]) and self-organizing maps (SOM) with the SOM-Toolbox version 2.1 [181] both running on Matlab®R2018B software).

Figure A.7 shows the U-matrix from the best SOM map selected along with the component planes of each of the components retrieved by PARAFAC. The U-matrix shows the distance between neighbouring neurons in the map, where large values (darker color) indicate highly dissimilar neurons. The component planes are useful to visualize the importance of different excitation-emission pairs or variables for each sample (neurons, from the SOM solution). We selected the pairs corresponding to the components proportions from PARAFAC (Figure A.6).

The distribution of the samples obtained from the solution of SOM is shown through the best matching unit (BMU) graphics. In Figure A.7 we show a combined image of the BMU overlapped with multiple hits histograms (colored hexagons) for each lake showing the importance of each neuron representing the lakes and the type of water (the larger the colored hexagon the higher number of hits in that neuron). The BMU is the best solution found by SOM and shows the distribution of the four lakes across the map for raw (R) and filtered (F) water. For example, samples associated to Lake B are located at different neurons in the map (the top-left and bottom-left in Figure A.7), indicating the differences in NOM composition from raw and filtered. Basically, raw water contains NOM and AOM (particulate + dissolved) and filtered water only contains the dissolved fraction of NOM and AOM. Thus, SOM maps locate raw and filtered water in different region (Figure A.7). Therefore, SOM allows discriminating differences in cell concentration between samples. We identify two clusters for Lake A: one (bottom-right) belongs to raw water from the lake while the other (middle) corresponds to filtered water through the well (Lake A supplies a bank filtration water system). Lakes C and C* show share similar neurons in the map, because they represent the same lake without (Lake C) and with (Lake C*) bloom conditions. For a given lake is seen that the SOM solution properly discriminate between raw and filtered water, particularly those with bloom condition (Lakes B and C*).

By comparing Figure A.6 and each component plane from Figure A.7 is possible to correlate that PARAFAC components C1(1), C6(1), C6(2) and C7(1) characterize Lake B. Furthermore, C6(1), C6(2) and C7(1) are essentially due to samples from Lake B. This allows us to conclude that Lake B is mostly characterized by humic acids-like and (Region V, Figure 5.4)

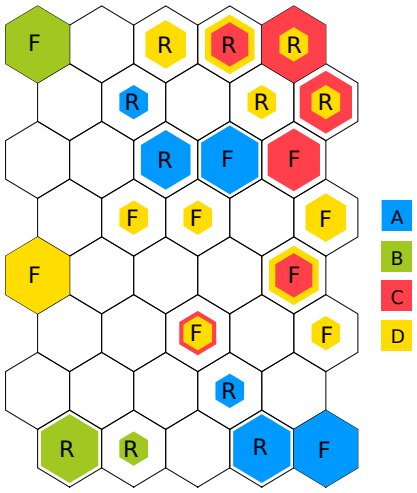

Figure A.7: SOM map with multiple hits overlapped showing the sites distribution for raw and filtered water.

and soluble microbial by-product-like (Region IV, Figure 5.4). Component planes show that raw water in Lake A is associated to C1(1), C5(1), C5(2) and C7(2), while filtered water correlates to C1(2), C3(1), C4(1) and C7(2). Here also the regions that characterize the lake are V and IV (Figure 5.4). Lakes C and C* are characterized by C1(2), C1(3), C3(2), C4(1) and C7(2), lying in regions V and IV.

By overlapping PARAFAC and SOM results, it is possible to distinguish components that characterise each lake. All four lake could be characterize by a reduced number of regions (Figure 5.4): region IV (humic acid-like) and V (soluble microbial by-product-like) (Table 5.4). By focusing on this FEEM region, it could be possible to make a relationship with NOM/AOM and DBP's formation and reactivity.

Combination of PARAFAC components and SOM allowed to characterize each lake with fewer components:

- Components C1(1), C6(1), C6(2) and C7(1) characterize Lake B
- Raw water in Lake A is associated to C1(1), C5(1), C5(2) and C7(2), while filtered water correlates to C1(2), C3(1), C4(1) and C7(2)

Table A.2: SOM and PARAFAC. Characteristic component of each lake

Lake	PARAFAC component
A	C1(1), C5(1), C5(2) and C7(2) (raw water)
A	C1(2), C3(1), C4(1) and C7(2) (filtered water)
B	C1(1), C6(1), C6(2) and C7(1)
C and C*	C1(2), C1(3), C3(2), C4(1) and C7(2)

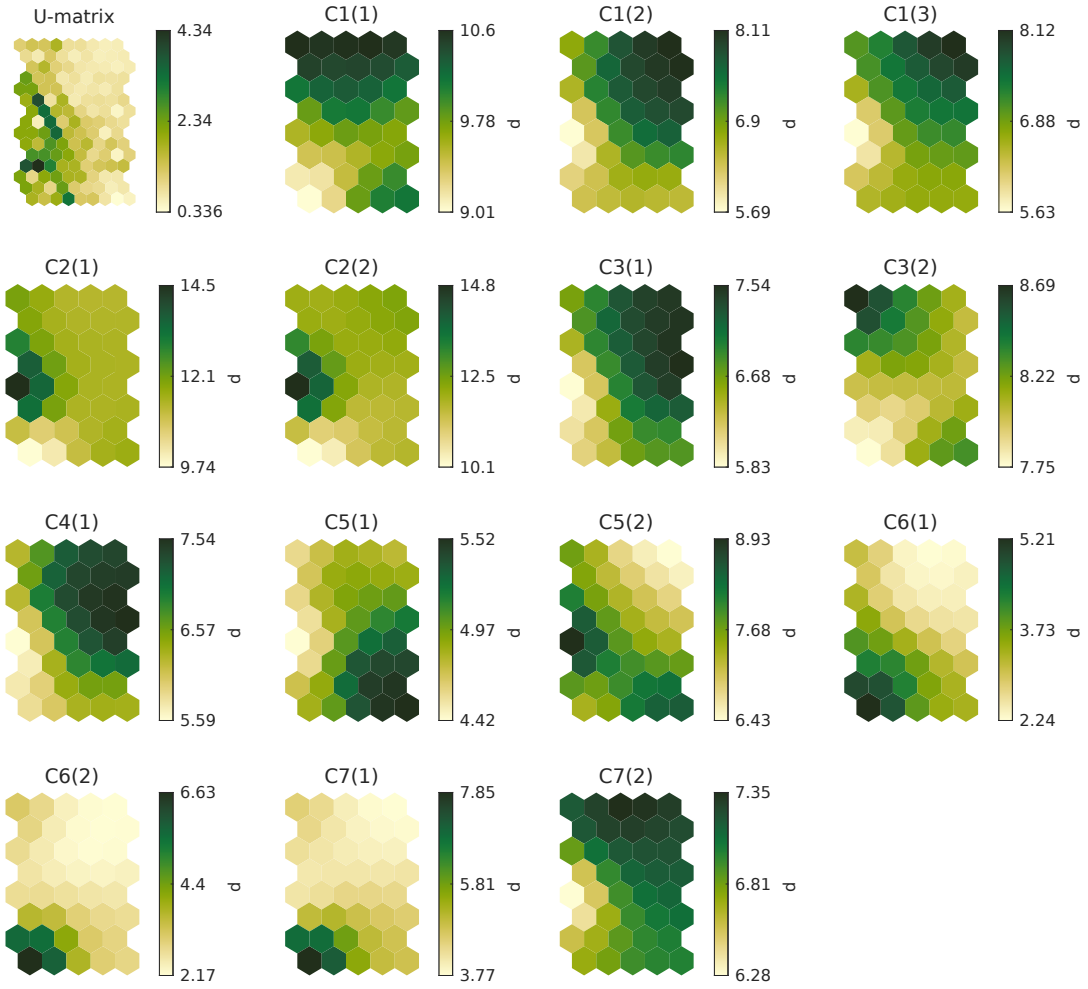

Figure A.8: U-matrix and component planes for the proportions of PARAFAC components resulted from SOM analysis.

Disinfection by-products formation: correlation data

Table A.3: Carbon fractions and yields values from DBP's formation correlation

	Yields, µg**F** µg(**THM or HAA**)$^{-1}$	
C or N fraction (F)	**THM**	**HAA**
DOC	27	43
DON	0.9	0.6
HS	20	28
BP	6.9	4.7
BB	3.8	7.2
LMW Ac	0.5	1.2
LMW Neutral	1.9	1.2

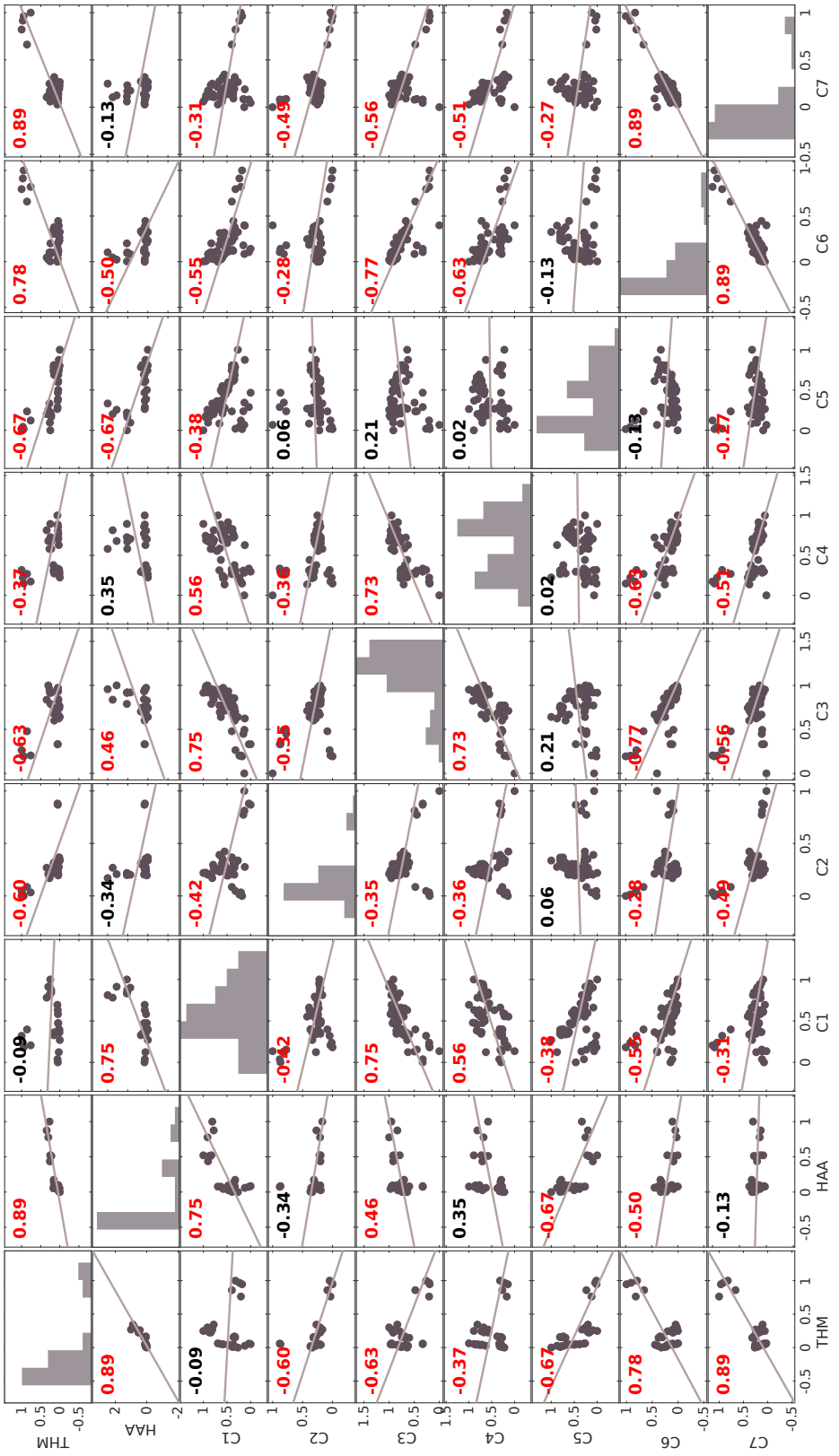

Figure A.9: THM and HAA correlation with PARAFAC compoments.

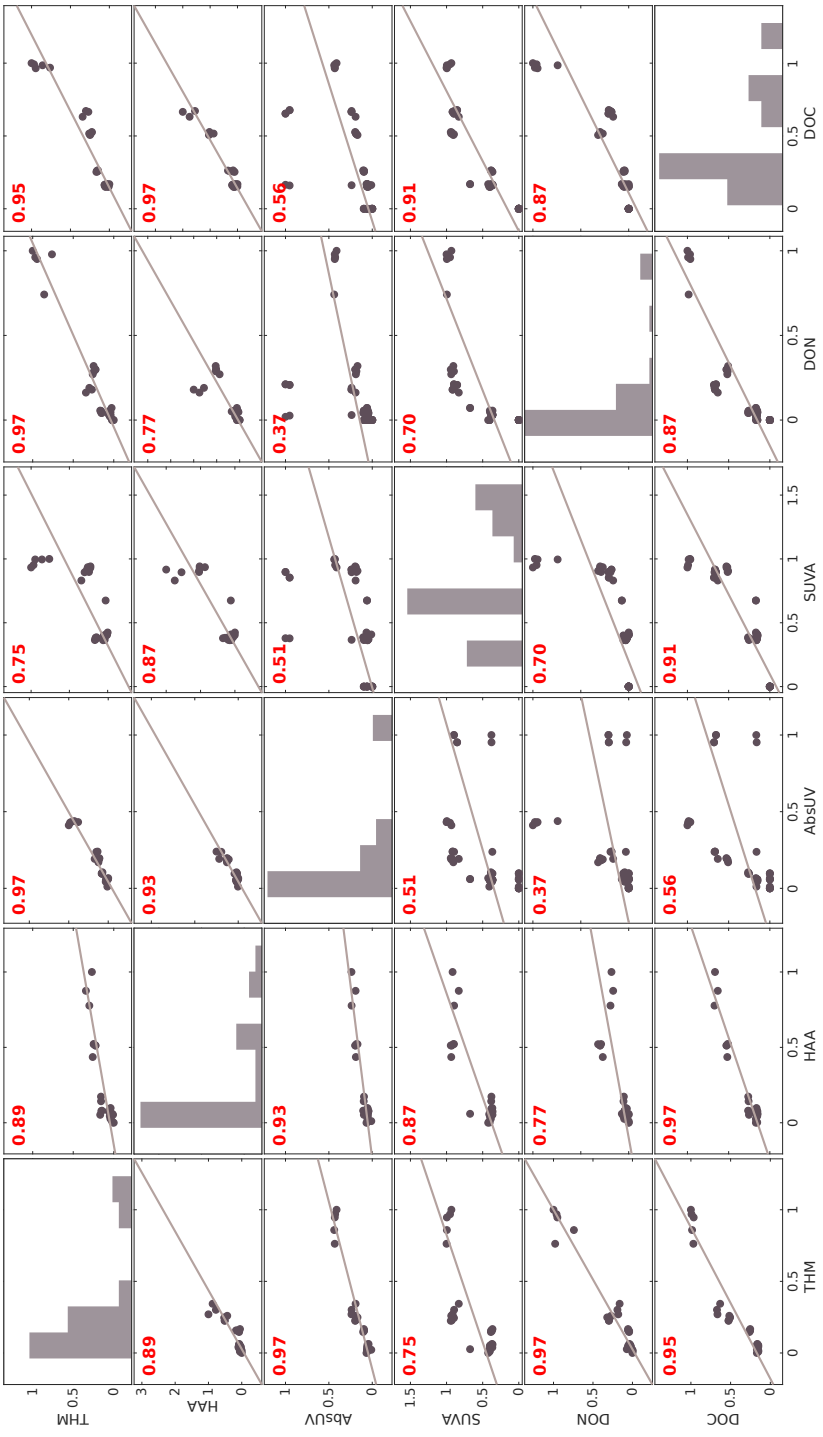

Figure A.10: THM and HAA correlation with UVA_{254}, SUVA, DON and DOC.